NTNU – Trondheim
Norwegian University of
Science and Technology

Probabilistic material modeling of iceberg for analysis of accidental impacts with ships and offshore structures

Simen Bøhlerengen

Marine Technology
Submission date: June 2013
Supervisor: Jørgen Amdahl, IMT
Co-supervisor: Martin Storheim, IMT
Ekaterina Kim, IMT

Norwegian University of Science and Technology
Department of Marine Technology

Abstract

There has been an increasing interest of maritime and offshore operations in the arctic regions for some decades now. In arctic regions there are icebergs which can't be neglected. The first part of this thesis is an introduction of the sea ice material and the material model developed by Zhenhui Liu. It will also be introduced some pressure relations, particularly the process pressure-area curve and the spatial pressure-area curve.

Development of numerical models which can be used in design process instead of full-scale measurements or model experiments would be very cost-efficient, and is therefore a hot topic these days. Modeling of an iceberg is associated with substantial challenges, due to the complexity of the material sea ice. Zhenhui Liu has developed a material model that gives reasonable load and pressure levels. This model has been evaluated and a parametric study has been performed. Zhenhui Liu's material model is homogenous. Earlier research has found that general icebergs are inhomogeneous with a mixture of hard and weak zones. Therefore Zhenhui Liu's material model has been further improved during this master thesis by developing a method that produces a stochastic variation of the some specific material parameters. This should improve the model, and give the iceberg inhomogeneous material properties.

This new modified model has been analyzed for both Ultimate Limit State (ULS) and Accidental Limit State (ALS). ULS only allows that the structure can undergo small deformations with no to limited elasto-plastic behavior. For ULS design maximum forces and pressures from the ice as structure crushes the ice are highly relevant. Therefore MATLAB scripts have been developed where forces and pressure-area curves can be plotted. ALS design accepts that the structure can undergo substantial deformations. For such impact scenarios, pressure-area curves are meaningless; and the more important results are the relative strength between the colliding objects. The level of structural damage in form of deformation and dissipation of energy are highly relevant for such impacts, which has led to development of more MATLAB scripts that produces relevant curves for ALS design.

The stochastic variation of the material parameters was a success. The new inhomogeneous iceberg model gave reasonable results, where especially local pressures and the location of occurrence of high pressure zones have been improved. From the ALS design analysis, the new inhomogeneous iceberg model gives considerable structural damage to the panel used. The new inhomogeneous iceberg model is stronger than the homogenous iceberg model, especially in the beginning phase of an impact scenario.

Sammendrag

Design av skip og offshorekonstruksjoner skal utføres ved prinsipper av "Ultimate Limit State" (ULS) og videre sjekkes for "Accidental Limit State" (ALS). ULS tillater kun små deformasjon med begrenset elasto-plastikk oppførsel. For ULS design er maksimum krefter og trykkrefter fra isfjellet når konstruksjonen knuser isen veldig relevant. På grunn av dette har det blitt utviklet et MATLAB skript som leser in en spesifikk fil LS-DYNA produserer, kalkulerer og plotter krefter og trykk-areal kurver. Det har i masteroppgaven blitt utviklet to typer trykk-areal kurver i MATLAB skriptet. Den ene typen er en såkalt "Process pressure-area curve", hvor kurven beskriver det gjennomsnittstrykket forandrer seg som funksjon av nominell kontakt-areal. Den andre typen er en såkalt "Spatial pressure-area curve", hvor kurven beskriver et gjennomsnitts trykk på sub-arealer av ulike størrelser innenfor et større areal for en bestemt tid i et kollisjonstilfelle.

Utviklingen av numeriske modeller som kan brukes i design prosessen, som muligens kunne erstatte full-skala målinger og modell forsøk ville være kostnadseffektivt. Noe som har ført et høyt fokus på utviklingen av slike modeller det siste tiåret. Modellering av isfjell har vært problematisk på grunn av det komplekse materialet til isfjellet. Det har tidligere vært utviklet noen numeriske modeller, Zhenhui Liu har utviklet en numerisk modell som gir fornuftige krefter og trykkrefter. Denne numeriske modellen har vært undersøkt, og en parametrisk studie har blitt utført. Det parametriske studiet undersøkte sensitiviteten til modellen ved endring av noen bestemte material parametere. Modellen har også gjennom masteroppgaven blitt modifisert. Isfjell modellen er nå fått tilført inhomogen mekaniske egenskaper. Dette har blitt oppnådd ved å tilegne bestemte material parametere en stokastisk variasjon. Den mest fornuftige input verdiene for material parameterne til isfjell modellen har også blitt undersøkt. Det har også blitt gitt anbefalte input verdier som skal representere et generelt isfjell meget bra.

Den nye modifiserte modellen har deretter blitt evaluert og sammenlignet med et tidligere eksperiment. Trykk distribusjonen over kontakt-arealet har også blitt evaluert. Den nye modifiserte modellen gir lovende resultater. Spesielt distribusjonen av lokale trykk og posisjonen av såkalte høy trykk soner ser mere fornuftig ut enn tidligere modell. Den modifiserte modellen har blitt analysert på 3 forskjellige deformerbare paneler, og det viser seg at den nye modifiserte modellen gir meget store strukturell skader for selv det sterkeste panelet. Effekten av inhomogen isfjell har også blitt undersøkt med hensyn på størrelsen på strukturell skade på et bestemt panel. Resultatene viser at et inhomogent isfjell gir større strukturell skade enn et homogent isfjell i tidlig fase av et kollisjonstilfelle.

Scope of work

MASTER THESIS 2013

for

Stud. techn. Simen Bøhlerengen

Probabilistic material modeling of iceberg for analysis of accidental impacts with ships and offshore structures

The Arctic waters are becoming an attractive area due to its large reservoir of oil and gas. Explorations in such areas will meet with harsh environmental elements, such as ice loads and low temperatures. The sea ice extent and thickness have diminished over the past few years due to global warming. This diminishing ice may provide access to new sailing routes in these waters in the years to come. The probability of collisions between ships and icebergs may increase due to this increased activity. The assessment of the loads caused by iceberg impacts is an important issue for ship designers. In modern ship and offshore structure design, the design should always be carried out under the principle of the Ultimate Limit State (ULS) and further checked with the requirements for the Accidental Limit State (ALS).

Although it is not explicitly stated, the conventional design of ship structures is carried out in the ULS format. This design implies that the structure is only allowed to undergo small deformations with no or limited elasto-plastic behavior. The task is then to determine the scantlings such that the structure can resist the maximum pressures and forces from the ice as the ship is crushing the ice. Consequently, the ice action is characterized as pressure versus contact area curves; the smaller the contact area, the larger is the indentation pressure. Substantial efforts have been invested over the past decades to determine pressure-area relationships for crushing ice. A variety of formulations can be found in ship classification codes and rules for arctic offshore structures, such as IACS and ISO 19906. The return periods for the ice pressures are not always explicitly stated, but in general, vary from a few years to 100 years.

Pressure-area relationships are sometimes also given for very rare ice impact events, for example, for a return period of 10000 years. The intention is to use the pressure for design in the ALS format. Such pressure–area relationships are useful if the objective is to design the structure to be so strong that it can crush the ice with very moderate deformations, similar to the task in the ULS design. This approach will often lead to overly conservative design. In most codes, it is accepted that the structure may undergo substantial deformations in the ALS design; yielding, plastic mechanisms, buckling etc. are allowed, but the integrity of the structure with respect to global stability shall not be put in jeopardy. For a ship or offshore structures carrying dangerous cargo, it is also normally required that a spill into the environment should not occur. For a double-hull tanker, this requirement implies

that, while gross deformation and fracture of the outer shell may be accepted, puncturing of the inner shell (cargo tank) should not occur. For this kind of design, pressure-area curves are meaningless; the structural resistance will to a large extent limit the pressures on the ice-structure interface. The pressure depends on the relative resistance of the ship, the iceberg and the damage evolution. This can only be assessed with confidence in integrated analyses based on continuum mechanics modeling of both the ship and the iceberg.

Material modeling of icebergs is associated with substantial challenges. Ice is generally an inhomogeneous material, with a mixture of hard and weak zones. The knowledge of the statistical distribution of strength properties of the hard and weak zones is limited. It is also not known to what extent the variation of the mechanical properties is important with respect to assessment of damage in the side of a ship or an offshore structure.

The objective of the present work is perform systematic variation of iceberg material properties and from integrated iceberg impact analyses study their effect on the level and distribution of structural damage.

The work is proposed to be carried out in the following steps:

1. Review of the physical basis behind determination of pressure area relationships for ice as given in various code formulations.
2. Reanalysis of the pressure-area relationships obtained in the ice impact simulations conducted in the project work. The pressure-area relation can be divided into process and *spatial* pressure-area. It is desired to identify the maximum pressure-area relationship within the contact zone for the various time instances (thereby *spatial* PA) as well as maximum of all maxima for the entire ice crushing history (thereby *process* PA). It is suggested to develop robust MATLAB ALGORITHMS to verify process and spatial pressure –area-relation, actual area vs. nominal area relation and dissipated energy.
3. Perform parametrical variations of the ice material parameters to study their effects on the pressure-area relationships. Depending on the outcome of pt.3, the effect of random variations of the ice parameters may be conducted. The extent of stochastic variations will depend on the demand for computer resources for the simulations. Stochastic variations could be easier to implement in the LS DYNA code rather than in the input deck. Method of implementation should be decided in cooperation with supervisors.
4. Investigate the effect of structural compliance on the pressure-area relationship. In collaboration with supervisors a characteristic stiffened panel is selected where the strength properties are varied systematically.
5. After the “best” ice material model has been established, perform systematic ice-structure interaction analysis for ALIE impacts. The shape of the iceberg shall be selected with due concern of the structural scantlings; i.e. stiffener/frame spacing, the relative strength of plating and stiffeners etc. What is the “worst” shape of the iceberg with respect to deformation of outer shell and penetration and rupture of inner shell.

6. Conclusions and recommendations for further work

Literature studies of specific topics relevant to the thesis work may be included.

The work scope may prove to be larger than initially anticipated. Subject to approval from the supervisors, topics may be deleted from the list above or reduced in extent.

In the thesis the candidate shall present his personal contribution to the resolution of problems within the scope of the thesis work.

Theories and conclusions should be based on mathematical derivations and/or logic reasoning identifying the various steps in the deduction.

The candidate should utilize the existing possibilities for obtaining relevant literature.

Thesis format

The thesis should be organized in a rational manner to give a clear exposition of results, assessments, and conclusions. The text should be brief and to the point, with a clear language. Telegraphic language should be avoided.

The thesis shall contain the following elements: A text defining the scope, preface, list of contents, summary, main body of thesis, conclusions with recommendations for further work, list of symbols and acronyms, references and (optional) appendices. All figures, tables and equations shall be numerated.

The supervisors may require that the candidate, in an early stage of the work, present a written plan for the completion of the work. The plan should include a budget for the use of computer and laboratory resources, which will be charged to the department. Overruns shall be reported to the supervisors.

The original contribution of the candidate and material taken from other sources shall be clearly defined. Work from other sources shall be properly referenced using an acknowledged referencing system.

The report shall be submitted in two copies:

- Signed by the candidate
- The text defining the scope included
- In bound volume(s)
- Drawings and/or computer prints that cannot be bound should be organised in a separate folder.

Ownership

NTNU has according to the present rules the ownership of the thesis. Any use of the thesis has to be approved by NTNU (or external partner when this applies). The department has the right to use the thesis as if a NTNU employee carried out the work, if nothing else has been agreed in advance.

Thesis supervisors

Prof. Jørgen Amdahl

Ph.D candidates Ekaterina Kim and Martin Storheim

Deadline: June 17, 2013

Trondheim, January 13, 2013

Jørgen Amdahl

Summary

It is a large amount of petroleum resources in total above the Arctic Circle. The U.S Geological Survey (USGS) has published an article where USGS has estimated that the above the Arctic Circle account for about 22 percent of the undiscovered, technically recoverable resources in the world. Also there are few shipping routes above the Arctic Circle which highly preferable for many countries, and therefore it has been a rapid increase in interest of operations and using of shipping routes above Arctic Circle. The probability of collisions between ships and icebergs may increase due to this increased interest and activity. The assessment of load caused by icebergs impacts has to be included in the structural design process.

The structural design should always follow the principle of Ultimate Limit State (ULS) and further check for Accidental Limit State (ALS). ULS only allows that the structure can undergo small deformation with no to limited elasto-plastic behavior. For ULS design maximum forces and pressures from the ice as structure crushes the ice are highly relevant. It has therefore been developed a post-processing MATLAB script that reads LS-DYNA output files, calculates and plots force and pressure-area curves. There are two types of pressure-area curves that are included in the MATLAB script. That is the process pressure-area curve and spatial pressure-area curve. Process pressure-area curve shows how the average pressure changes as a function of nominal contact-area during a collision. The spatial pressure-area curve on the other hand gives the average pressure on sub-areas of various sizes within a larger area at a specific time-step during a collision.

Developing numerical models which can be used in design process instead of full-scale measurements or model experiments would be very cost-efficient, and therefore it has been a hot topic the last decade. Modeling of icebergs is associated with substantial challenges, due to the complexity of the material sea ice. There has been develop a few numerical models from earlier research, Zhenhui Liu has developed a numerical model that gives reasonable load and pressure levels. This model is been used in this master thesis, and modified. This master thesis first investigates the most reasonable input values for the material parameters by comparing the NLFEA results with an earlier experiment. Thereafter a parametric study was performed where the sensitivity for a change in the different material parameters were identified. The numerical model developed by Zhenhui Liu is an idealized model that has a few simplifications. The model is simplified by assuming that the iceberg is homogenous, which is known from the literature and earlier research to be wrong. Icebergs are inhomogeneous and have a mixture of hard and weak zones. During this master thesis Zhenhui Liu's model has been modified. The iceberg model has been given a stochastic variation to some material parameters, which will make the iceberg model inhomogeneous.

The new modified iceberg model was than evaluated by comparing the forces and pressure levels to an earlier experiment. The local pressure distribution over the contact-area was also evaluated. The new modified iceberg model does give promising results, especially the local pressure distribution and the location of the high pressure zones is seems more reasonable.

For ALS design large deformation and fracture of outer hull may be accepted as long as the puncturing of inner hull does not occur. This makes the distribution and level of structural damage is highly relevant for ALS design. The new modified version of the Zhenhui Liu's numerical iceberg model has been analyzed for ALS design, where the level of structural damage on a panel is measured. The new modified iceberg model produced considerable structural damage to the panels that were used. The effect on the structural damage on the panel due to the stochastic variation of material properties was analyzed. The new inhomogeneous model produced more structural damage to the panel than the model without this inhomogeneity in the earlier stages of the impact scenario.

Preface

This report is the result of the master thesis for Stud. Techn. Simen Bøhlerengen at the Norwegian University of Science and Technology, NTNU, spring 2013.

This master thesis has given me a lot of new knowledge about nonlinear finite element analysis. It also gave great insight and literature about the sea ice, especially the material properties and the challenges this material brings into impact scenarios. The software used during this master thesis is MSC PATRAN, LS-DYNA, LS-PrePost and MATLAB. MSC PATRAN was a good tool to create the different models. The rest of the setup has been done by use of LS-PrePost, and all the nonlinear finite element analyses are performed by LS-DYNA.

The master thesis started out with making robust MATLAB scripts where different post-processing scripts were developed. Thereafter a parametric study of the Zhenhui Liu's material iceberg model was performed. The amount CPU-resources needed was large; therefore to be able to use one of the NTNU's servers to perform the analyses has been important. It appeared some difficulties with the license for the LS-DYNA program during the master thesis, which delayed me to performing analyses for some time. This might have limited my parametric study in some degree. Anyway, I am pleased with the end result, and the parametric study led to great insight on how sensitive the iceberg model is for some material parameters.

Share-energy design analyses for the modified inhomogeneous iceberg model have been performed, where the level of structural damage on a panel has been investigated. NTNU's servers used different operative system, which made it difficult to implement the new modified iceberg model to the servers. This led to performing the analyses with the new modified inhomogeneous iceberg model on my laptop, which made relative large limitations on the duration length, the model size and the amount of analyses performed. Therefore the analyses where limited to only investigated structural damage of outer hull, and neglecting to see how the iceberg might penetrate the inter hull of the panel. Still some reasonable results were obtained and discussed.

Besides Zhenhui Liu which provided the material model, I would like to thank my supervisor Professor Jørgen Amdahl for good guidance during the master thesis. I will also give special thanks to both Ph.D. candidates Ekaterina Kim and Martin Storheim which has provided interesting discussions and good guidance throughout the whole master thesis.

Tyholt, Trondheim, June 17, 2013

Simen Bøhlerengen

Contents

Figure list

Table list

Nomenclature

F_G	-	Global crushing force, associated with global action
p_G	-	Ice pressure averaged over the nominal contact area
p_L	-	Local ice pressure
δ	-	Penetration depth
p_1, p_2	-	Smaller and larger root of the yield function respectively
p	-	Hydrostatic pressure
q	-	Von Mises stress
J_2	-	Second invariant of deviatoric stress tensor
A_N	-	Nominal contact area
w_L	-	Width of the loaded area
a	-	Height of the loaded area
A	-	Areal
a_0, a_1, a_2	-	Material constants
s_{ij}	-	Deviatoric stress tensor
τ	-	Octahedral stress
ε_0	-	Initial strain
ε_f	-	Failure strain
$\varepsilon^p{}_{ij}$	-	Equivalent plastic strain
p_{cut}	-	Cut-off pressure
E	-	E-modulus
K	-	Bulk modulus

G	-	Shear modulus
M	-	Mass Matrix
C	-	Damping Matrix
R	-	Internal force Matrix
P	-	External load
v_n	-	Velocity at time step n
a_n	-	Acceleration at time step n
u_n	-	Displacement at time step n
V	-	Volume
v	-	Velocity
ρ	-	Density
υ_e	-	Characteristic volume
L_e, L_s	-	Characteristic length
c	-	Sound of speed
Δt	-	Time step
Δt_e	-	Critical time step
E_s	-	Strain energy
μ	-	Expected value
σ	-	Standard deviation
δ_{plate}	-	displacement of the chosen nodes on the deformable plate
δ_{pusher}	-	displacment of the rigid plate that pushes the ice
δ_{ice}	-	erosion/crushing distance of iceberg

Acronyms

ADAMC	-	The analysis with Derradji-Aouat's material constants
AKMC	-	The analysis with Kierkegaard's material constants
ARFMC1	-	The analysis with Riska's and Frederking's material constants data set 1
ARFMC2	-	The analysis with Riska's and Frederking's material constants data set 2
FEM	-	Finite element method
ISO	-	International Organization for Standardization
NLFE	-	Nonlinear finite element
NLFEM	-	Nonlinear finite element method
NLFEA	-	Nonlinear finite element analysis
NRC	-	National Research Council Canada
STePS^2	-	Sustainable Technology for Polar Ships and Structures
PPAC	-	Process pressure-area curve
SPAC	-	Spatial pressure-area curve
SPACs	-	Spatial pressure-area curves
CP	-	Contour plot
CPs	-	Contour plots
MC	-	Material constants
TS	-	Time-step

1 Introduction

The U.S Geological Survey (USGS) published an article in 2008 [25], where they made estimation of the total available petroleum resources above the Arctic Circle. They have estimated that the resources above the Arctic Circle accounts for about 22 percent of the undiscovered, technically recoverable resources in the world. Figure 1 below shows the measured probability of at least one undiscovered oil/gas field with recoverable resources greater than 50 million barrels of oil [17].

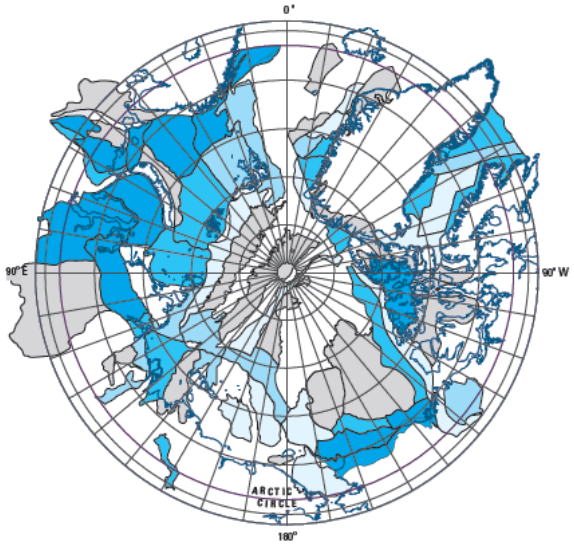

Figure 1 - Measured probability of oil/gas field greater than 50 million barrels of oil, [17].

Due to this enormous potential for petroleum industry, the interest of operation above the Arctic Circle has rapidly increased in the last decades. There is also a lot of research going on related to the changes of environment in the arctic regions. The arctic sea ice is decreasing, and the big question is if it is because of natural variations or because of the rising temperatures linked to global warming. Many will say a combination of these two reasons is most probably correct. Figure 2 below shows the daily arctic sea ice extent. It clearly indicates that the arctic regions have a decreasing extent of sea ice, especially in the late summer months.

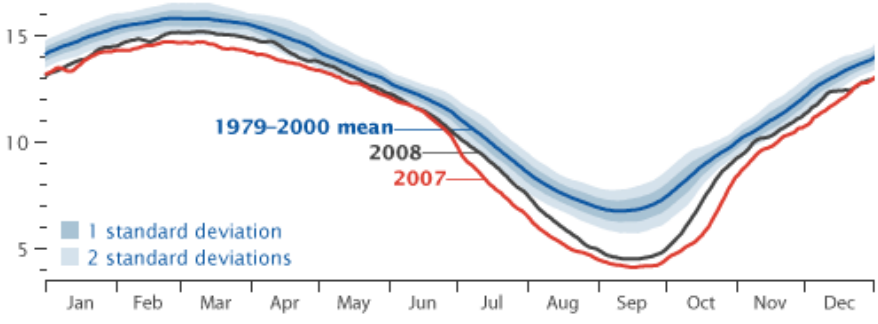

Figure 2 - Arctic daily Sea Ice Extent (Millions of square kilometers) [22].

This makes the Northwest and Northeast Passage increasingly less expensive and easier to pass through due to fewer areas with sea ice during the year. Especially the Northeast Passage during late summer months, there is little to no sea ice through this route at that period during the year. Therefore the maritime industry has also had a rapid increase of interest for ship design in arctic regions. The increase in both petroleum and maritime industry give increasing need for standards and recommended practices for design of maritime and offshore structures in arctic environmental conditions. Standards exist, but they are still relatively fresh. The standards are also continuously under development for more comprehensive recommend practices.

In arctic regions there are icebergs of which large icebergs relatively easily may be avoided due the visibility of the iceberg from the ship's radars and/or from people's eyes aboard. However it can be difficult to spot a middle size iceberg (bergy bit) in bad weather, and the radar might not spot the bergy bit either. Therefore iceberg collisions are possible and have to be investigated during the structural design. Figure 3 shows some critical locations where bergy bits have been observed.

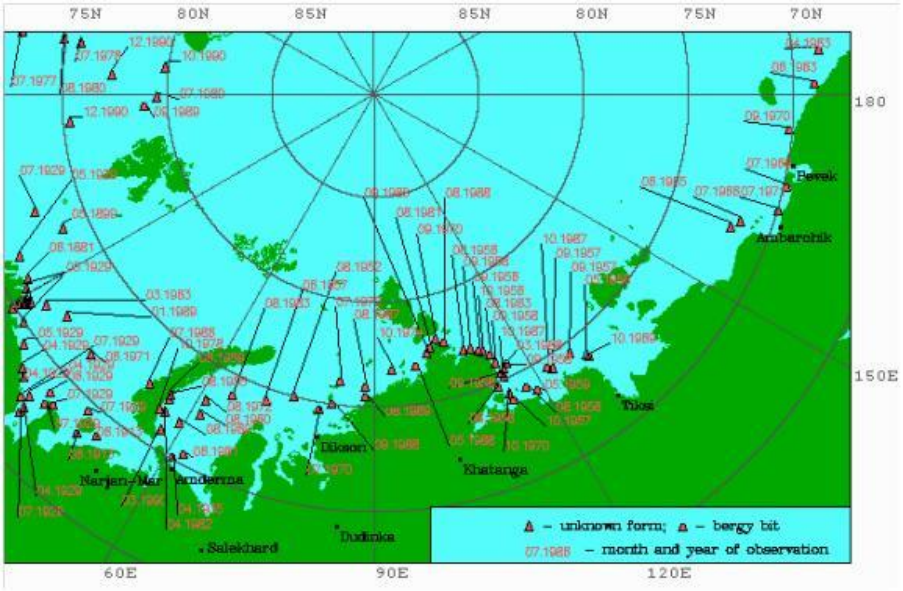

Figure 3 - Locations of observed bergy bits [1].

Figure 3 shows that many bergy bits are observed in Northeast Passage which ships might encounter. Therefore having a good design method against bergy bits is important. Different standards have made some effort to design for such collision scenarios. ISO is an international organization who develops voluntary international standards. Due to the recent increasing interest in offshore operation in artic regions, ISO has made a few recommended standards for design of offshore structures in artic waters. According to ISO-19906, [13], ice actions can be divided into two groups, local and global ice actions.

The ISO recommended practices describe how to preform calculation for local and global ice actions [13]. For determination of global ice action, ISO recommends a combination of full-scale measurements and model experiments. Theoretical methods can be used as long as suitable calibration has been done from either full-scale measurements or experiments. For determinations of local ice action, ISO recommends full-scale measurements or established theoretical methods. The local ice action has to be considered due to the local structural configuration.

From an engineering point of view, making full-scale measurements and models experiments are very expensive, therefore numerical method is much more preferable. Up to now it has been put only limited effort into developing such numerical models. Zhenhui Liu is one person who has developed a model that yields reasonable results, which is continuously under evaluation and further development by NTNU. Material modeling of icebergs is associated with substantial challenges. Iceberg is generally inhomogeneous, with a mixture of weak and strong zones. The knowledge of the statistical distribution of strength properties of the weak and strong zones is limited. It is also not known how important this mixture of zones with different mechanical properties is with respect to assessment of structural damage for impact scenarios. The model developed by Zhenhui Liu is an idealized model, where the model is homogenous. This model will be further improved in this master thesis by suggest a method to include inhomogeneous mechanical properties to the iceberg model. Thereafter the new modified model will be analyzed for ALS design, where the level of structural damage on a panel is measured.

2 Background

There is a lot of research going on around iceberg impacts, due to increasing interest from companies to operate in arctic region. Arctic routes are favorable for transport of import and export for many countries, and new oil and gas fields are being discovered and will be explored in the near future in the arctic region. The Shtokman field is one example, and many other fields are explored and will be operated on in the future. This increasing interest has resulted in research for design against ice loads. The next subsection will give some examples of previous work that addresses some of the topics in this report.

2.1 Previous work

There have been quite a few researchers on the theme ice interaction with structures. One of the most recently experiments conducted as a part of the STePS^2 (Sustainable Technology for Polar Ships and Structures) research project at Memorial University, St. John`s, Canada, [10]. The object of this experiment was to study the response of a full size structural grillage for both quasi-static and dynamic ice loads. The contact pressure profiles at each time step were obtained, which revealed the shape and the variability of the high pressure zones that exist during an ice-structure impact.

Jones (1982), [14], carried out a compressive triaxial test, where randomly oriented, laboratory-made, polycrystalline ice, between strain-rates of 10^{-7} and 10^{-1} [s^{-1}], and with confining pressures from 0.1 to 85 [MPa] were investigated. Jones made a good effort to investigate the dependence of strain-rate during ice impacts.

Wells, Jordan, Derradji-Aouat and Taylor (2010) [26], have performed laboratory indentation tests were the processes of ice failure during indention and the pressure distribution at the contact area were investigated. The test gave interesting results, where failure modes and pressure distributions over the contact area for different rates were discussed. The results from the test were consistent with theory obtained so far, and with earlier experiments.

Daley has made great contribution the last decade, where his research on ice impact has resulted in many published articles. Daley has made a great contribution to theory and description of how the pressure-area curves is developed. His articles of pressure-area curves [6] have been of great value during this master thesis.

There has been developed two different model in LS-DYNA, one by Gagnon [9], and one by Liu [18]. Gagnon has also done laboratory growler impact tests, where Gagnon compared growler model in LS-DYNA with the laboratory growler test. The LS-DYNA model produced reasonable results compared with the laboratory growler tests. The model is based on crushable foam material with a certain criteria that shall simulate the crushing of the ice. Liu's ice model which also is used in this master thesis is plastic model. This model was evaluated in an earlier project, and it will be further evaluated in this master thesis and also improved.

This report will make use of the following 4 earlier experiments that have conducted the material constants a_0, a_1 and a_2. These 4 experiments are done by the following researchers:

- A. Derradji-Aouat (2000)
- H. Kierkegaard (1993)
- Data set 1 Riska and Frederking (1987)
- Data set 2 Riska and Frederking (1987)

3 Ice in general and Zhenhui Liu's material model

There has been an increasing interest in maritime and offshore operation in the arctic regions for some decades now. In arctic regions there are icebergs which can't be neglected. Therefore research on iceberg collision and modeling of numerical iceberg models with real mechanical properties are hot topic the last decade. Due to the complexity of the sea ice material, modeling physical correct numerical models have been very difficult. Ph.D. student Zhenhui Liu has developed a model that predicts reasonable results in strength design. The model is then assumed to give adequate accuracy for share-energy design. Zhenhui Liu's material model of an iceberg will be used, evaluated and also improved during this report. Therefore a short review of the ice model describe in his doctoral thesis [18], will be given in this chapter. It will also be given general theory of the material properties of sea ice, and how sea ice behaves in different scenarios.

Iceberg is a complex material. It is general inhomogeneous and the mechanical properties depend on many different parameters, [18]:

1 Temperature
2 Porosity
3 grain size
4 strain rate
5 confinement
6 shape
7 imperfections

Generally icebergs are weaker and softer with increasing temperature, porosity and grain size. The strain rate, which affects the strength of the iceberg, is still under discussion. Schulson's research, [24], shows that the strength increases with increasing strain rate up to a threshold value. This threshold value is the transition from ductile to brittle failure, and has a value of about 10^{-3} as shown in figure 4.

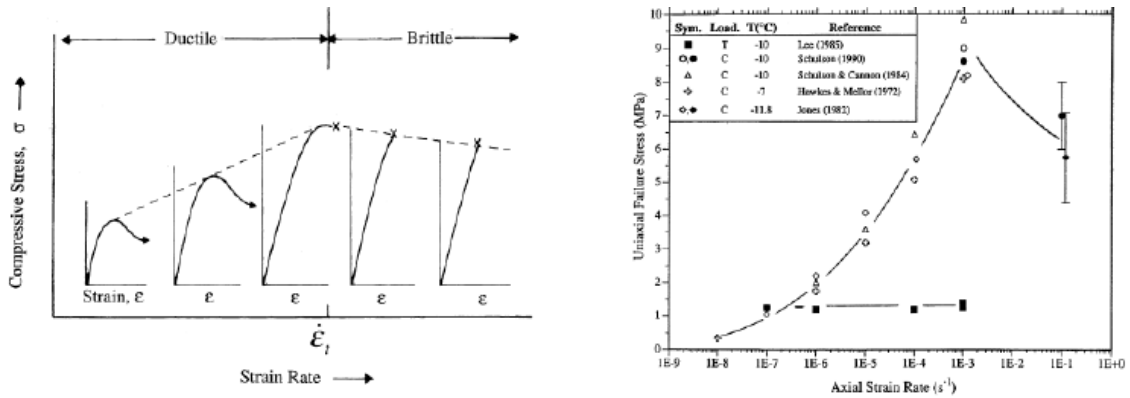

Figure 4 - Strain rate and transition (ductile to brittle)

Sea ice properties depend on many variables as mention above. There are also other factors that decide the size of ice load, and that is what failure mode the ice takes in an ice-structure interaction scenario. According to ISO [13], there are several different failure modes for ice actions. There is crushing, shear, flexure and creep modes, and the key parameters for determine the failure mode are:

- Ice thickness
- Presence of ridges
- Ice velocity
- Ice temperature
- Structure shape

There will mainly be focus on the crushing failure mode, since it is the dominate failure mode for iceberg impacts. Crushing is a very complex failure process, where development of damaged layer, flakes, spalls, horizontal splits and cleavage cracks take place. The crushing process is highly irregular, due to the cracks and spalls which are developed in the process. This leads to development of high pressure zones, which must be accounted for in the local analysis. From observations there has been shown that ice process change from creeping to fracture and spalls for impacts, when the velocity reaches a certain threshold. The threshold observed is about 1 [mm/s]. This implies that crushing failure mode dominates in iceberg impacts, since iceberg impacts usually are of higher velocity then the threshold value.

Overview of the crushing process during impacts

According to ISO [13] the crushing process can be described as follows; During the impact the ice develop high pressure zones. These zones have triaxial stress state, and the zones are most often of high confinement near the center and low confinement near the edges. Due to occurrence of fractures, these high pressure zones vary in space and time. The high pressure zones cause the ice to be crushed in relative small pieces. The high pressure zones tend to occur in the most confined region of the iceberg, at the core of the iceberg. Therefore these zones are often located close to the center of contact-area. Still due to fracture the high pressure zones location changes and the new high pressure zones often occurs other places then the most likely location. Figure 5 on the next page taken from ISO-19906 [13], gives an overview of the crushing process.

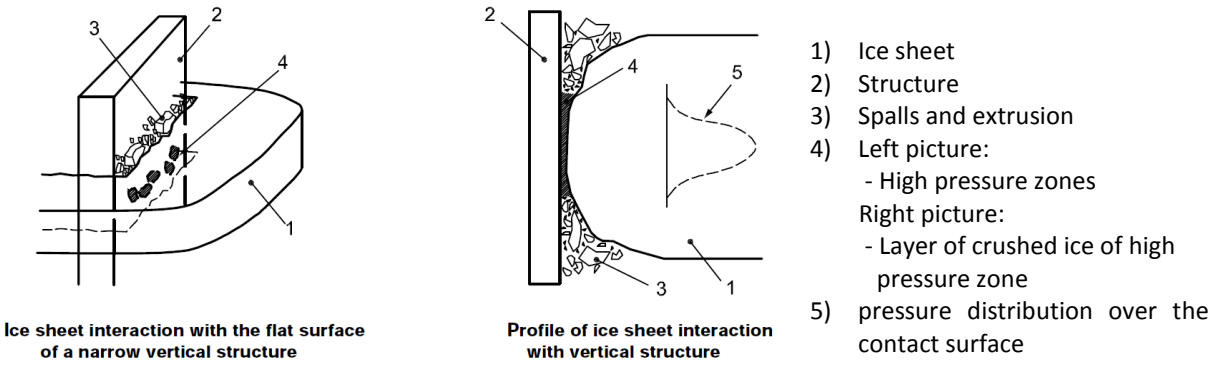

Figure 5 - Description of ice crushing process, [13].

The crushing process described above, gives the reason for local and global ice actions. The global ice action uses the average pressure over nominal contact area. Within the nominal contact area there can be many areas with higher local pressures. Ice actions must therefore be considered both globally and locally.

Zhenhui Liu's model is an idealized model, where the main focus was to establish a NLFEA model that gives correct load levels, rather than physically correct ice process during impact. The idealized model has an isotropic material property which means that the material model properties are the same in all directions. The model is based on plasticity theory, where it is assumed that the material is an elastic-perfect plastic material. In the plastic model a Tsai-Wu yield surface is used, which is fitted to experimental data. The model is also strain-rate and temperature independent. The importance of the dependency of temperature and strain-rate is still not quite clear. Zhenhui Liu has therefore simplified the model by neglecting them.

Iceberg has generally more confined particles in the center of the iceberg. This implies that high pressure zones should be produced more frequently in the center of the contact-area during impact. This confinement makes the ice behave in a triaxial stress state, therefore triaxial experiments should be used to find proper yield surface. The Tsai-Wu yield surface and the failure strain curve are explained in detail in Zhenhui Liu's doctoral thesis [18], and a short summary will be given here. There exists many yield surface techniques. Ice is best represented by the Tsai-Wu yield surface. The Tsai-Wu is a special case of the yield surface purposed by Derradji-Aouat. The yield surface proposed by Derradji-Aouat, [7], is defined as:

$$\left(\frac{\tau-\eta}{\tau_{\max}}\right)^2+\left(\frac{p-\lambda}{p_c}\right)^2=1 \tag{3.1}$$

where $\eta, \tau_{\max}, \lambda$ and p_c are constants, $\tau=\sqrt{\frac{s_{ij}:s_{ij}}{3}}$ is the octahedral stress, s_{ij} is the deviatoric stress tensor and p is the hydrostatic pressure. The Derradji-Aouat yield surface is

mathematically the same as the Tsai-Wu yield surface when $\eta = 0$. The Tsai-Wu yield surface can for an isotropic material be written as:

$$f(p,q) = q - \sqrt{a_0 + a_1 p + a_2 p^2} \tag{3.2}$$

where $p = \frac{\sigma_{kk}}{3} = \frac{I_1}{3}$ is the hydrostatic pressure, $q = \frac{3}{2}\sqrt{s_{ij}s_{ij}}$ is the Von Mises stress, and a_0, a_1 and a_2 are constants that require fitting to experimental data. The more convenient form to write the Tsai-Wu yield surface is to transform it into the $p - J_2$ space:

$$f(p,J_2) = J_2 - \left(a_0 + a_1 p + a_2 p^2\right) = 0 \tag{3.3}$$

where J_2 is the second invariant of deviatoric stress tensor. There are still limited amount of experiments preformed, and the experiments preformed gives very inconsistent values for the material constants a_0, a_1 and a_2. The main reason for this is probably due to the data source and the fitting methods used. In figure 6 the yielding surface for 4 different input values of the material constants are plotted. The material constants are obtained from earlier experiments and plotted against each other. The variation in range and amplitude in the $p - J_2$ space for the different yield surfaces are clearly shown.

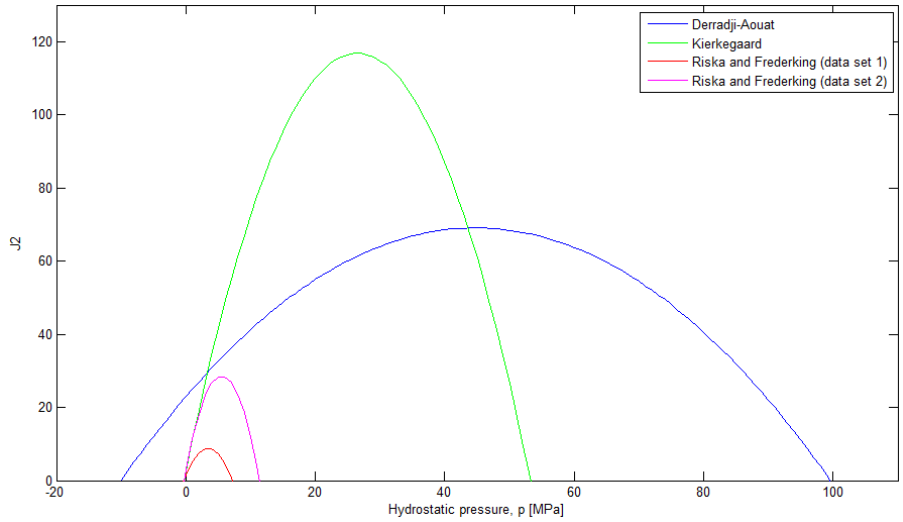

Figure 6 - Tsai-Wu yield surface for different constants

The temperate effect on the iceberg has been investigated in earlier research. The temperature effect can be included in the equation by letting the constant a_0, a_1 and a_3 be temperature dependent:

$$f(p,J_2) = J_2 - \left(a_0(T) + a_1(T)p + a_2(T)p^2\right) = 0 \tag{3.4}$$

Earlier research published by NRC (National Research Council Canada) [15], shows that there is a temperature gradient from the submerged surface to the core of the iceberg. This temperature gradient is also neglected in Zhenhui Liu's iceberg model.

The failure strain is purely empirical, and is based on effective plastic strain and hydrostatic pressure. To simulate the failure of the ice, a technique called "erosion" is used. The "erosion" of elements is activated when the $\varepsilon_{eq}^{p} > \varepsilon_{f}$, or if the pressure is not greater than the cut-off pressure p_{cut}.

Equivalent plastic strain:
$$\varepsilon_{eq}^{p} = \sqrt{\frac{2}{3}\varepsilon_{ij}^{p}\varepsilon_{ij}^{p}} \tag{3.5}$$

Failure strain:
$$\varepsilon_{f} = \varepsilon_{0} + \left(\frac{p}{p_{2}} - 0.5\right)^{2} \tag{3.6}$$

where ε_{eq}^{p} is the equivalent plastic strain, ε_{f} is the failure strain, ε_{0} is the initial failure strain and p_{2} is the larger root of the yield function. The initial failure strain should be set by experimental data.

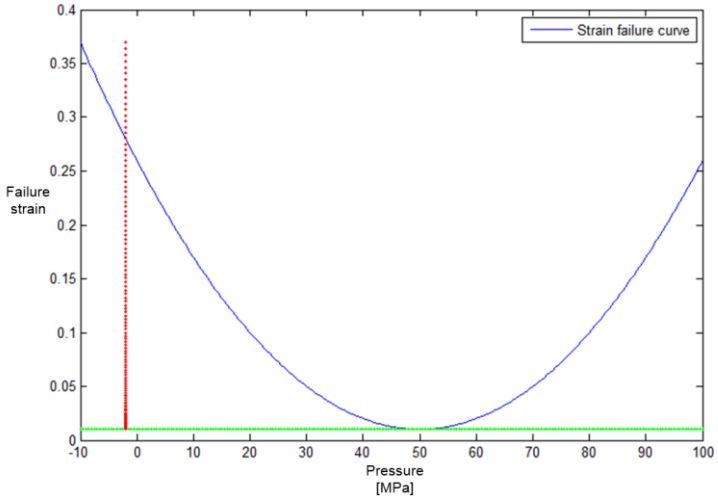

Figure 7 - Strain failure curve

Figure 7 gives graphically the erosion/failure criteria for all pressures. The red line is the cut-off pressure and the green line is the initial failure strain.

3.1 Modification to the Zhenhui Liu's model

Zhenhui Liu's material model of the iceberg yields relative good results, but still there are some simplifications that have been included in the model. Most of them are mention above, and the one which is removed will be discussed below. Zhenhui Liu's model is an idealization model where every element has the same strength. Ice in general is complex material where a mixture of hard and weak zones exists. Sea ice is developed by nature over a period of cold temperature. The sea ice can grow into many different types of ice, and each ice type has different amount of brine cells, grain size etc. Iceberg is developed over many years and it is most certain that there is some extent of material variation within an iceberg model.

Therefore during this master thesis the iceberg model has been modified with a stochastic variation of a few chosen material parameters. The chosen parameters that are given a stochastic variation are the material constants $(a_0, a_1$ and $a_2)$, which control the yielding surface. The other parameters are the initial failure strain (ε_0) and the E-modulus. There will be performed a number of analyses to obtain the best stochastic variation of the material parameters. These results will be presented and discussed in chapter 11. Most interesting to evaluate is how the overall load level and local pressures is affected by the stochastic variation.

Below in figure 8 a graphical illustration of how the stochastic variation of a random material parameter is shown for the modified Zhenhui Liu's material model of an iceberg.

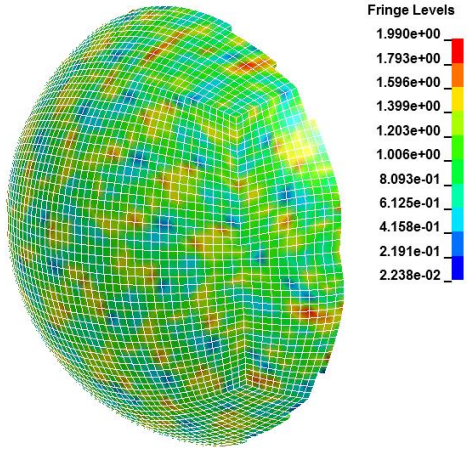

Figure 8 - Modified Zhenhui Liu's model, with stochastic variation of material parameters

The scale in figure 8 shows a value range between 0 and 2, and this value is a factor which either is multiplied or divided on the initial value of the random material parameter mention above. This will lead to variation of mechanical properties within the iceberg, and the element strength will therefore vary. This stochastic variation should make iceberg model more physical correct, and make the material inhomogeneous. This stochastic variation will be further discussed in chapter 11, and how this stochastic variation is implemented in the LS-DYNA code will also be given.

4 Pressure-area relationships

There exist many pressure-area relations and there will in this master thesis emphases on some specific pressure-area relations. It will be large focus on both the process pressure-area curve and the spatial pressure-area curve. This chapter will also discuss how the well-used pressure-area curve given in ISO-19906 [13] is obtained, and what the curve is based on. But first the definition between local and global ice actions will be given, and ISO [13] gives the following definition.

4.1 Global ice action

Global ice action calculates the average pressures over the nominal contact-area, and do not consider the local pressures within that contact area. There are many different ice failure modes, but for global ice action only crushing is being considered. This is because it will be the dominated failure mode in the collision scenario which is being analyzed in this master thesis. According to ISO [13] the global crushing force can be described as:

$$F_G = p_G \bullet A_N \tag{4.1}$$

where

$p_G =$ the ice pressure averaged over the nominal contact area associated with the global action

$A_N =$ the nominal contact area, which is the projected area of the intact ice feature on the structure

The average ice pressure is calculated differently depending on the scenario. Considering an iceberg impact, the average ice pressure is given as:

$$p_G = C_p A_N^{D_p} \tag{4.2}$$

$$A_N = C_A \delta^{D_A} \tag{4.3}$$

where

$C_A, D_A =$ local ice shape coefficient for ice feature

$A_N =$ nominal contact area

$\delta =$ penetration depth

The nominal contact-area is the projected contact-area of the ice feature on the surface of the structure for a given penetration into the ice feature. The constants C_p *and* D_p can be obtained by calibration against existent database. The large ship ramming database (Kigoriak, Polar Sea, MV Arctic, Manhattan and Oden) recommend C_p to be lognormal distributed with a mean equal to 3, and with a deviation of 1.5. For D_p the ship ramming

database recommend a normal distributed value with a mean equal to -0.4 [MPa], and with a deviation of 0.2. When designing a structure against ice actions, p_G is usually the most important parameter, and has to be carefully calculated or chosen. This parameter depends on many parameters and factors, and is therefore very difficult to calculate properly. Below is a list of the factors that p_G depends on:

- Ice temperature
- Nominal contact area
- Shape or aspect ratio (contact area)
- Nature of the contact
- Relative speed
- Displacement between ice and structure
- Compliance of the structure

4.2 Local ice action

Ice to structure interaction will have varying pressures within the nominal contact-area, due to the complexity of the material and the crushing process of ice. This means that there can be many areas within the nominal contact-area that are subjected to higher local pressures. Therefore consideration of local pressures is necessary. These local pressures have to be considered with respect to the structural configurations. This is done by splitting up the nominal contact-area into smaller contact-areas that fits the structural configuration. Figure 9 below shows the nominal contact-area divided up into smaller areas and some definitions given by ISO-19906 [13].

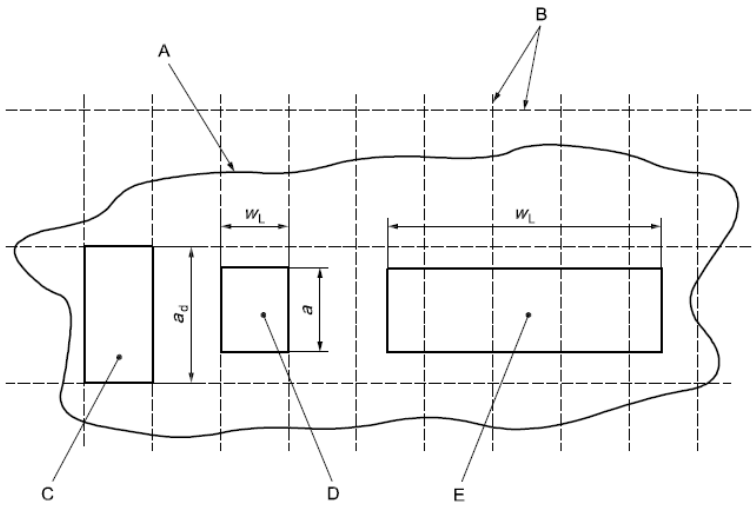

A global interaction area (grows as interaction proceeds)
B frames and stiffeners
C local area for plate design
D loaded area for plate design
E loaded area for stiffener design

a loaded height
a_d frame spacing
w_L loaded width

Figure 9 - Definition of loaded areas for local actions [13]

According to ISO [13] ice interaction can produce local pressures that can be considered as constant over an area:

$$A = a \bullet w_L \tag{4.4}$$

where

$a =$ height of the loaded area

$w_L =$ width of the loaded area

The local pressure due to massive ice features such as icebergs can be determined by the equation (4.5), which is the suggested local pressure-area curve given by ISO-19906 [13]:

$$\begin{aligned} p_L &= 7.40A^{-0.70} \quad for \;\; A \le 10[m^2] \\ p_L &= 1.48 \qquad\quad for \;\; A > 10[m^2] \end{aligned} \tag{4.5}$$

This equation is obtained based on more than just one measurement. One of the measurements it is based on is the Molikpaq indention test in Beaufort Sea. This is an important design curve for design against iceberg collisions for both maritime and offshore structures.

4.3 The pressure-area curve in ISO code

The pressure-area relation for impact scenarios between ice features and maritime and offshore structures has been of huge interest for local structural design of structures operating in arctic waters. Earlier research strongly indicates that the size of the contact-area matters. The pressure has been observed to decrease with increasing contact-area, and the general pressure-area relation has been found and is given by equation (4.6) [4]:

$$p = kA^n \tag{4.6}$$

where p is ice pressure, A is loaded area, k and n is constants and n being less than 1. This relation is much used within structural design of structures operation in arctic waters. Therefore some standards have now a recommended pressure-area relation to use in structural design of structure planning to operate in arctic waters. ISO is one of them, which is a very well-known and recognized international organization that develops standards. The ISO code suggested a pressure-area relation with k set to 7.40 and n set to -0.70, and the relation is given in equation (4.5). There should be no confusion about what data the curve is based on, and what the curve actually represent. The curve is usually based on several data from different full-scale measurements and model experiments. Different code have different suggested curve, it all depends on which full-scale measurements and model experiments that the curve includes.

The ISO pressure-area relation curve is based on following data:

A $3m^2$ Pond Inlet test data
B flat jack test data
C 1989 Hobson's Choice test data
D Molikpaq BW data
E Molikpaq N face data
F F Molikpaq E face data

The data has been divided into bins, and a mean and standard deviation has been determined for each bin. A regression line has been fitted to the average plus 3 times standard deviation points for the bins. The results is the pressure-area relation given in equation (4.5), and the pressure-area curve given in figure 10 below.

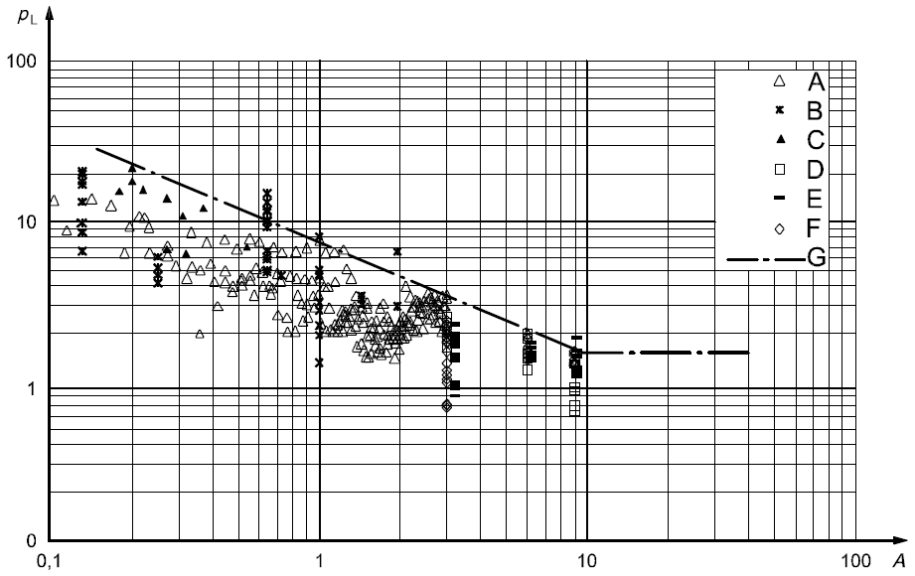

Figure 10 - ISO recommended local pressure curve

Figure 10 above is the ISO's recommended pressure-area curve for local pressure design, the curves is given with a logarithmic scale for both the local pressure and area axes. The ISO curve lies above most of the data measured, this is due to the curve is the mean plus three times the standard deviation, which should ensure that the local pressure in an iceberg collision should not exceed the ISO curve.

The various data sets the ISO curve is based on is very different from each other. Molikpaq data sets are obtained by full-scale measurements, and a detailed description of the full-scale measurements is given by NRC Publications Archive [16]. Molikpaq is a platform which was deployed in Canadian Beaufort Sea in 1984, and was heavily instrumented with equipment that could monitor the ice load that was present. The monitor equipment were 31 Medof panels, each panel is 1.135 [m] wide and 2.715 [m] high. The capacity of each

Medof panel was 20 MN and the panels were arranged in clusters of four to five panels. The panel measured the total force on each panel. It was also equipped with over 200 strain gauges, and several extensometers and Accelerometers. The ISO curve includes a few model experiments, which is “Pond Inlet 1984” tests and “Hobson’s choice 1989” tests. These two model experiments, has been described and results has been well documented by Claude Daley [5]. “Pond Inlet 1984” tests were of medium scale, and the indentor had a large spherical shape which was pushed in to an ice face. The ice face used in these tests, was in a lateral tunnel excavated into the side of a grounded iceberg. “Hobson’s choice 1989” indentor tests were also of medium scale and these tests were done in a trench excavated in a multi-year ice. There were performed 10 indention tests, 5 with 1280 [mm] radius and spherical shape and 5 with various flat indentors. For the flat indentor, the ice face was formed to vertical wedges. The ISO curve has also few more data included, but the above data set is of most relevance to this master thesis. Especially “Pond inlet 1984” tests which has many similarities to the case analyzed in this master thesis. Due to all the similarities the results obtained from many of analyses performed during this master thesis will be compared with “Pond Inlet 1984” tests.

4.4 Pressure-area curve types

During all decades with research about ice loads in arctic waters, it has been performed a lot of full-scale measurements and model tests. These full-scale measurements and model tests have all documented the results in their own way, and therefore what type of result that is documented in experiments often varies. The result that almost always is included is the force-indention curves and the pressure-area curves. From earlier research there has been identified two fundamentally different types of the pressure-area relation [8], which is the process pressure-area curve (PPAC) and the spatial pressure-area curve (SPAC).

The process pressure-area curve shows how the average pressure changes as a function of nominal contact-area during a collision. This is the pressure-area curve that is heavily documented in earlier research and experiments. The ISO curve is based on experiments and full scale measurements where this process pressure-area curves is obtained. The nominal contact area can easily be calculated when knowing the shape of the ice and the indentation depth. The process pressure-area curves in this master thesis are plotted by taking the measured force and divide it on the nominal contact-area at each time-step during the collision. There is a few methods on how to calculate the nominal contact-area, it will be analytically calculated in this master thesis by use of the Sagitta relation [19]. Sagitta is a geometric relation for calculating different types of lengths for a spherical cap. This relation is very useful for obtaining the indentation length and the nominal contact-area of the iceberg shape encountered in this master thesis. The relation is given in equation (4.7) below, and figure 11 visualize the different geometric lengths that are used in equation (4.7).

$$\left(r-s\right)^2+h^2=r^2 \rightarrow s^2-2rs+h^2=0$$

using the quadratic equation:

$$s=r\pm\sqrt{r^2-h^2},\ h\rightarrow 0, s\rightarrow 0$$

gives:

$$s=r-\sqrt{r^2-h^2}$$

$$h=\sqrt{2rs-s^2} \tag{4.7}$$

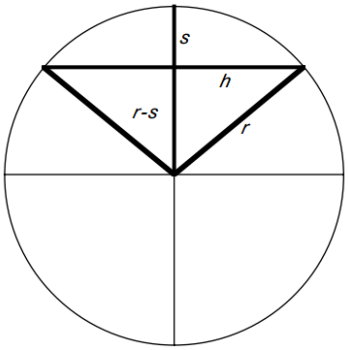

Figure 11 - Sagitta geometric explanation, [19].

The spatial pressure-area curve gives the average pressure on sub-areas of various sizes within a larger area at a specific time during a collision. Spatial pressure-area curve is especially made for determine the design load for local design such as framing and plating. The complexity of the crushing process and the ice material described earlier produce several high pressure zones within the contact-area in each time step. These high pressure zones change locations within the contact-area during the crushing process. These zones have to be accounted for during structural design, and spatial pressure-area curve can be used as a design tool to account for these critical high pressure zones. Spatial pressure-area curves are recently developed curves, and earlier research and experiments has not documented these types of curve until the latest years. The reason is due to the need of advanced equipment. There has been performed a few experiments that are focusing on obtaining such curves. Kim, Daley and Ulan-Kvitberg have performed some experiments with use of high-precision pressure measurement films to obtain such curves [12]. The spatial pressure-area curve uses the actual area instead of the nominal area, which is smaller due to the crushing process during impact.

Spatial pressure-area curves can be plotted in various ways. In this master thesis 5 different methods is developed, and below the 5 different methods is explained:

1 A) Expand-maxima method (square areas)
   B) Expand-maxima method (irregular areas)
2 Box-averaging method
3 Contour-averaging method
4 Iterative-search method

The Box-averaging and the Contour-averaging methods have been developed in earlier research [12]. Still only a description on how the results were obtained and plotted was given. A MATLAB-script has been developed during this master thesis. The Expand-maxima and the Iterative-search methods are completely new methods, and were also developed during this master thesis. The Box-averaging method works such that a starting point for the first sub-area is chosen, and then the area expands uniformly in all directions to obtain the next sub-area. This continues until the whole contact-area is included. Figure 12 below illustrate how the area expands for a chosen time-step by the Box-averaging method.

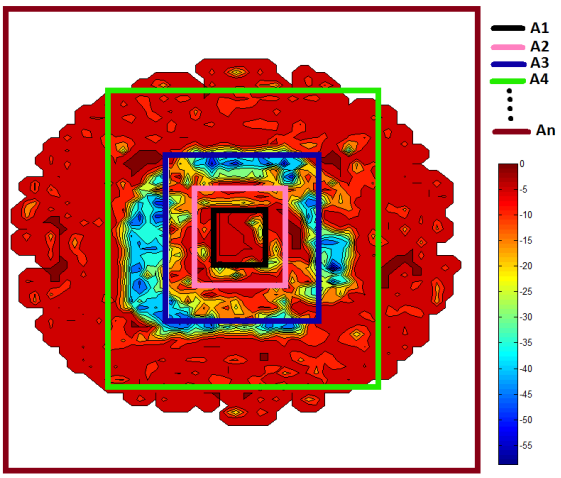

Figure 12 - Box-Averaging Method

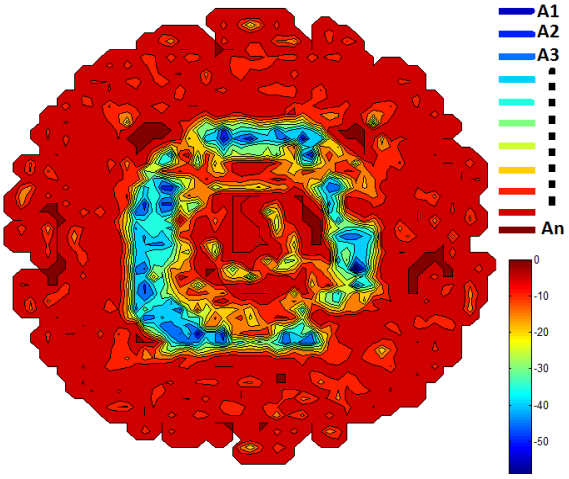

Figure 13 - Contour-Averaging Method

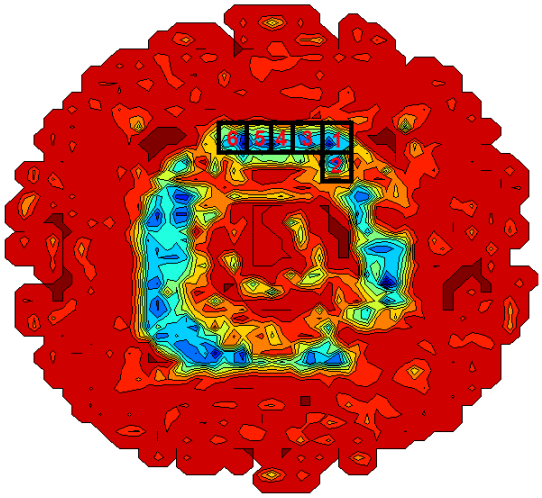

Figure 14 - Expand-maxima Method

Figure 15 - Zoomed picture of figure 14

Contour-averaging method is averaging method that starts with taking the sub-area at the location with maximum pressure. The next sub-area that is added on is the second largest pressure within the entire contact-area, regardless of the position of the first sub-area. Sub-areas with different pressures levels are in descending order added on until total pressure within the contact-area is obtained. Figure 13 illustrates the Contour-averaging method. The figure is a contour plot with 11 colors, each color represent a pressure range. The Contour-averaging method will start with the dark blue areas (maximum pressure areas), then add on areas in the pressure range right below the current pressure range. This continuous until the lowest pressure range is included (dark red color in figure 13).

Expand-maxima method is a method that first search through all the sub-areas within the contact-area for sub-areas with the highest pressures. Chosen number of sub-areas with the highest pressures is obtained. The algorithm for plotting the spatial pressure-area curve will be repeated until each of the saved sub-areas with these highest pressures has been analyzed. The algorithm starts with one of the sub-areas with high pressure, and then the sub-area expands to a neighbor sub-area that has the highest pressure. The sub-area continuously expands to neighbor sub-areas that have the highest pressure until the whole contact-area is included. Figure 14 and 15 illustrate the Expand-maxima method. The numbers in the figure is the order the sub-area is expanding. Square 1 represents the area with the highest pressure. Square 2 has a higher pressure than square 3, and it continuously expand to square 6 where the pressure also is high. This method continues to expand to neighbor sub-area until all the pressures on contact-area are included. It has been developed to variants of this method, one that gives irregular shaped sub-areas, and one that constrains the sub-areas to be rectangular shaped. This is done by summing the sub-areas one each side of the sub-area and then expand to the side with the largest average pressure, and it continues to expand to the side with largest average pressure until the total pressure in the contact-area is included.

Figure 16 shows 5 possible starting sub-areas for the Expand-maxima method. The spatial pressure-area curve for different starting sub-area, will give slightly different curves since the pressure field around the high pressure zone will vary. The highest value for each sub-area size between the SPACs plotted from the 5 different starting sub-areas will be used and plotted. The search-pattern for the irregular shaped variant has also been given two options, one that search for all 9 directions, and one that search for only 4 directions(right, left, up and down). Figure 17 visualize the search-pattern.

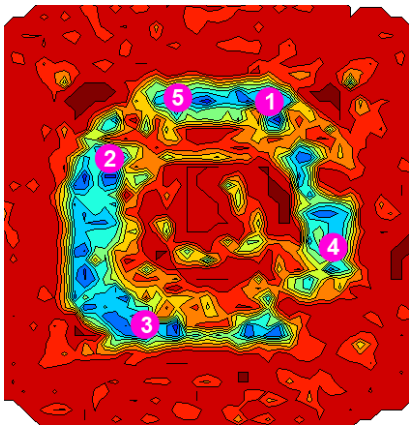

Figure 16 - High pressure zones, starting location

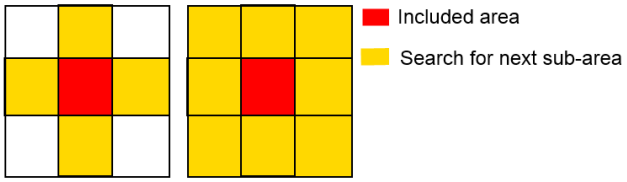

Figure 17 - Search pattern, (left) 4 directions, (right) 9 directions.

The search pattern with 4 directions is the active one in the script, since it gives more compact areas.

Iterative-search method is a method that starts with a small sub-area and steps the sub-area through every possible location on the plate, and obtains the pressure on each location. The algorithm than saves the pressure and position of the sub-area that gave the highest pressure. Thereafter the sub-area increases with one sub-area to the left, and the same stepping procedure is performed. The sub-area continuous to expand to the left until width vs. height ratio reaches 3. Then the sub-area expands downwards, and the width of the sub-area reduces to same width as the first sub-area. The same procedure as above continues until every possible sub-area shape and size is stepped through the plate. It is also a constraint of height vs. width ratio, which should not exceed 3. Therefore the acceptable sub-area shapes in this method will be all rectangular shapes that fulfill the width vs. height ratio 1:3 and 3:1.The position on the plate where the various sub-areas has theirs highest pressure will be included in the spatial pressure area curve. For all the sub-areas with equal size, only the sub-area with the highest pressure will be included in the SPAC.

The shape limitations mention above; rectangular shaped with width vs. height ratio 1:3 and 3:1 is given because of in structural design the framing and spacing in structures is usually rectangular shaped. The ratio limitations are implemented since the iceberg most probably will not have high pressure zones exceeding the ratio limit. Also larger ratios are normally not that critical due to the structural design of maritime and offshore structures. The stepping process for all the different sub-areas makes this method very CPU-consuming, and limiting the number of possible sub-areas will reduce the CPU-time drastically. Still with this limitation above, the method still require a lot of CPU-time. Anyway this method is very useful in structural design of local pressures, since it gives sub-areas that are reasonable easy to handle for structural design, and it is simple to modify. The method will also always choose the sub-area with the largest pressure, which cannot be ensured in the Box-averaging method and Expand-maxima method. Figure 18 below shows the method for a very simple case, where a square is divided up in 4 sub-areas.

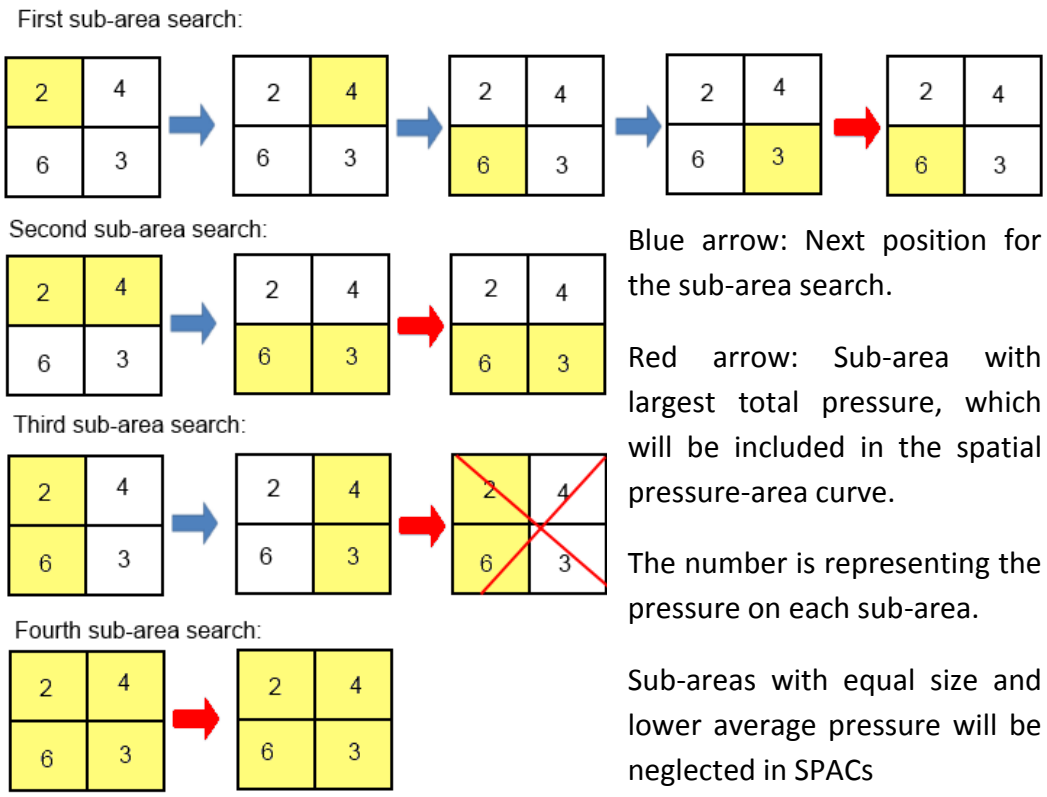

Figure 18 - Iterative-search Method, Illustration

The spatial pressure-area curve gives similarly information as a contour plot, but with this spatial pressure-area curve it is easier to evaluate the results. A contour plot is a 2D plot where the colors represent different value range, and the plot will graphically give the local variation of the investigated value, in this case the pressure. This master thesis will mainly focus on Contour-Averaging Method and the iterative-search method since the method gives the most interesting results. Contour-averaging method gives the amount of each pressure level that exists locally within the contact-area, and the iterative-search method gives interesting results for structural design. Box-averaging method will also be of interest; since it shows how high the pressure level is at the center of contact-area, and how the average pressure level changes with increasing sub-area. The difference between the methods is graphically shown in appendix C. In appendix C spatial pressure-area curves for given time-steps is plotted and how the sub-areas expands is graphically shown, which indicates how the different method works.

There is a link between the process pressure-area curve and the spatial pressure area curves, if the process pressure-area curve is plotted based on the force divided on the actual contact-area instead of the nominal contact-area. Than the end of each spatial pressure-area curve will hit the process pressure-area curve (highlighted with a red dot) , as shown in figure 19. The blue dots are representing the data points from process pressure-area curve based on actual contact-area. The other colored lines representing spatial pressure-are curves for given time-steps, and the upper red line representing the ISO curve mention earlier.

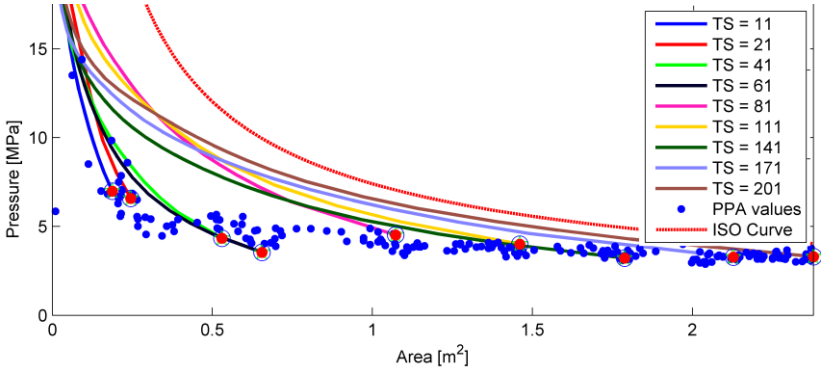

Figure 19 - Link between PPAC and SPACs

5 MATLAB scripts

LS-DYNA is an advanced NLFEM program that gives out a lot of information and all kind of results. Still the LS-DYNA does not present the results that well, and therefore several post-processing scripts have been developed in MATLAB during this master thesis. To be able to perform a good evaluation of the iceberg model to Zhenhui Liu and also suggest possible improvements, it is important to compare results with earlier experiments. In that regard the force and process pressure-area curve is important results. The spatial pressure-area curves have started to get increased interest, due to the importance of accounting for the high pressure zones in local design. It is difficult to obtain the spatial pressure-are curve, and therefore few of earlier experiments have these curves, due to improved equipment over the years some scientists have attempted to obtain such curves. There is also a request for some specific results in the scope of work for his mater thesis, which is the pressure curves mention above, actual vs. nominal area, dissipated energy curves etc. Therefore MATLAB scripts have been developed to post-process out these results mention above, and some other important results for shared-energy design. The results from the share-energy design analysis will be total force vs. relative displacement length to each object, and internal energy curves.

5.1 Overview and output from MATLAB scripts

The MATLAB scripts produce many results. Below a MATLAB overview chart is given where all the scripts name and what output they produces is given:

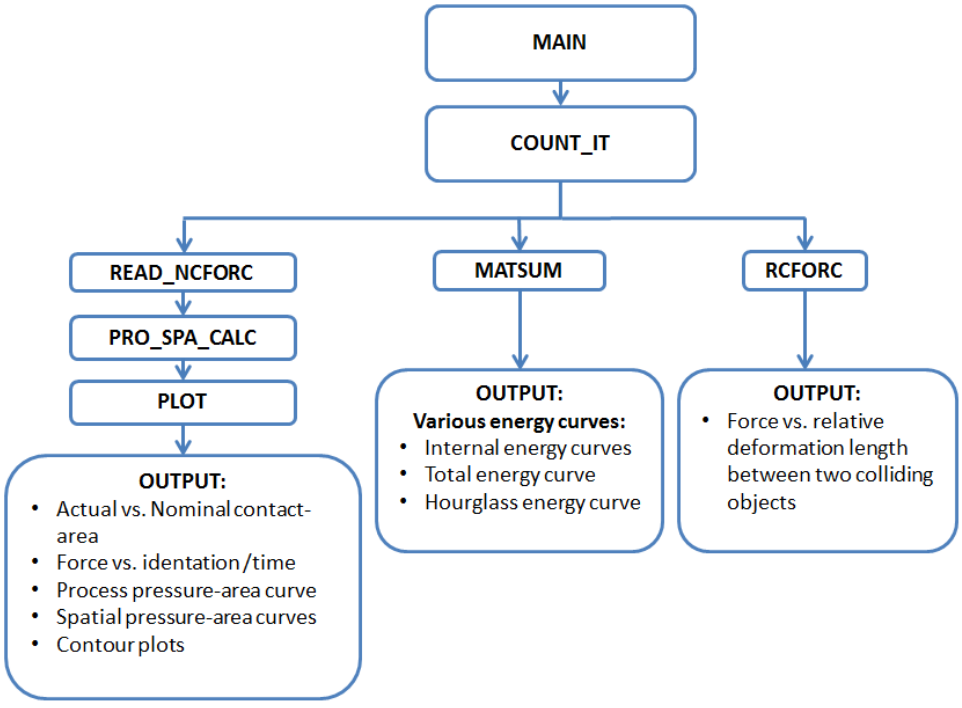

Figure 20 – MATALB overview chart

The MATLAB scripts make use of 3 output files from LS-DYNA, which is the “NCFORC”, “MATSUM” and “RCFORC” files. And below will a brief description of these MATLAB scripts be given:

MAIN and COUNT_IT

MAIN script only runs all the scripts in correct order and the CONT_IT script uses “NCFORC” output file and count the number of nodes and time-steps that the analysis has created. The amount of nodes and time-steps is important input to the other MATLAB scripts. Both MAIN and COUN_IT scripts can be found in appendix B.

READ_NCFORC and PLOT

The READ_NCFORC script simply reads in the large “NCFORC” output file, and the PLOT script plots various plots by using the matrices created in the PRO_SPA_CALC script. How the “NCFORC” output file is read can be view in appendix B.

PRO_SPA_CALC

It post-processes and calculates the values and matrices needed to plot the output given in figure 20. To understand the code it is important to understand the “NCFORC” file. The file contains the coordinates, component forces (x-, y- and z-direction), pressure at each node for a given time-step. First part of the script calculates values and matrices need to plot actual vs. nominal contact-area, force vs. indentation length and the process pressure-area curve. For detailed description on how the calculation is done can be view by looking at the MATLAB scripts in appendix B. The second part of the script shows how the 5 SPAC methods are mathematically obtained. A good description of each method is given in chapter 4.4, but a more mathematically description can be seen in the MATLAB scripts in appendix B.

MATSUM

The MATSUM script is more straight-forward. The output file from LS-DYNA contains energy values for the internal-, kinetic-, total-, and hourglass-energy, which this script reads and then produces a few energy verses time plots. In this script also relative strength between the structure and the iceberg is plotted, by plotting the total internal energy of the iceberg and the structure against each other. This MATLAB script is also given in appendix B.

RCFORCE

This script uses the “RCFORC” file and some graphs that can be obtained from the LS-PrePost program. From that program the nodes with largest displacement after the impact can be chosen. Then the displacement of the chosen nodes can be plotted against the time. The total force, displacement for the chosen nodes and the speed of the iceberg is now known. This makes it possible to obtain the crushing distance of the iceberg by the following equation (5.1):

$$\delta_{ice} = \delta_{pusher} - \delta_{plate} \tag{5.1}$$

where, δ_{ice} = erosion/crushing distance of iceberg

δ_{pusher} = displacment of the rigid plate that pushes the ice

δ_{plate} = displacement of the chosen nodes on the deformable plate

Then can the relative strength between the structure and the iceberg can be measured by plotting the total force vs. relative displacement (the displacement of the plate vs. the crushing distance). This script can also be viewed in appendix B.

6 Impact design methods

Impact analyses are usually separated into external and internal mechanics. The external part refers to the translational and the rotational momentum and energy balance. The internal part refers to the local deformation of the objects that are in interacting in the collision. The external mechanics gives the demand for energy dissipation, which gives a good indication on the total damage output of the collision. The demand of dissipation is determined by calculating the kinetic energy before and after the collision. Those two objects have a given total kinetic energy before and after the collision, and the loss of kinetic energy after the collision has to be dissipated as strain energy during the impact. In this master thesis only the internal mechanics will be considered by an integrated analysis. The reason is that in this master thesis the main goal is to evaluate and improve the iceberg model, where the demand of energy is less important since there is no design requirement to look at. Therefore an arbitrary iceberg collision is being analyzed and the demand of energy is less important.

When considering the distribution of energy dissipation, the design principles can be divided into three different designs given by NORSOK [23], and shown in the figure 21 below.

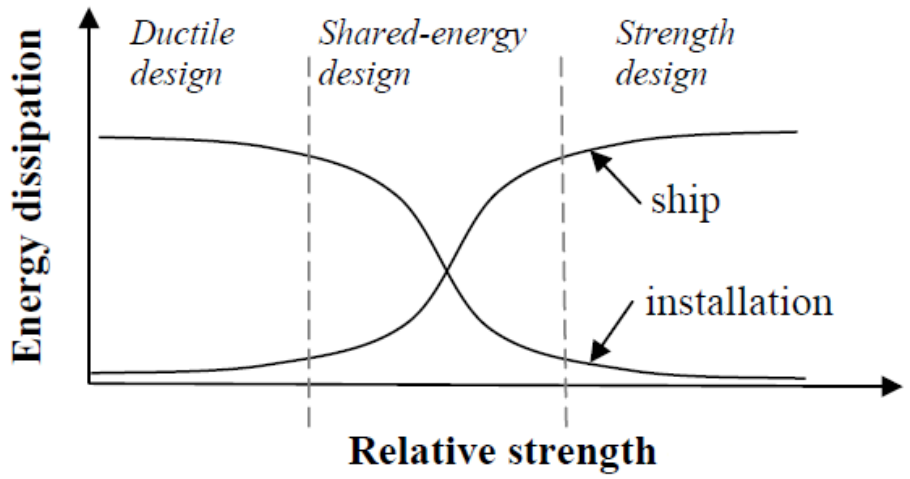

Figure 21 - Energy dissipation for strength, ductile and shared-energy design, [23].

Strength design implies the structure that is being analyzed is strong enough to withstand the collision, which means that the object colliding into the structure is taking the most of the demanded strain energy. While the ductile design is the opposite, in this design the structure is taking most of the demanded strain energy and the object is strong enough to withstand the collision. The last design principle is the share-energy design, which implies that both structure and the object contribute considerably to the energy dissipation. In the master thesis strength design and share-energy design will be analyzed.

The strength design is favorable for analyzing pressures, since the analysis will be much less complex, and obtaining pressure during the impact is easier. If share-energy design is used the dissipation of energy in the structure will give reduction in the pressure-area curves, which will make the results more complex to analyses. When studying energy dissipation and other energy-term, share-energy design is preferable, since strength design produces too conservative results. Still for strength design the energy dissipation gives some indication on how strong the iceberg model is during the impact.

The energy dissipation is of large importance for colliding objects, since the energy dissipation gives the produced strain energy in collision. Therefore it is a good indicator of how much structural damage the object has been given after the collision. For share-energy design the distribution of energy dissipation between the colliding objects is highly relevant. In figure 22 load-deformation curves for strength design and share-energy design is shown.

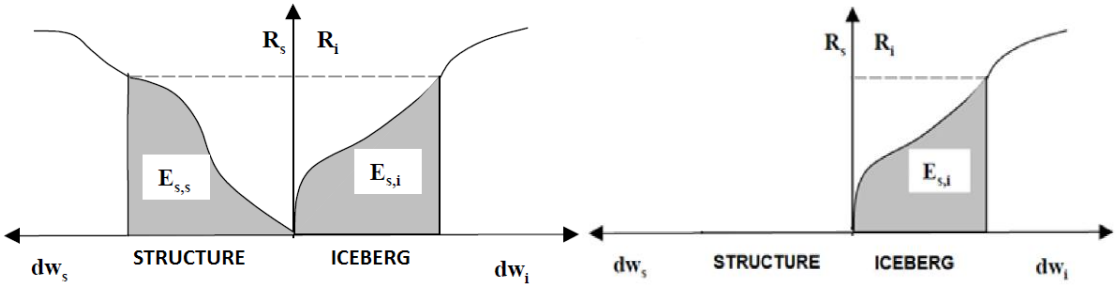

Figure 22 - Load-deformation curves, (a) share-energy design, (b) strength design, [23].

The load-deformation curve gives the strain energy by integrating the force over indentation length as given in NORSOK [23], and equation (6.1) below:

$$E_S = E_{S,S} + E_{S,i} = \int_0^{W_{S,max}} R_i dw_i \tag{6.1}$$

7 Applied Software

The following three programs have been used to setup the analysis in this master thesis:

1 MSC PATRAN
2 LS-PrePost
3 LS-DYNA

MSC PATRAN was used to construct the different parts, and the reason for using MSC PATRAN is due to the powerful modeling tools it contains. LS-PrePost was used to set up the whole analysis. That includes; Material choice, boundary condition, initial velocity, etc. More details regarding the setup are given in chapter 8.1.4. LS-DYNA is the nonlinear finite element program that simulates and solves the analysis.

MSC PATRAN

MSC PATRAN is one of the most widely used pre/post-processing software for finite element analysis. It provides solid modeling, meshing, analysis setup and post-processing for multiple solvers, [2], where LS-DYNA is one of them. The software contains many advanced modeling tools, which makes the modeling of complex part easier. MSC PATRAN also provides powerful meshing tools, which made construction of the models much more efficient. The software was used to construct the different parts and give them a suitable mesh.

LS-PrePost

LS-PrePost is an advanced pre/post-processing software that is delivered by Livermore software Technology Corporation. This software has a very efficient interface, which made it easy to establish the setup for the analysis. LS-PrePost was used to setup all the pre-processing configurations except the construction of the part and meshing.

LS-DYNA

LS-DYNA is a general nonlinear program that uses explicit time integration to solve the analysis. LS-DYNA included all three nonlinearities, which are nonlinear boundary condition effects, nonlinear geometric effects and nonlinear material effects. Since the program solve the problem explicit, the program is especially design to solve analysis of high velocity and short duration where inertial forces is important, [20]. Information and theory about nonlinear finite element method can either be found in LS-DYNA theory manual online, or short introduction is given in appendix E.

8 Integrated analysis of iceberg impacts

Two types of analysis have been carried out during this master thesis. These two types are strength design and share-energy design, and these design methods are described in chapter 6 and now the setup of these two analyses will be given.

8.1 Strength design analysis

8.1.1 Case overview

The analysis has two main parts, i.e. the rigid plate and the solid object. The plate is representing a shipside, and the solid object is representing a part of the iceberg. The iceberg part is push with a constant velocity against the plate by a rigid plate pusher, which is shown in figure 23. The analysis stops after a chosen time. During the analysis the iceberg deforms and elements erode after reaching the failure criterion. All the specifics about the integrated analysis will be given in this chapter, starting with the modeling of the two objects.

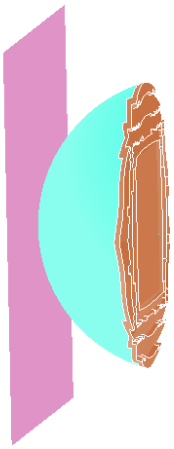

Figure 23 - Overview of the analysis

The nonlinear finite element analysis includes two models, and the iceberg model is built up by two parts. There are a lot of options that need consideration for obtaining accurate results in the analysis. Some of the key modeling choices for each model will be given below. In the analysis there have only been used linear elements, since higher order element is not suited in NLFEA. The reason is that higher order elements yield higher maximum frequencies. This also makes the analysis very efficient even with relative small element size in the models.

8.1.2 Iceberg model

The iceberg model is divided into two parts, one part represents the deformable ice and the other represents a rigid plate that pushes the ice during the analysis. The model has the geometry as a segment of a sphere, and the model is graphically shown in figure 24 and 25. The geometrical lengths of the iceberg model are given in table 1:

Length	Values [m]
Sphere radius	1.50
Sagitta length	1.05-1.15
Chord length	2.85-2.90

Table 1 - Geometry; iceberg model

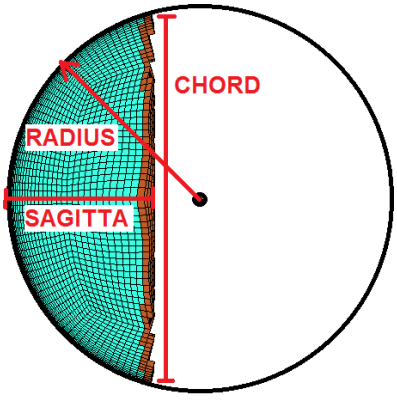

Figure 24 - Length definitions

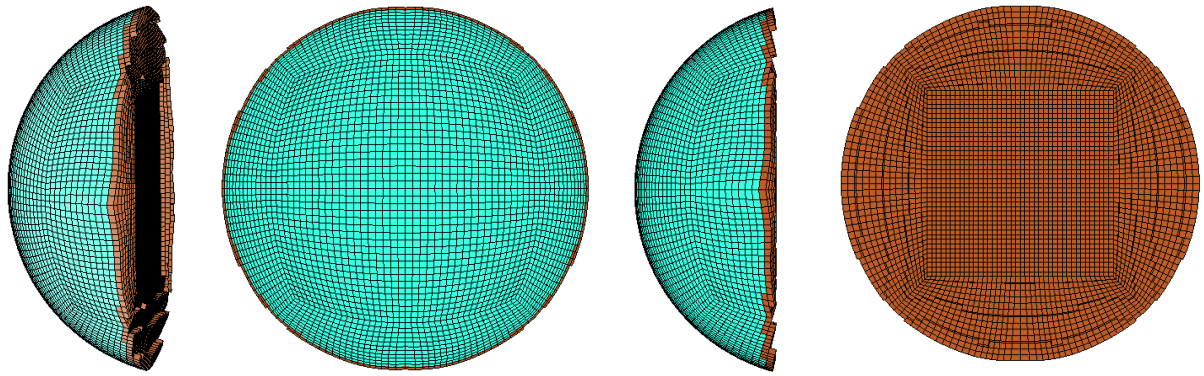

Figure 25 - Iceberg model, standard, front, side, back view respectively

The iceberg model was created by using the tool "Creating a Solid Sphere and Hex mesh" in MSC PATRAN, which is one of many powerful modeling tools MSC PATRAN offers. What it does is to create cubic box, than put deformed cubic elements around the cubic box in layers to make a sphere. The length of each cubic core side is 0.75 [m]. The discretization gives small cubic elements were the element size is important. Zhenhui Liu has made some efforts into investigating the optimal element size for the iceberg model, which is documented in his doctoral thesis, [18]. The optimal element size due to accuracy and CPU-time was concluded to be $50x50[mm]$. In this master thesis $50x50[mm]$ mesh-size is used. However the mesh-size has been varied between $25x25[mm]$, $50x50[mm]$ and $100x100[mm]$ in the parametric study to clarify if Zhenhui Liu's conclusion is good. The chosen element type is the 8-node constant stress solid element. This element type makes the analysis very accurate due to the small element size, and still very efficient.

8.1.3 Plate model

The plate model is only build-up of one part. That is a rigid plate, which is representing the shipside. The plate dimension is $4x4[m]$, and the plate thickness is 16 [mm]. The element size has been varied between $25x25[mm]$, $50x50[mm]$ and $100x100[mm]$, to ensure that the result is accurate and still efficient due to CPU-time. The plate has been given the 4 node Belytschko-Tsay shell element type with 5 integration points over the thickness. For more information of the Belytschko-Tsay shell element, see LS-DYNA theory manual [11]. In figure 26 a modeling view of the plate is shown.

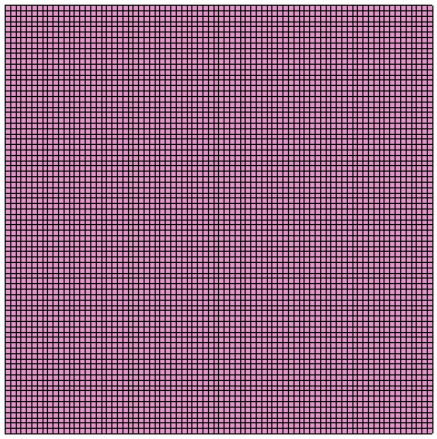

Figure 26 - Plate model 50x50[mm]

8.1.4 Setup (pre-processing)

Applied Materials

LS-DYNA has a large material library, where in this analysis two of the materials are used. The LS-DYNA material manual has a description of all the materials and suggested input for each of the materials [21]. A short summary of the two materials used will be given below, and what values the important input parameters has been given.

MAT_RIGID (20)

Material 20 is a material that makes the part rigid, and is therefore a very efficient and useful material to use in this strength design analysis. Material 20 has configurations that give options of how the rigid part may be constrained in both the translational and rotational directions. This makes it easy and efficient to add boundary conditions to the analysis. This material 20 is applied in two parts of the analysis. The plate in the analysis has this material property, which represents the shipside. The ice pusher plate in the analysis also has the same material property. The ice pusher plate is located at the back of the iceberg model, and represents the connection between the iceberg tip and the rest of the iceberg. In table 2 the input of the material properties is given for both the plate representing the shipside, and the plate which pushes the iceberg model.

	Density [kg/m^3]	E-modulus [MPa]	Poisson's ratio [-]
Plate	7890	210 000	0.3
Ice pusher	900	9500	0.3

Table 2 - Material input; rigid plate

MAT_USER_DEFINED (41)

A user defined material has been developed by Zhenhui Liu. This user defined material created in LS-DYNA should give the iceberg model reasonable material properties during impacts. This should make the iceberg model produce load levels as an actually iceberg. The theory about the material is given in chapter 3, and the material inputs are given in table 3. Before the parametric study in chapter 10, this strength design analysis was performed for 4 times with different input of material constants. The values given to these material constants have been obtained from earlier experiments, and are also given in table 3.

	Density [kg/m^3]	E-modulus [MPa]	Poisson's ratio [-]
	900	9500	0.3
	Bulk modulus [MPa]	Shear modulus [MPa]	E_0 [-]
	7916.6	3653.8	0.01
Analysis with different material constants:	Material constants		
	a_0 [MPa^2]	a_1 [MPa]	a_2 [-]
Derradji-Aouat (2000)	22.930	2.06	-0.023
Kierkegaard (1993)	2.588	8.63	-0.163
Riska and Frederking Data set 1 (1987)	1.600	4.26	-0.62
Riska and Frederking Data set 2 (1987)	3.100	9.20	-0.83

Table 3 - Material input; iceberg model

Initial and boundary conditions

*Initial condition

The iceberg model is set to have an initial velocity. This is important since the early acceleration of the body may give the iceberg model some initial stress levels that should not occur. The initial velocity of the iceberg is set to 2[m/s] in the x-direction.

*Boundary conditions

Two parts have boundaries or so called constraints in the analysis. That is the rigid plate and the rigid ice pusher. The rigid plate has constraints in all translational and rotational directions. The rigid ice pusher has the same constraints, except it is allowed to move in x-direction. A prescribed displacement curve has also been created. The curve is linear and will represent a constant velocity of 2[m/s]. Then a *PRESCREBED_MOTION_SET is made where the curve is added to a node in the ice pusher part to create the constant velocity to the iceberg model.

*Contact

The analysis was defined with two contacts:

1) *CONTACT_ERODING_SURFACE_TO_SURFACE
2) *CONTACT_ERODING_SINGLE_SURFACE

The first contact creates the contact between the plate and the ice. The second contact creates the self-contact, which will be needed due ice crushing. Configuration of the contact also decides Master-Slave part in the analysis, and which part that should be included in the results. The contact configurations have many options. One of them is the static friction coefficient which is set to 0.15, which seems reasonable. Rest of the configurations was mostly set to default.

Duration and time step

***Time step**

Initial time step is set to zero, so that LS-DYNA automatically chooses the most favorable initial time step.

***Termination**

The termination of the analysis is set to 0.4[s] which will give the iceberg an indentation length of about 0.8 [m].

8.2 Shared-energy design analysis

8.2.1 Case overview

This analysis is very similar to the strength design case described above. The only difference is that the rigid plate in the above case is traded out with a panel model which is allowed to deform. A graphical overview of the analysis is given in figure 27.

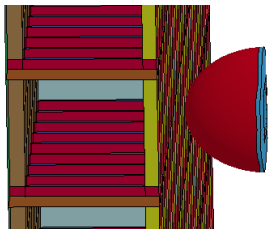

Figure 27 - Share-energy design overview

8.2.2 Iceberg model

The iceberg model for the shared energy design was created in the same matter as in the strength design. For the shared-energy design analysis two different iceberg shapes have been created, and the shapes are displayed in figure 28 below:

Circular shaped iceberg **Circular shaped iceberg scaled 1.5**

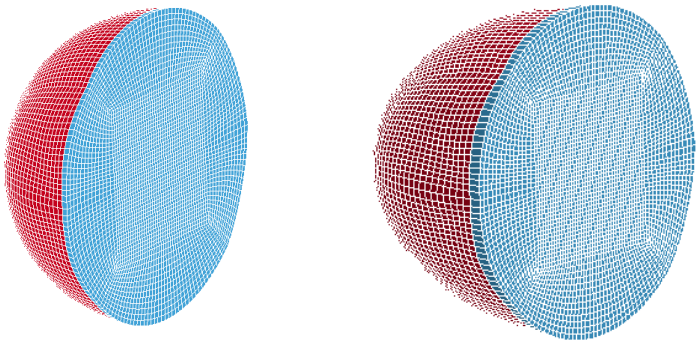

Figure 28 - Iceberg models, shared energy design

Both iceberg shapes have a cubic core side of 0.75 [m]. The iceberg models in the figure above are modeled similarly, but the sharper shaped iceberg has been scaled 1.5 in the direction away from the ice pusher plate. The distance between the ice pusher plate and the tip of the iceberg is 1.4 [m] for the circular shaped model and 2.1 [m] for 1.5 scaled model. Element type is the 8-node constant stress solid element, and the average element-size is

close to $50x50[mm]$. The scaled models will have an increase in element length in same direction as the scaling.

8.2.3 Panel model

The panel models used in this master thesis is provided by Torstein Myhre. Torstein Myhre has created 3 panels with different strength. The panels are very similarly modeled, and a graphical overview of one of the panels is given in figure 29.

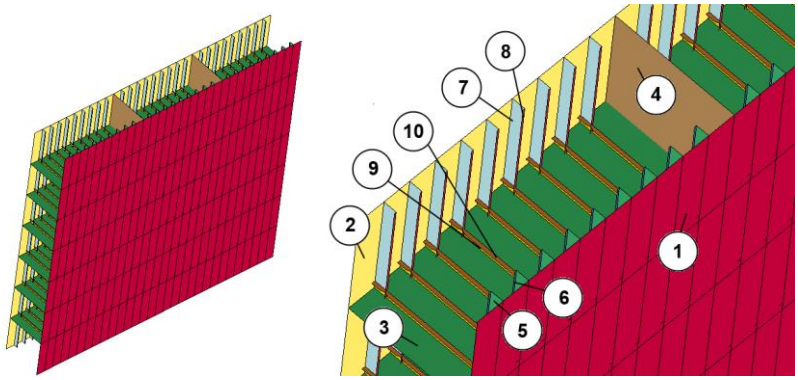

1. Inner hull
2. Outer hull
3. Girder
4. Stringer
5. Inner stiffener web
6. Inner stiffener flange
7. Outer stiffener web
8. Outer stiffener flange
9. Girder stiffener web
10. Girder stiffener flange

Figure 29 - Overview and description of the panel

The main dimension for the different components in these panels is given in table 4:

	Panel 1	Panel 2 (strength level 1)	Panel 3 (strength level 2)
Web frame spacing	3.2 [m]	3.36 [m]	3.36 [m]
Web frame plating thickness	15.5 [mm]	20 [mm]	20 [mm]
Stiffener spacing	0.8 [m]	0.864 [m]	0.864 [m]
Outer stiffener	L370x13/ 53.5x38.4 [mm]	L325x12/ 150x15 [mm]	L450x12/ 150x15 [mm]
Inner stiffener	L370x13/ 53.5x38.4 [mm]	L350x12/ 150x15 [mm]	L350x12/ 150x15 [mm]
Web frame stiffeners	L250x11.5/ 100x15 [mm]	FB200x12 [mm]	FB200x12 [mm]
Outer plate thickness	17 [mm]	21 [mm]	30 [mm]
Inner plate thickness	15 [mm]	18 [mm]	18 [mm]
Stringer spacing	8 [m]	7.8 [m]	7.8 [m]
Stringer plating thickness	12[mm]	12 [mm]	12 [mm]
Size of modeled field	22.4x24 [m]	23.5x23.3 [m]	23.5x23.3 [m]
Distance from inner to outer plating	3.6 [m]	2.41 [m]	2.41 [m]

Table 4 - Panel dimensions

The element type in the panel is 4 node Belyscho-Tsay shell elements with 5 integration points over the thickness. The mesh-size has been given a proper size, were the accuracy and efficiency is well balanced. The panels has in total around 100 000 to 150 000 elements depending on which panel model that are used.

8.2.4 Setup (pre-processing)

The setup is almost the same as for the strength deign analysis. There have been some changes which will be given below.

Applied Materials

POWER_LAW_PLASTICITY (18)

The panel has been given the material "POWER_LAW_PLASTICITY". This material accounts for elasto-plastic behavior with isotropic hardening and is a well-known material in nonlinear finite element programs. The LS-DYNA theory manual [11], explains how the material behaves and which rules it follows. The most important mechanical equations the material type follows will be given below. For further information about the material see the LS-DYNA theory manual [11].

The yield stress, σ_y, is a function of the plastic strain an follows the following equation:

$$\sigma_y = k\varepsilon^n = k\left(\varepsilon_{yp} + \bar{\varepsilon}^p\right)^n \tag{8.1}$$

Where ε_{yp} is the elastic part of the strain and the $\bar{\varepsilon}^p$ is the effective plastic strain. If the initial yield stress is set to a value non-zero and greater than 0.02 which is the case for the analysis conducted in this master thesis, the elastic strain is given by the equation (8.2):

$$\varepsilon_{yp} = \left(\frac{E}{k}\right)^{\left[\frac{1}{n-1}\right]} \tag{8.2}$$

The strain rate is also incorporated by using the Cowper and Symonds model which scales the yield stress with the factor below:

$$1+\left(\frac{\dot{\varepsilon}}{C}\right)^{\frac{1}{p}} \tag{8.3}$$

where $\dot{\varepsilon}$ is the strain rate. The material input values are given in the table 5:

Density [kg/m^3]	Young's Modulus [MPa]	Poisson's [-]	Strength coefficient [MPa]	Hardening exponent [-]	Initial yield stress [MPa]
7890	$2.1 \cdot 10^5$	0.3	740	0.24	275

Table 5 - Steel material properties, input.

Initial and boundary conditions

Since the structure now is allowed to deform boundary conditions have to be given to the structure. The panel has been fixed for translation and rotation in all directions for all nodes that are located at either side on the panel. Figure 30 below shows graphically which nodes that have been constrained. The iceberg is still set to have a 2 [m/s] initial velocity, where the iceberg is also set to have a constant velocity during the whole impact.

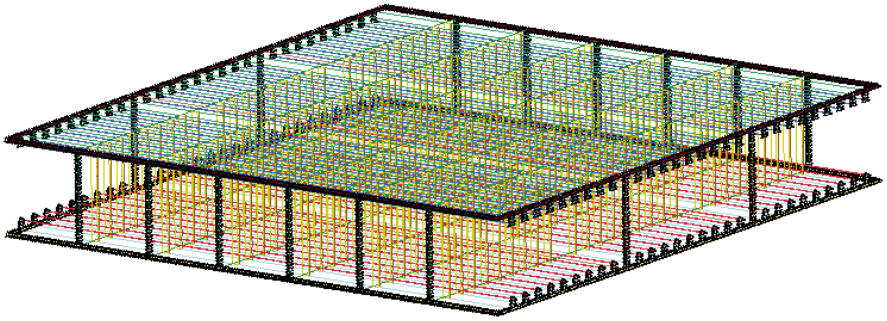

Figure 30 - Boundary conditions

*Contact

There is also a new contact defined in the share energy design analysis, since the analysis now has a deformable panel instead of a rigid plate. The panel is allowed to deform, which makes defining a contact for the panel important. The contact type selected for the panel is *AUTOMATIC_SINGLE_SURFACE, where the static friction coefficient is set to 0.3. Most of the other options are set to default. The two early mention contacts are also included.

Duration and time step

Initial time-step is set to zero, so that LS-DYNA automatically chooses the most favorable initial time-step. The analysis terminates when 0.4 [s] is reached.

9 Short reanalysis of project work

In an earlier project a collision scenario was analyzed. The collision scenario is given in chapter 8.1, and the scenario is an iceberg impact on a rigid plate with a given velocity. The analysis was performed 4 times with different material input; each run had different input for the material constants. These values of the material constants have been obtained from earlier experiments. It will now be given a short preview and a reanalysis of those 4 analyses. Table 6 gives material constants for the 4 different analyses.

Analyses/Cases:	Material constants		
	a_0 [MPa^2]	a_1 [MPa]	a_2 [-]
Derradji-Aouat (2000)	22.930	2.06	-0.023
Kierkegaard (1993)	2.588	8.63	-0.163
Riska and Frederking Data set 1 (1987)	1.600	4.26	-0.62
Riska and Frederking Data set 2 (1987)	3.100	9.20	-0.83

Table 6 - Material constants, from different experiments.

For evaluation of the material model and for finding the most reasonable input values for the iceberg model, the analyses will be compared with the “Pond Inlet 1984” experiment. “Pond Inlet 1984” is a well-performed experiment, which has many similarities to the NLFEA conducted in this master thesis. The most important similarities are the shape and the size of the indentor. There is one large difference between the “Pond Inlet 1984” experiment and the NLFEA, which is that the indentor is rigid and the wall is of ice. The opposite is the case in NLFEA. The differences between using a steel indentor (rigid) against an ice wall and using an ice indentor against a steel wall (rigid) has been investigated in earlier research. Ulan-Kvitberg, Kim and Daley have conducted ramming tests with both scenarios [3], and it appeared that the difference on maximum force during the impact was relative low and quite equal. The ramming tests gave good indication that despite of the differences in the nature of the indentor between the “Pond Inlet 1984” tests and the NLFEA, they still should give relative similar results. This requires an assumption that the ice material in the NLFEA and the “Pond Inlet 1984” tests is similar.

The input values for the material parameters which gives the most similar result as the "Pond Inlet 1984" experiment will be set as initial values for the parametric study performed in chapter 10. The results obtained from the analyses are given below, where the green curves in the figures 31 and 32 representing the obtained results from the "Pond Inlet 1984" experiment.

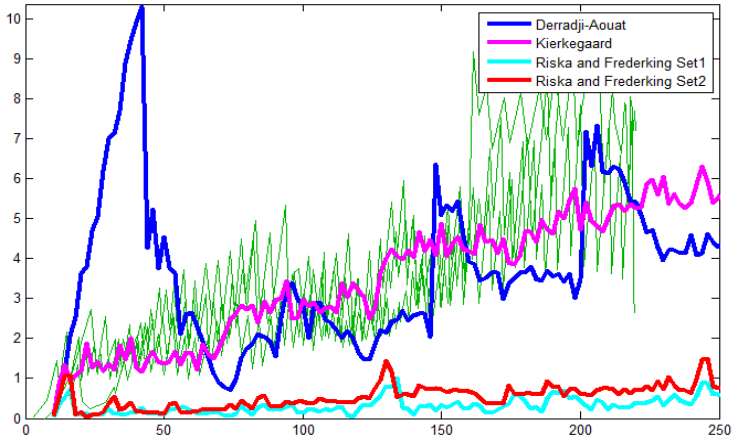

Figure 31 - Force comparison with Pond Inlet tests

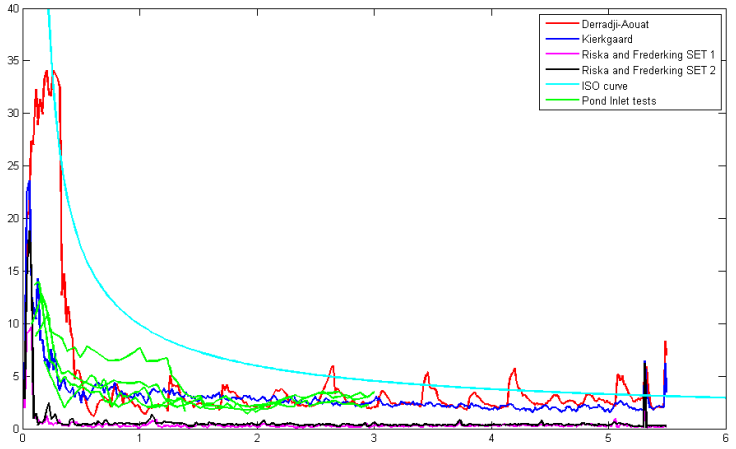

Figure 32 - Process pressure-area curves comparison with Pond Inlet tests

Figure 31 and 32 show that the material model developed by Zhenhui Liu can represent a large range of ice types, and the input parameters has a large influence on the strength of the material model. Figure 31 and 32 clearly indicate that the Riska and Frederking's input of material constants give to low values, which means that the material constants represent very soft ice relative to the other material constants. Derradji-Aouat's input of material constants gives relatively similar results as the "Pond Inlet 1984" tests, but the load and pressure levels is too high at the beginning of the impact compared to "Pond Inlet 1984" tests. The analysis with Kierkegaard's input of material constants gives very similar results as the "Pond Inlet 1984" tests. Also Kierkegaard's material constants give seemingly less random load peaks, which is good. There should definitely be some peaks due to the nature of the crushing process of the ice, but the amplitude produces in analysis with Derradji-Aouat material constants seems to be too high. Some of the reason is most probably due to a numerical error.

Based on the above results (figure 31 and 32) the Kierkegaard's material constants give the most reasonable results. Both the force and the process pressure-area curves from the analysis are very similar to what curves that were obtained in the "Pond Inlet 1984" experiment. The initial values of the material constants in the parametric study given in chapter 10 will therefore be set to the same values as what Kierkegaard obtained. The ice material is known to have varying material properties and strength for different arctic regions, due to the fact that the material properties depend on so many factors. Therefore it do not exists one set of input parameters that can represent all the different icebergs that exists in the different arctic regions. However the iceberg used in the "Pond Inlet 1984" tests is assumed in this master thesis to represent a relative strong and general iceberg that can be encountered in several arctic regions.

The remaining figure in this chapter (figure 33 to 38) will be results obtained from the analysis performed with Kierkegaard's material constants. Figure 33 below shows the SPACs for 9 different time-steps. The curves below are plotted by contour-averaging method. The time-step numbers are given in the figure, and the end of each line shows what the total actual area is for the given time-step (highlighted with red dot).

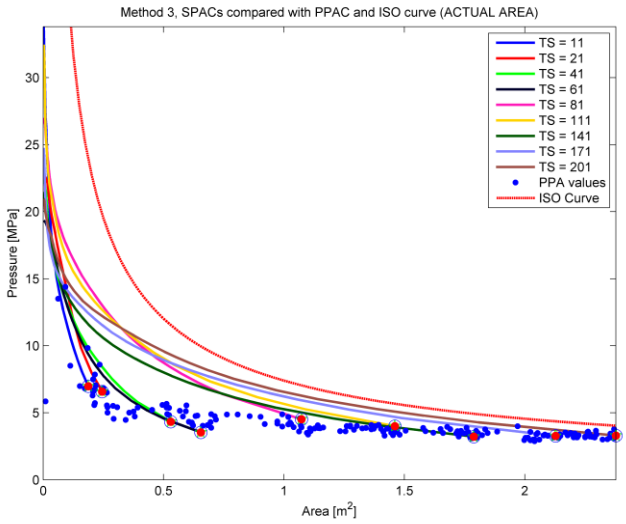

Figure 33 – SPACs, Contour-averaging method (Kierkegaard's MC)

It is interesting to see how little the maximum pressure in the high pressure zones changes, which can be seen by looking at the different SPACs for different time-steps at the smallest areas. From figure 33 it shows that the maximum pressure in the high pressure zones and that the pressure contours is relative similar for all 9 time-steps chosen. This indicates that the local pressure and pressure contours behaves relative similar for the whole duration of the impact.

Figure 34 below shows the SPACs from Kierkegaard's material constants analysis for 9 different time-steps. Here the curves in the left figure are plotted by box-averaging method, and the curves in the right figure are plotted by iterative-search method.

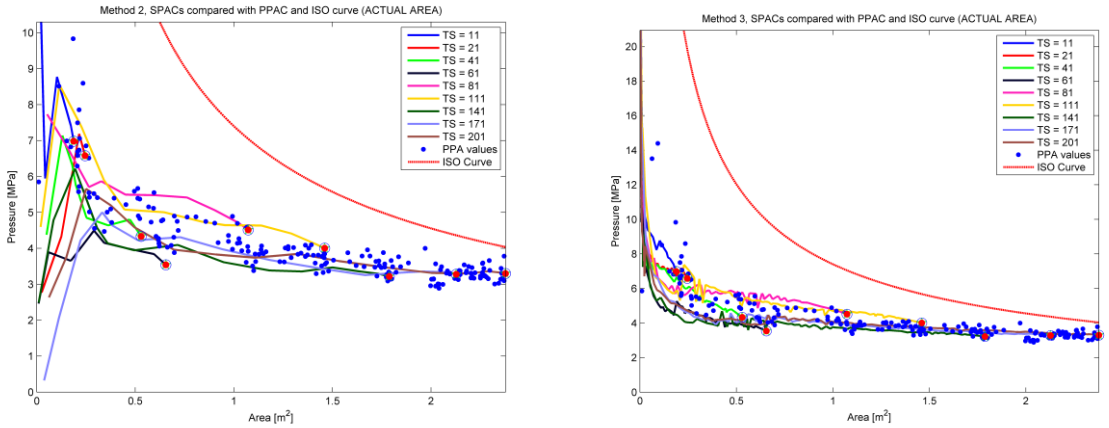

Figure 34 - SPACs, (left) Box-averaging method, (right) Iterative-search method (Kierkegaard's MC)

Figure 34 shows some concerning results. From literature the icebergs shall have increasing confinement near the center of contact-area, which also is mentioned in chapter 3. Figure 34 disagrees with that by having very low pressure field and few high pressure zones in the center of the contact-area. Comparison of figure 33 and 34 makes it even clearer. The comparison of these figures does also indicate that the high pressure zones are of small area size and has large spread within the nominal contact-area. This is seen by comparing how fast the SPACs reduce for increasing area size between iterative-search method and contour-averaging method.

Below the total force and process pressure-area curve is given verses both the indentation length and time:

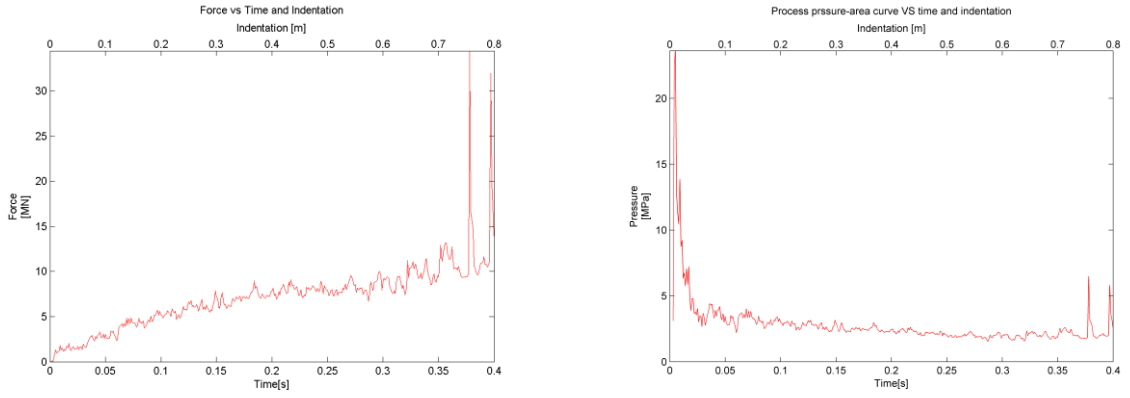

Figure 35 - (right) force curve, (left) Process pressure-area curve (Kierkegaard's MC)

Figure 35 gives the total force and the total pressure over the contact-area for the whole duration of the impact.

From the analysis the area-ratio between actual contact-area and nominal contact-area was obtained, and some very interesting results has been revealed (see figure 36).

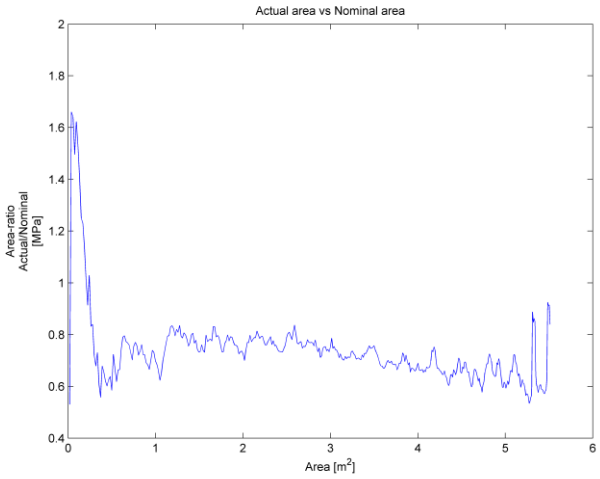

Figure 36 - Area-ratio curve (Kierkegaard's MC)

Due to the complex crushing process which occurs during the impact a lower actual contact-area than nominal contact-area is predicted. The material model is strain rate independent, and iceberg collision is assumed to have strain rate above the transition between ductile and brittle failure mode. Still figure 36 shows that there is some deformation in the material model in the beginning before element is crushed or eroded away. This is shown by having an actual contact-area larger than the nominal contact-area at the beginning of impact. When elements start to erode the actual contact-area reduces to about 80 percent of the nominal contact-area, and it kept around that level for the remaining time of the impact duration. A 20 percent difference is a relative large percentage. It is unknown how low the actual contact-area should be. However that the actual contact-area is less than the nominal contact-area seems reasonable due to the effect of ice crushing, where damaged layer, flakes, spalls, horizontal splits and cleavage cracks takes place for real icebergs.

The contour plots in figure 37 confirm the same as figure 34, that there is too low pressure in the center of contact-area. Figure 37 shows very clearly how the elements erode. The elements erode in layers, especially in the center of contact-area. This layer effect produces this low pressure zone at the center and lack of high pressure zones in the center of contact-area for most of the time-steps in the impact scenario.

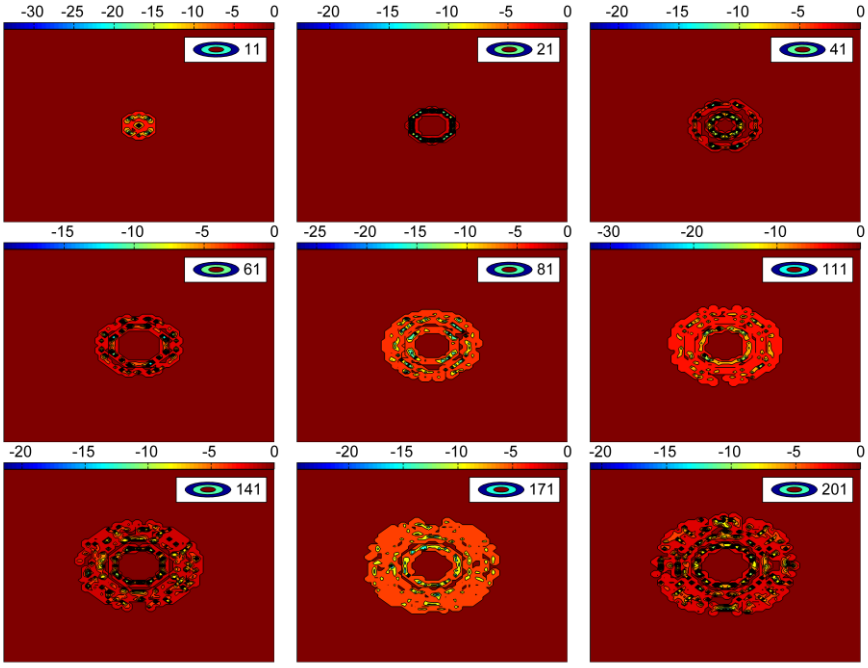

Figure 37 - Contour plots (Kierkegaard's MC)

Plotting the internal energy vs. time gives the amount of ice damage that is produced. The internal energy is in the iceberg model divided up into two parts; internal energy of intact/deformed elements and internal energy of eroded elements. In figure 38 the internal energy of intact/deformed elements and hourglass energy are plotted. The hourglass energy gives an indication of how much energy that are produced due to spurious modes, that is nonphysical, zero-energy modes of deformation that produce zero strain and zero stress. Hourglass energy should be as small as possible; a rule of thumb is that the hourglass energy should be less than 10 percent of the internal energy. This rule does not quite apply to this model, since the elements are eroded before significant deformation takes place. This makes the internal energy for intact/deformed elements in the ice material very low. This can be confirmed by looking at figure 38 below.

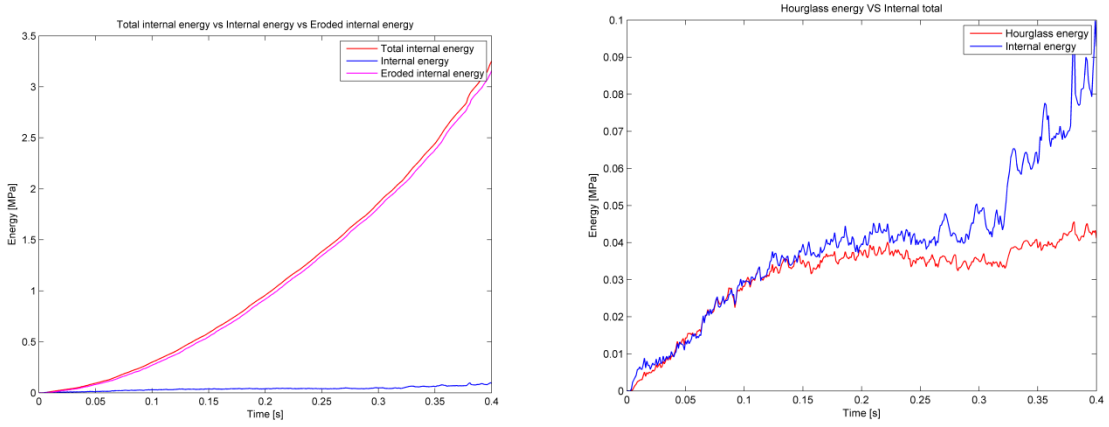

Figure 38 - (left) Internal energies, (right) intact/deformed Internal energy vs. hourglass energy

10 Parametrical study of the iceberg model

A parametric study is very efficient method for evaluating the importance of each parameter in the material model of the iceberg. Table 7 gives an overview of which parameters that is included in the parametric study, and what parametric change each parameter has been given:

Parametric variation overview					
	reduction in percent	Decreased or changed to	Kierkegaard values	Increased or changed to	increase in percent
Material constant 1	30 %	1.8116	2.588	3.3644	30 %
Material constant 2	30 %	6.041	8.630	11.219	30 %
Material constant 3	30 %	-0.1141	-0.163	-0.2119	30 %
Initial failure	100%	0.0001	0.01	0.03	200%
Mesh size	50%	25 [mm]	50 [mm]	100 [mm]	100%

Table 7 - Overview of the parametric study

It was also attempted to vary the E-modulus and develop different failure curve shapes. The result from changing the shape of the failure curve gave unphysical results; the load level and the process pressure-area curve were no longer comparable to the “Pond Inlet 1984” experiments. Therefore the purely empirical strain failure curve developed by Zhenhui Liu (see chapter 3) will be used in all the analyses, and it will be assumed to be the most fitting failure curve to use for the current iceberg model. The results from changing the E-modulus gave often peculiar results, and were therefore excluded from the parametric study. The parametric study will be evaluated by discussing the change in the following results:

- Force vs. time
- PPAC vs. time
- SPAC for specific time-steps
- Energy vs. time
- Contour plots

The results are obtained by the MATLAB scripts which were developed during this master thesis. It reads the “NCFORC” and “MATSUM” files that LS-DYNA produces, and does some post-processing calculations to obtain the results mention above. The spatial pressure-area curves are plotted for some specific time-steps, and the chosen time-steps are given in table 8.

SPACs number	1	2	3	4	5	6	7	8	9
Chosen time-step	11	21	41	61	81	111	141	171	201
Time [s]	0.01	0.02	0.04	0.06	0.08	0.11	0.14	0.17	0.2
Indentation length [m]	0.02	0.04	0.08	0.12	0.16	0.22	0.28	0.34	0.4

Table 8 - Time-step chosen for SPACs

The interval length between each time-steps increases for increasing time-step number. The reason is because the process pressure-area curve has relative high pressure peak at the beginning of impact, but relatively fast converges to a value around 1.48 [MPa]. It will also be important to investigate the load level differences between the analyses for each time-step. The load level difference can be divided up in two parts. One part will be the overall increase of the force due to the parametric change. Second part will be the coincidence of a time-step hitting one of many load peaks that exist during the impact, which will give a considerable contribution to the load level. These load peaks exist due to the complexity of the ice crushing process, and there is also a numerical effect which occurs. These load peaks have to be accounted for when comparing the analyses.

It has been plotted to types of force curves. One force curve that gives actual values (normal curve), where pressure peaks exists. The other force curve (smooth curve) uses an averaging method, which will reduce the peaks significantly. This curve shows more how the overall force changes with time. The smoothing works such that every point is an average of the 50th closest points on the actual curve. Table 9 below shows the difference in force between the normal curve and the smooth curve. A large value for a given time-step indicates that the analysis has a force peak at or very close to that time-step, which must be taken into consideration when comparing the different analyses.

	Normal curve vs. smooth curve (actual force – averaging value) [MN]								
ANALYSES	TS 11	TS 21	TS 41	TS 61	TS 81	TS 111	TS 141	TS 171	TS 201
ICE1-Kierk	0.19	0.10	-0.11	-1.18	0.50	0.45	-0.45	-0.06	0.11
K-C1-H	0.12	0.10	-0.01	-1.13	0.34	0.17	-0.63	0.26	0.13
K-C1-L	0.14	-0.06	0.03	-0.91	0.63	-0.03	-0.39	-0.31	-0.08
K-C2-H	0.34	-0.04	0.12	-1.07	0.35	0.01	0.25	-0.71	0.35
K-C2-L	0.00	-0.09	0.09	-0.35	0.16	0.21	-0.32	-0.05	0.40
K-C3-H	0.18	0.25	0.07	-0.63	0.14	0.03	-0.26	-0.40	0.43
K-C3-L	-0.14	0.58	0.13	-1.04	0.73	0.57	-0.61	-0.44	0.07
K-inif-H	2.27	0.31	-0.09	-0.76	0.62	-0.31	-1.21	0.07	0.05
K-inif-L	0.12	-0.06	0.22	-0.76	0.42	-0.01	-0.66	-0.05	0.39
ICE100K	0.39	0.82	0.48	-0.97	-0.81	-0.55	0.72	-0.31	1.71
ICE25K	0.06	0.36	0.00	-0.21	0.60	0.33	0.11	-0.01	0.40

Table 9 - Parametric force differences, TS = time-step number

A more complete description of what the different names of the analyses means in the parametric study (given in tables and figures) are listed below:

- KIERKEGAARD's input values = ICE1-Kierk
- Material constants 1 (A0) HIGH (30% increase) = K_C1_H
- Material constants 1 (A0) LOW (30% decrease) = K_C1_L
- Material constants 2 (A1) HIGH (30% increase) = K_C2_H
- Material constants 2 (A1) LOW (30% decrease) = K_C2_L
- Material constants 3 (A2) HIGH (30% increase) = K_C3_H
- Material constants 3 (A2) LOW (30% decrease) = K_C3_L
- Initial failure strain HIGH (30% increase) = K-inif-H
- Initial failure strain LOW (30% decrease) = K-inif-L
- Mesh-size 100[mm] = ICE100K
- Mesh-size 25[mm] = ICE25K

To evaluate the sensitivity in force due to the parametric change, there are some choices to be made. The first choice was to simply choose specific time-step to use for the evaluation. This will give the same scenario for all analyses, which means same nominal contact-area, indentation length, etc. To have the same scenario is essential to evaluate the results from the parametric study. This will lead to neglecting the most critical time-step for each analysis, which is at the positive force peaks. The main goal in this parametric study is to see how much each parameter affects the results, not investigate how critical each analysis is. Since the force level is low at the beginning and affected by the boundary conditions and mesh construction at the end of the impact (see chapter 8). Therefore the most reasonable time-steps to compare the force level will be some time-steps at the middle of the impact scenario. The time-steps number 101 and 201 are chosen. The effects on the force due to the parametric change can be evaluated by looking at table 10 and the force curves in figure 39 and 40. Table 10 shows the force difference in percentage between the initial analysis (no parametric change) and the other analysis in the parametric study. The force difference in percentage is given for both the normal and smooth curve. The smooth curve is now an average of the 50 closest points.

Analysis	Increase in Percentage [%]			
	NORMAL		SMOOTH	
	TS 100	TS 201	TS 100	TS 201
ICE1-Kierk	0.0	0.0	0.0	0.0
K-C1-H	-3.4	2.1	1.0	1.8
K-C1-L	-5.9	-3.9	-1.4	-1.5
K-C2-H	14.9	29.7	23.3	27.0
K-C2-L	-28.2	-26.3	-28.0	-30.4
K-C3-H	-22.8	-23.5	-26.0	-28.0
K-C3-L	29.3	40.8	36.0	41.8
K-inif-H	25.9	16.8	18.4	17.7
K-inif-L	-11.1	-6.1	-8.8	-9.8
ICE100K	13.7	32.9	15.6	12.6
ICE25K	-8.5	3.5	-4.6	-0.3

Table 10 - Forces difference at TS100 and TS201, TS = time-step number

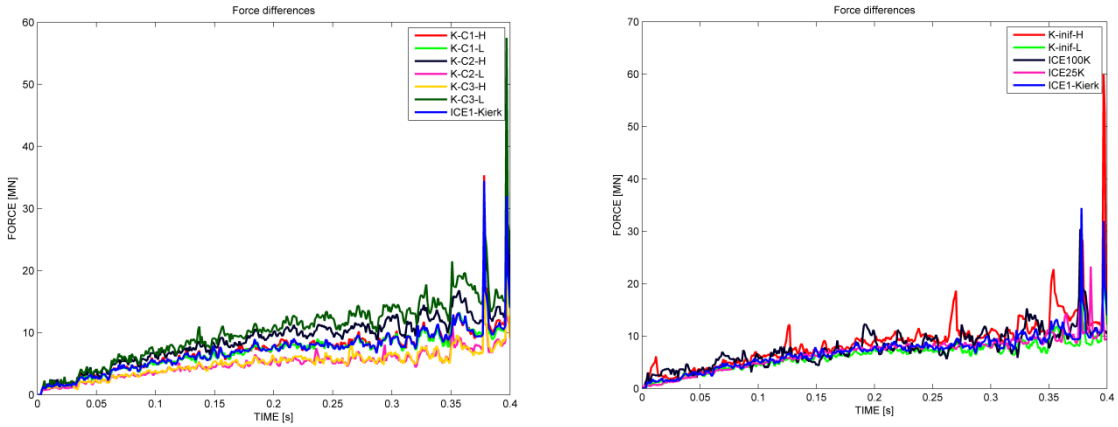

Figure 39 - Force differences (normal curve), parametric study.

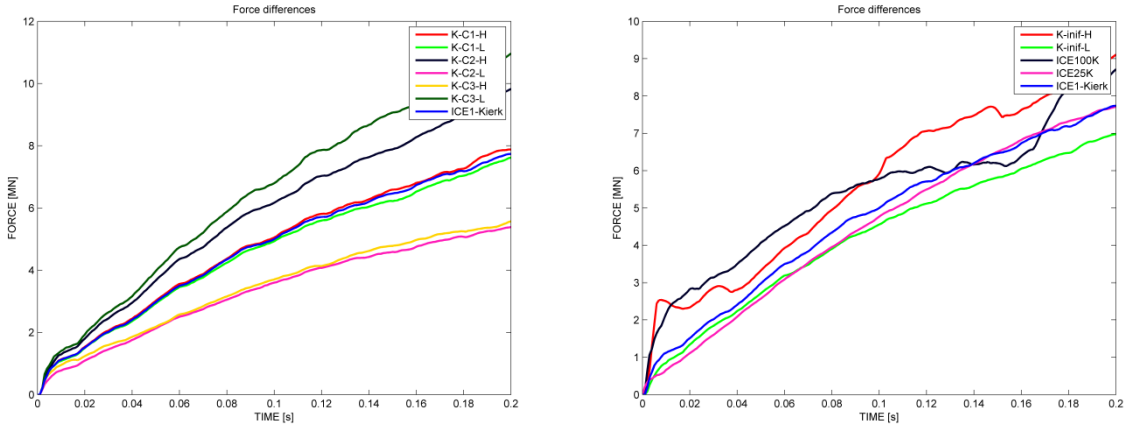

Figure 40 - Force differences (smooth curve), 50th closest points averaged

The smooth curves in figures above will be used to evaluate the effect on the overall force level due to a parametric change. This is because the irregular force curve above is difficult use in the evaluation, due to the irregular curves. Choosing the correct mesh-size in all types of FEA is important. The mesh-size plays an important role for deciding the accuracy and the efficiency of an analysis. Figure 40 indicates very clearly that mesh-size 100 [mm] gives a

different overall force during the collision compared to the analysis with 50 [mm] mesh-size. The analysis with 25 [mm] mesh-size on the other hand gives very similar overall force as the 50 [mm] mesh-size analysis for the whole duration of the impact. This indicates that the 50 [mm] mesh-size is sufficient to be used in the iceberg model. The force level seems to converge for a mesh-size around 50 [mm], and by accounting for both CPU-time and accuracy the optimal mesh-size is concluded to be 50 [mm].

The initial failure strain parameter is also under consideration. By looking at table 10 and the smooth curves above, it shows that the initial failure strain is an important parameter to the analysis. A large initial failure strain gives many high force peaks, which makes it difficult to evaluate. Even for averaging 50 data points it still gives a quite irregular curve. The smooth curve however yields that a high initial failure strain gives a considerable increase in load level for the total duration of the impact. For indentation length between 0.15-0.25 [mm] and 0.35-0.45 [mm] the total average force has increased by 18.4 % and 17.7 %, respectively. This is relative high percentage increase; still the initial failure stain was increased by 200 % (from 0.01 to 0.03). The effect on the force level is therefore not that high considering how large of a change the initial failure strain was given.

The material constants are also evaluated in the parametric study; each parameter is increased or reduced with 30 % from the initial value. The outcome of these parametric changes is the following: The material constant a_0 has a relative small effect on the force level for the total duration of the analysis. The material constants a_1 and a_2 have relative large effect. The effect from the material constants seems mathematically correct (see eq.(3.3)). The Material constant a_1 is multiplied by the pressure and the value is usually relative high, which it also is in this case. For the material constant a_2, it is multiplied by p^2 and therefore will affect the result largely even for small values of a_2.

From table 10 the effect on the force level due to a parametric change in each of the material constants is given, and the following was obtained:

- A 30 % increase of the material constant a_0 increased the force by about 1-2 % for both time-steps TS101 and TS201. A 30 % reduction of the material constant a_0 reduced the force with 1-2 % for both time-steps TS101 and TS201.
- A 30 % increase of the material constant a_1 increased the force by 23.3 % and 27 % for TS101 and TS202 respectively. A 30 % reduction of the material constant a_1 reduced the force by 28 % at TS101 and 30.4 % at TS201.
- A 30 % increase of the material constant a_2 reduced the force by 26 % at TS101 and 28 % at TS201. A 30 % reduction of the material constant a_2 increased the force by 36 % at TS101 and 41.8 % at TS201.

The process pressure-area curves should yield the similar effects as the force curves; due to the only variable that affects the process pressure-area curves is the force term. The process pressure-area curve is plotted by dividing the total force in each time-step on the nominal contact-area for each time-step. The nominal contact-area is analytical calculated, and therefore are not affected by a change in material properties. This makes the nominal contact-area the same for all the analyses in the parametric study, which makes the force term the only part that will change the process pressure-area curve.

Figure 41 below shows the process pressure-area curves for the different analyses. Comparing figure 39 and 41 indicates how similar the force curve and process pressure-area curve is affected by the parametric change. There is definitely more difficult to see the effect in figure 41, due to the large pressure peak at the beginning of the analyses.

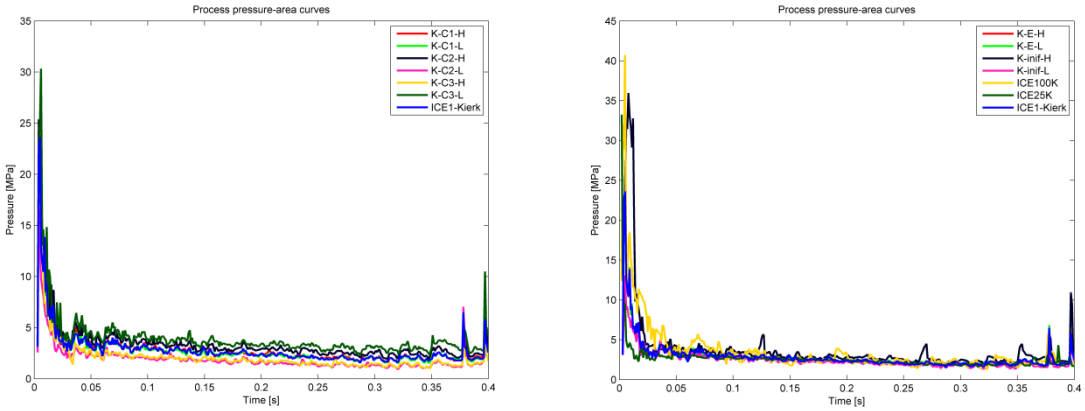

Figure 41 - PPAC differences, parametric study

During the master thesis it has been developed some methods to calculate the spatial pressure-area curve for a given time-step. It has been developed 5 different methods to calculate the spatial pressure-curve, where each has their own advantages. The different methods are earlier described in chapter 4.4.

Figure 42 and 43 show spatial pressure-area curves plotted by the contour-averaging method. The result below indicates also that the SPACs are significantly affected by the parametric change. Some parametric change affects the SPACs more the others, which clearly can be viewed by looking at figure 42 and 43.

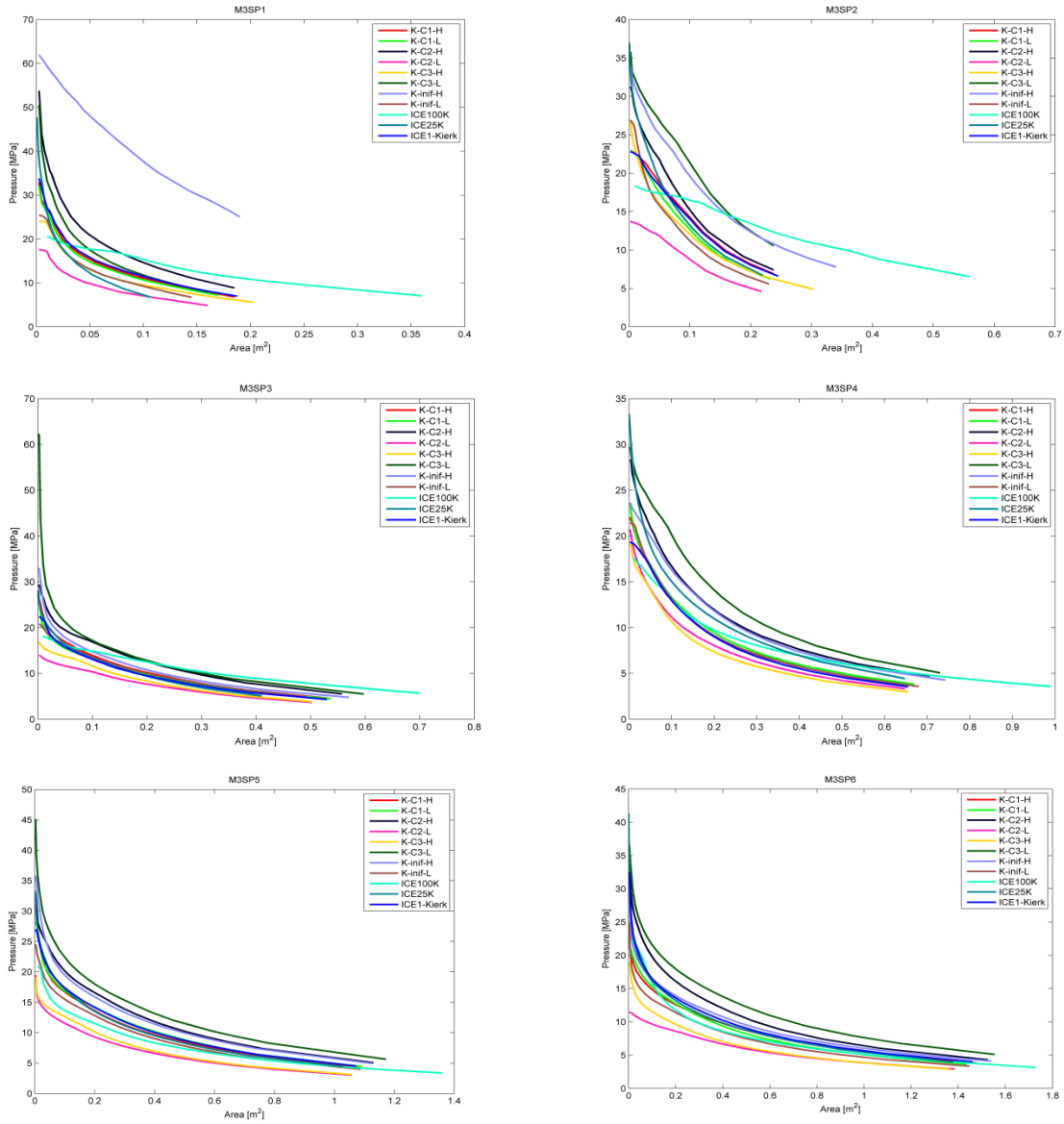

Figure 42 - SPACs differences SP 1-6, parametric study

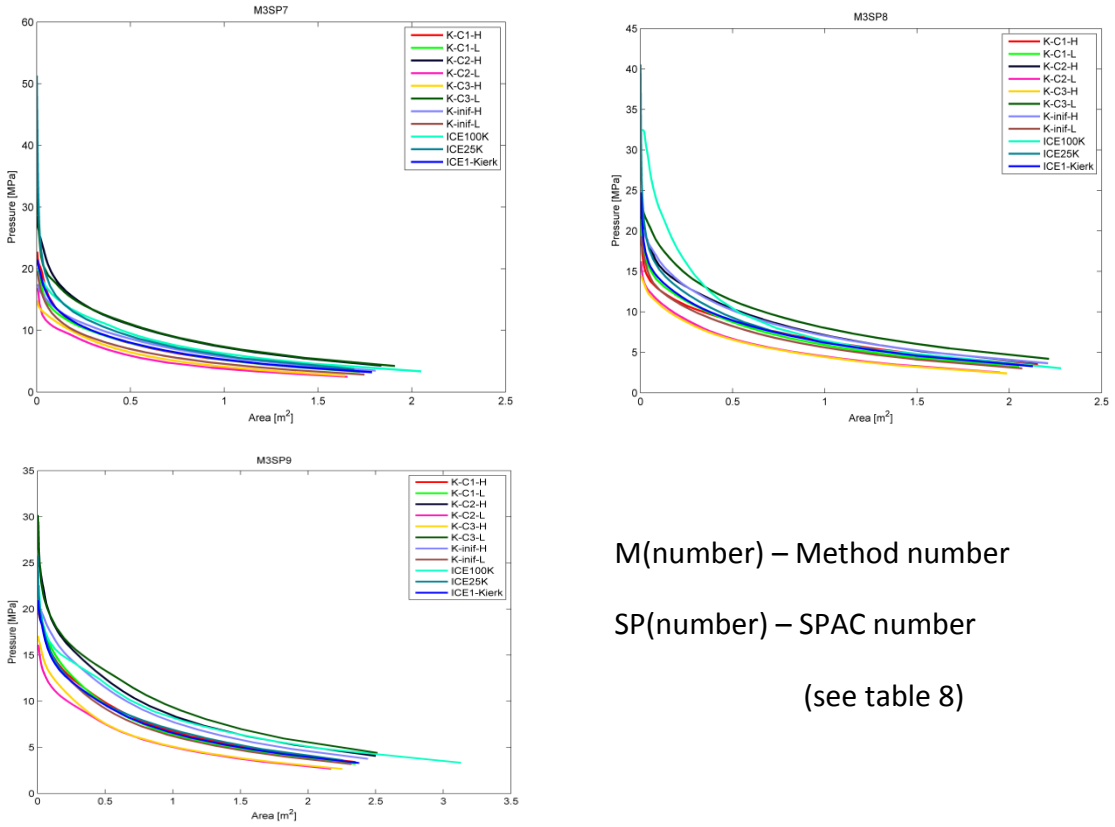

Figure 43 – SPACs differences SP 7-9, parametric study

Figures 42 and 43 are SPACs plotted by the contour-averaging method. This means that these figures show the maximum pressure at the high pressure zones, and how large area each pressure level covers within total contact-area. Most of the SPACs changes in the same matter as the PPAC due to the parametric change, but there is some few curves that deviate unexpectedly more than the others. The first time-steps (M3SP1 and M3SP2) have some curves that deviate significantly from the other curves. The analysis with a 100 [mm] mesh-size, gives relatively high SPAC for time-step number 11 and 21, and the reason for that is numerical. The contact-area in the beginning of the impact is very small, and therefore the 100 [mm] mesh has difficulties to give reasonable results, since each element is relative large. The 100 [mm] mesh-size analysis has problem obtaining the highest pressure and how rapidly the SPACs decreases by increasing sub-area.

High initial failure strain yields relative high forces, PPAC and SPACs in the beginning of the impact. This is mostly due to the initial failure stain parameter shift failure curve upwards, which means that for every pressure level the needed strain for erosion of an element is increased. Therefore larger deformation is needed before erosion can occur, which will result in an increase in force and pressure. For the high initial failure strain analysis the first spatial pressure-area curve M3SP1 hits a force peak, and therefore gives a lot higher values then the rest of the curves for that time-step. The other SPACs behave as expected. Figures 42 and 43 clearly show that there exist high-pressure zones where it is very high pressures. The figures also show that the pressure level reduces relative fast for increasing contact-area.

From earlier experiments and full-scale measurements the force and pressure have been in focus. Still one of the most important variables to consider for collisions is the internal energy. The amount of internal energy shows how much damage each colliding object has obtained during the collision. Below in figure 44 to 46 the internal energy from deformed element, eroded elements and both added together (total internal energy) is plotted. The material model developed by Zhenhui Liu erodes the elements very early. This can be viewed in figure 44 to 46, where the internal energy for deformed elements are very low compared to eroded internal energy. This is true for all the analyses. This means that the elements are eroded relatively early and before significant deformation is allowed to take place. This behavior seem realistic taking the crushing process into account, since the crushing process should be in the brittle region and therefore less deformation will occur before fracture.

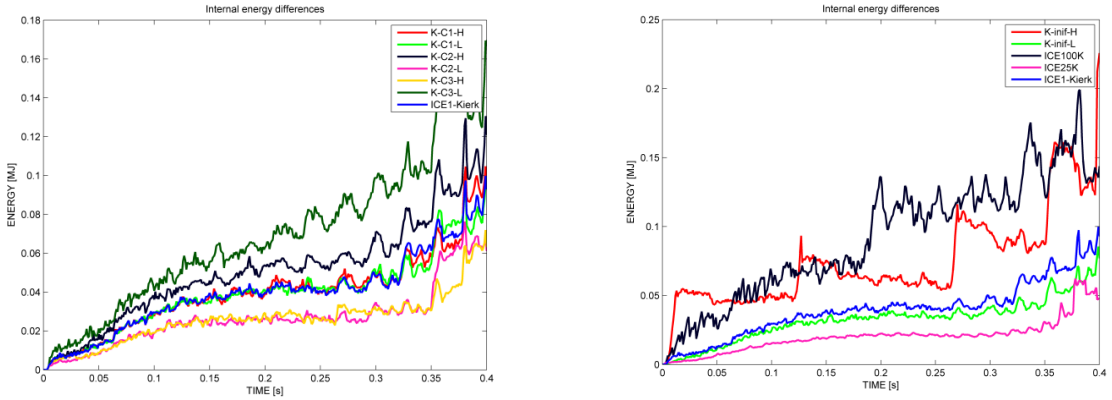

Figure 44 - Deformed internal energy

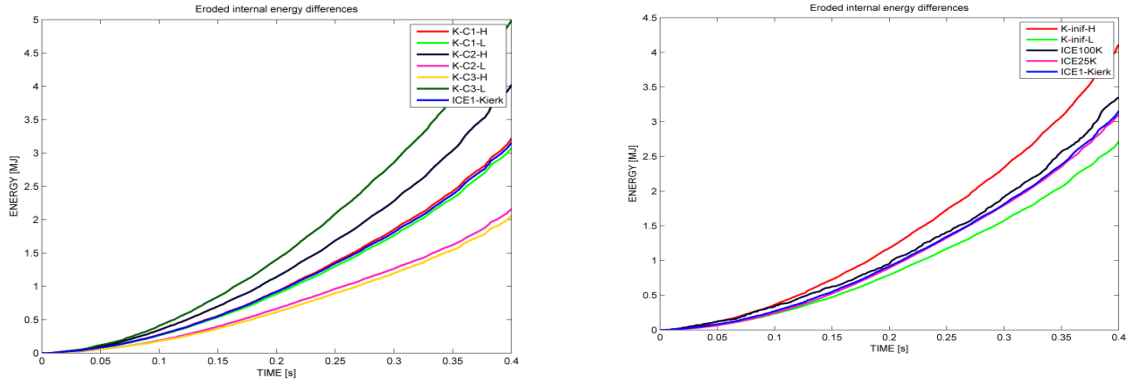

Figure 45 - Eroded internal energy

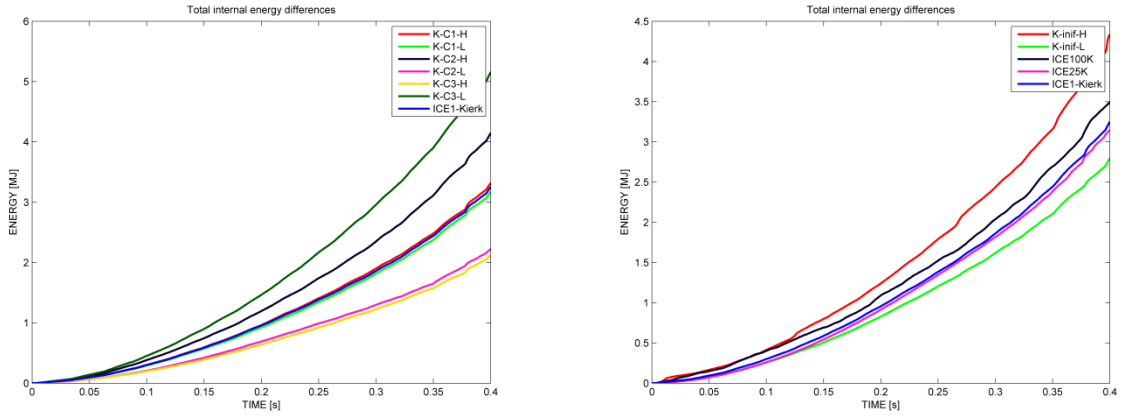

Figure 46 - Total internal energy

Figure 44 to 46 gave some very interesting results. First the 100 [mm] mesh-size analysis gives too high internal energy and eroded internal energy, and therefore also too large total internal energy. The total internal energy should not vary with different mesh-size, and the parametric study shows therefore that using 100 [mm] will result in inaccurate results. The 50 [mm] mesh-size gives almost the same total internal energy curve, which means that 50 [mm] should be sufficient considering the energy output. The analyses with 30 % higher initial failure strain shifts the failure curve (figure 7) upwards and therefore will result in an increase of required straining before the elements start to erode. This will increase all the energy curves given above, which also can be confirmed by looking at figure 44 to 46. The opposite effect occurs for a reduction in the initial failure strain which also can be seen from figure 44 to 46. The effect on the energy curves by a parametric change in the material constants, are also shown in figure 44 to 46. The material constants defines the yielding surface, and an increase in the yielding surface should increase the internal energy, and the opposite effect should occur for reduction in the yielding surface, which is confirmed in the figures above.

The parametric study has up to now only considered specific time-steps chosen. These chosen time-steps do not include the most critical time-step as mention earlier. Neither should they, since the critical time-steps where the load level is large, will vary in time for the different analyses. Comparing different analysis for different time wouldn't give comparable results since the scenario would be different. The analyses need to have the same time, indention length, nominal contact-area, etc. In other word, a parametric study needs to be based on one specific scenario. This means that the different analyses need the same setup and the results needs to be obtained at the same time. Now a comparison of critical time-steps and the specific time-steps chosen will be given. It will be interesting to see how large impact this force peaks has on the SPACs. It is the initial analysis with no parametric change that will be used in the evaluation of the effect of these force peaks. The effect of these force peaks will be found by comparing the selected time-steps with critical time-steps close to the selected time-steps.

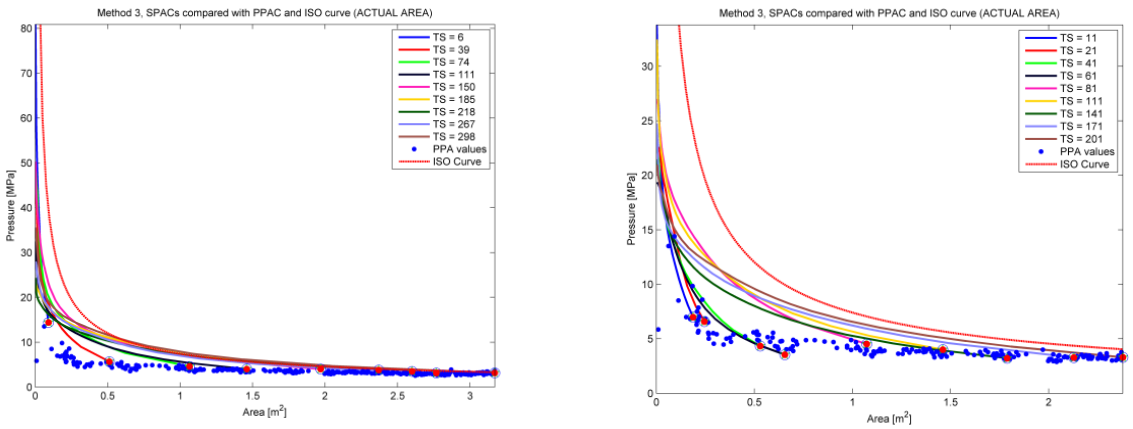

Figure 47 – SPACs; Contour-averaging method; (LEFT) At force peaks, (RIGHT) at selected time-steps

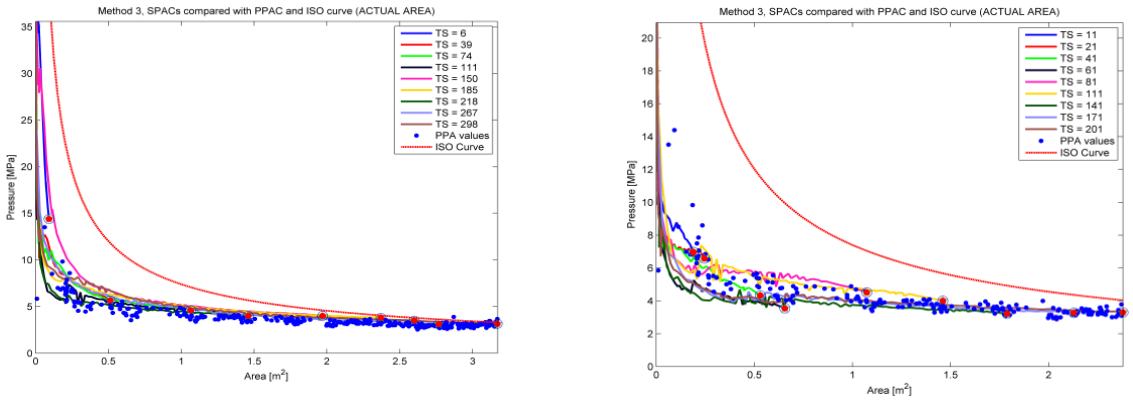

Figure 48 – SPACs Iterative-search method; (LEFT) at force peaks, (RIGHT) at selected time-steps

Figure 47 and 48 shows that the SPACs increases significantly when chosen time-steps are located at force peaks. The figures also show that the maximum pressure at high pressure zones increases, which makes local pressure more critical.

After the parametric study a lot of results were obtained, and the significance of each material parameter has been presented, discussed and found. The main goal was to evaluate the parameters significance on the results mention above, and also suggest good input parameters to the material model that gives the most realistic iceberg loads for a general iceberg during impact. The parametric study gives good insight in how each parameter changes the outcome. The material constant a_0 gives minimal changes to the results and are therefore less important than the material constants a_1 and a_2. Both these parameters have very significant effects on the outcome and have to be carefully chosen. The initial failure strain ε_0 is also relatively significant. Form the obtained results; it seems that the initial failure strain should be carefully varied. A too high initial failure strain will give unstable results, where most probably numerical errors and high amount of hourglass energy will develop. Also high initial failure strain gave very untrustworthy and unphysical energy curves. Therefore it is only suggested to adjust the initial failure strain to empirical data. The suggested input parameters for the material model after the parametric study is actually the same input values as for the Kierkegaard's material constants analysis. There is of course different combination of the material constants that will give about the same results as the

Kierkegaard's analysis. But since the Kierkegaard's material constants analysis fits the "Pond Inlet 1984" tests that well, the Kierkegaard's input values for the material parameters seem like the best values to use in the material model of the iceberg.

11 Stochastic variation of mechanical properties

Material modeling of icebergs is associated with substantial challenges. From literature and earlier research it is known that the ice material is inhomogeneous, and that the iceberg consists of a mixture of hard and weak zones. The knowledge of the statistical distribution of the hard and weak zones is limited. The Zhenhui Liu's model has up to now been simplified to have a homogenous material. It will in this chapter be attempted to modify the current Zhenhui Liu's model by including inhomogeneity to the material model. The material model developed by Zhenhui Liu gives reasonable load and pressure levels. However, the location of where the high pressure zones occur during impact seems to be too far from the center of the contact-area. Figure 49 below shows this graphically.

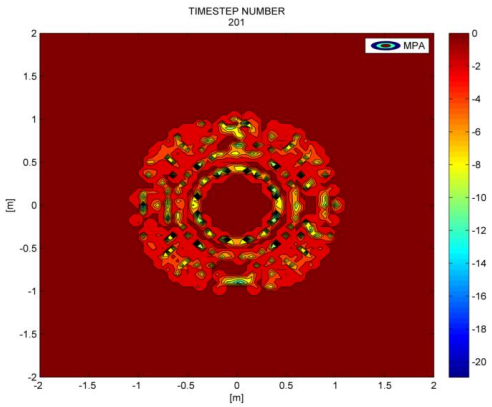

Figure 49 - Contour plot, Kierkegaard's (analysis)

From physics and literature it would be more correct if the model would have an increasing strength at the center of the contact-area, due to the increasing confinement between neighbor elements in core of the iceberg. This should lead to an increase of pressure level and more often development of high pressure zones in the center of contact-area compared to elsewhere. The reason for why the high pressure zones in model often appear a distance from the center is a combination of model geometry, shape of the failure curve and failure criteria. The elements in contact-area first "erode" at the center and the "erosion" of elements continuous outward in uniform direction to the edge of contact-area is reached. This will result in that most time-steps have no pressure at the center of contact-area due to the centered elements have already been "eroded". Modifying the model to be inhomogeneous will hopefully eliminate or reduce this non-physical zero pressure area at the center of contact-area. Inhomogeneity will give the iceberg a mixture of hard and weak zones, and the elements in the hard zones will "erode" later than the other elements. Some of these hard zones will most probably be located at the center of contact-area, and therefore will lead to more high pressure zones closer to the center of contact-area. This should lead to a reduction in this non-physical zero pressure area, which is seen in figure 49.

11.1 The method for incorporating stochastic variation

The method used to incorporate inhomogeneity is to systematically perform a stochastic variation of some chosen material parameters. The chosen material parameters that are included in the stochastic variation are the material constants (a_0, a_1 and a_2), the initial failure strain (ε_0) and the E-modulus. The reason behind the chosen material parameters is that they all affect the strength of the ice material in different ways. The material constant affects the yielding curve. The initial failure strain affects the failure curve, and the E-modulus affects stiffness of the material.

There is limited access to the FORTRAN77 code LS-DYNA uses. However, the FORTRAN77 code implemented in LS-DYNA gives the opportunity to element-wise change the initial value of the material input parameters before the analysis starts to simulate. This was done by implementing a subroutine in the FORTRAN77 code that produces a stochastic variation on the chosen material parameters on each element. Due to the degree of irregularity of the ice material for real iceberg and the limited knowledge of this irregularity, it is logical to produce a stochastic variation to have certain degree of randomization of the material parameters. The main goal of this randomization is to make the material model more physical correct, and still give the same total load and pressure level as before this stochastic variation. A more physical correct material model means an iceberg model that is inhomogeneous where it exist a mixture of weak and hard zones. Also these high pressure zones which can be seen in figure 49 should be located closer to the center of the contact-area.

The distribution of hard and weak zones in a real iceberg is unknown. The material model produces relative good load and pressure levels as mentioned earlier. Therefore the stochastic variation should only affect the location of the high pressure zones and the spatial pressure-area curves. To obtain that, the stochastic variation has been given a normal distribution with the expected value (μ) and the standard deviation (σ). Using a normal distribution with expected value equal to initial value should ensure that the load and pressure levels are unchanged. Thus the difference between the process pressure-area curve before and after the variation should be small. The expected value of a random variable is the weighted average of all possible values that can occur. The standard deviation defines how much variation that occurs from the expected value. There is also included one more variable that makes a small modification to the normal distribution. It has been created a variable that creates a limit for the maximum and minimum deviation from the expected value. If the function in the code produces random variables that exceed the limit set, the function immediately reproduces the number until it is within the limit. The figure 50 shows how the distribution will look like with different expected value, standard deviation and limit.

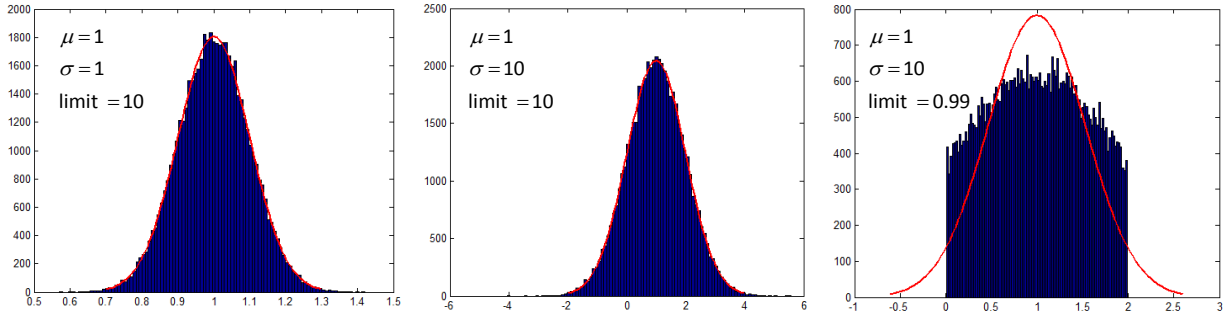

Figure 50 - Ex. on distributions for the stochastic variation of the material parameters

Figure 50 clearly shows how the expected value, standard deviation and the limit variable affect the distribution. The figure also shows that a combination of a low limit value and a large standard deviation value will give a distribution close to a uniform distribution. The limit value actually only limits the variation by cutting off the tails of the normal distribution. Below will the mathematically description on how the stochastic variation is performed on each element:

$$devi = \left(rand(1) - 0.5\right) \bullet \sigma + \mu \tag{11.1}$$

$$\begin{aligned} &if \;\; devi > \text{limit} + \mu \\ &\quad \text{Do equation 5.5 again} \\ &elseif \;\; devi < \text{limit} - \mu \\ &\quad \text{Do equation 5.5 again} \\ &else \\ &\quad Continue \end{aligned} \tag{11.2}$$

$$\begin{aligned} parameter^{(+)} &= parameter^{(+)} \bullet devi \\ &or \\ parameter^{(-)} &= parameter^{(-)} / devi \end{aligned} \tag{11.3}$$

Where rand(1) is a random number between 0 and 1 and follows a normal distribution. Expected value (μ) is set equal to 1, since value 1 gives the parameter no change from initial value. The *limit* value should be set to a value less than 1, since larger values of *limit* will allow negative values of *devi* if σ is sufficiently large. Negative values will give problems and wrong results.

Due to the restricted access to the FORTRAN77 code in LS-DYNA, the subroutine was first developed in MATLAB. Then an equivalent subroutine was developed in FORTRAN77. Both codes; the MATLAB code and FORTRAN77 code that create the stochastic variation can be found in appendix C. The MATLAB code works properly, but it appeared a problem in the FORTRAN77 code.

The problem is that LS-DYNA that uses the FRORTAN77 subroutine does not create the expected spread as the MATLAB code produces. The FORTRAN77 code has to handle some of the code differently than MATLAB. The following suggested error source is given: Either the random function used in FORTRAN77 is too poor, which might lead to a problem. However the random function was tested and it will be quite surprising if the random function could make this error. Another possible error source is that the restricted FORTRAN77 code does something to the variables after the subroutine has performed the stochastic variation. Anyway a stochastic variation with a normal distribution was performed, but the problem explained above gave limitations to the stochastic variation. The distributions given in figure 50 are produced by an equivalent MATLAB code, and figure 51 gives the distribution the LS-DYNA gets after implementing the FORTRAN77 subroutine.

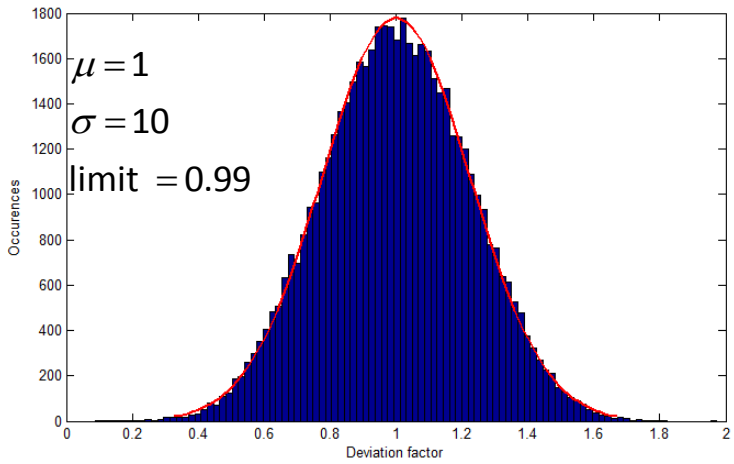

Figure 51 - Stochastic variation of the material parameters

The distribution in figure 51 has very reduced spread compared to the distribution given in figure 50 with equal input. Still the limited variation is better than none. Also there are 5 material parameters included in the stochastic variation, and a small stochastic variation on each of those parameters can give relative large change in material properties. Therefore the limited stochastic variation produced from the FORTRAN77 subroutine should be enough.

11.2 Results from the stochastic variation of the material properties

The expected change after the stochastic variation of the material parameters is that the SPACs should be affected. The highest pressure level in a high pressure zones should increase, which should increase the maximum pressure value for the smallest sub-area in the SPACs. This stochastic variation will also most probably lead to an increase of the high pressure zone size. The locations of the high pressure zones will also change, and a more irregular pattern of the location of these high pressure zones should occur.

It has been performed a lot of analyses with various input values for expected value (μ), standard deviation (σ) and limit. The results from the most relevant analyses performed will be given below:

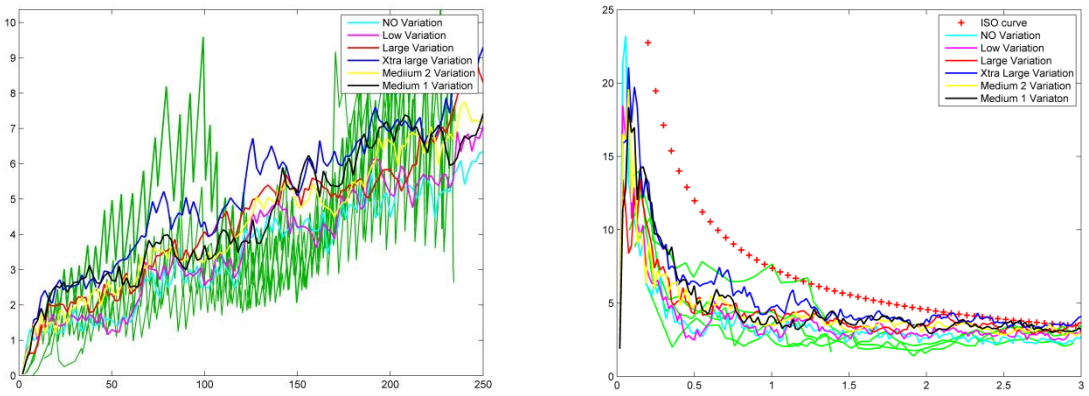

Figure 52 - Various input for the Stochastic variation, comparison with "Pond Inlet 1984" tests (green lines)

Figure 52 indicates implementation of the stochastic variation does affect the force level and therefore also the process pressure curve. Still the change in overall load and pressure level during the impact duration is relatively small. All of the analyses given in figure 52 are within acceptable range of what the "Pond Inlet 1984" experiment has measured. The Medium 1 Variation (black line) is concluded to have the optimal variation. It produces reasonable load and pressure levels for the whole impact duration, which is shown in figure 52. A minor concern is that the chosen stochastic variation produces a PPAC that converge to high pressure value than the PPAC without the stochastic variation. This value the PPAC converges to seems too high compared to what ISO recommends. However the difference is relatively small and therefore the "Medium 1 Variation" is concluded to produce reasonable PPAC.

This inhomogeneous property should really affect the local pressure, and therefore the SPACs. Below in figure 53 and 54 there will be given both SPACs and contour plots to show the effects this stochastic variation of material properties has on the local pressures.

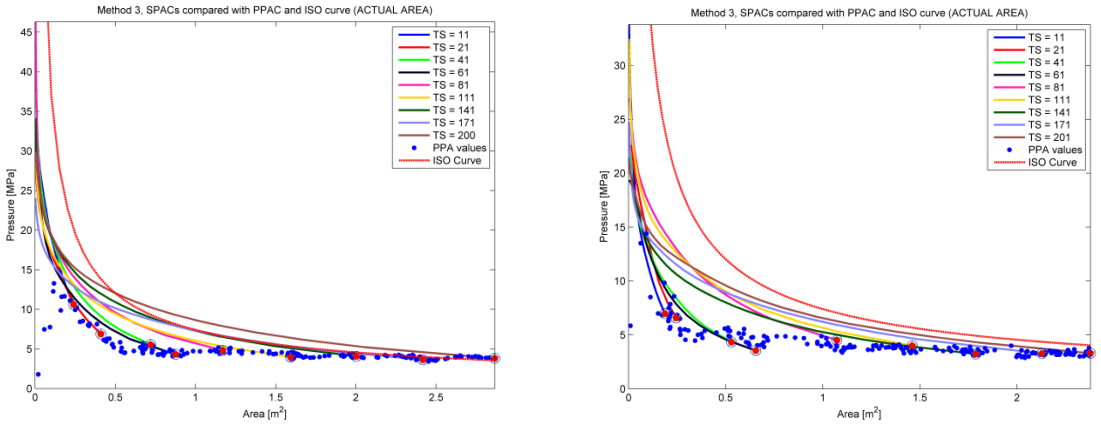

Figure 53 – SPACs; (left) inhomogeneous iceberg, (right) homogenous iceberg

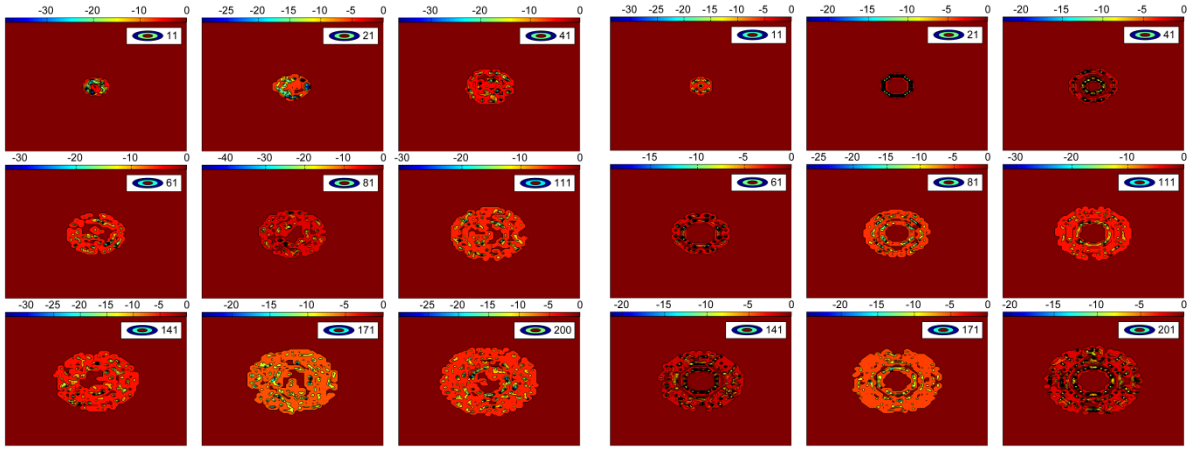

Figure 54 – CPs; (left) inhomogeneous iceberg, (right) homogenous iceberg

The SPACs in figure 53 show a significant increase of maximum pressure at the high pressure zones, and also for increasing area size the SPACs gives higher pressure levels. The contour plots in figure 54 indicate that the high pressure zones now has an more irregular pattern, and also the zero-pressure area circle at center of contact-area is eliminated. The energy curves were also investigated and they seem logical. The internal energy has increased, which is logical due to the increase in total force and pressure levels. A few of the energy curves are given in appendix C. Figure 55 shows the area-ratio (actual/nominal). The area-ratio still seems reasonable. Since the area-ratio is unknown and the fact that area-ratio most probably varies a lot in real iceberg impacts, none of the curve below is more correct than the other. The area-ratio value above 1 in the beginning is due to ice deformation before erosion occurs.

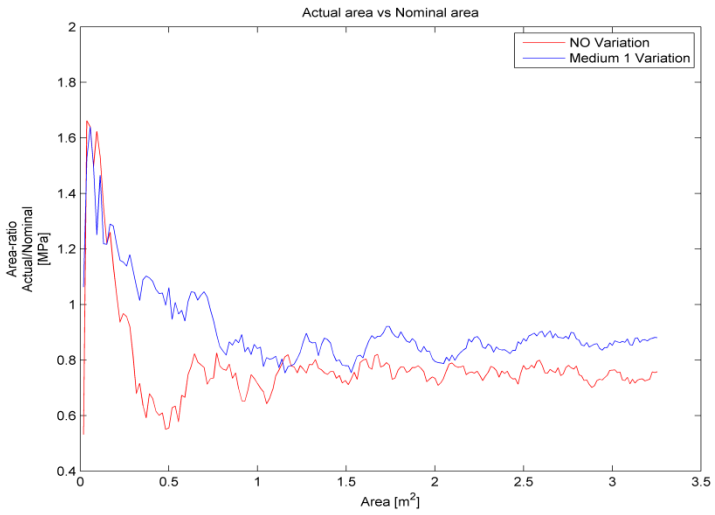

Figure 55 - Area-ratio, NO stochastic variation vs. Medium 1 Variation

It is difficult to find the reason for this suddenly increases in total force and pressure levels, which can be seen in figure 52. The inhomogeneous iceberg model as shown above is a small percentage stronger than the homogenous iceberg model. The increase in total load and pressure level has to come from the inhomogeneous property. The method that produces the distribution to the stochastic variation which is added on certain material parameters does not give a perfect normal distribution. The distribution of the stochastic variation which is produced for the “Medium 1 Variation” analysis to each material parameter is given on the next page:

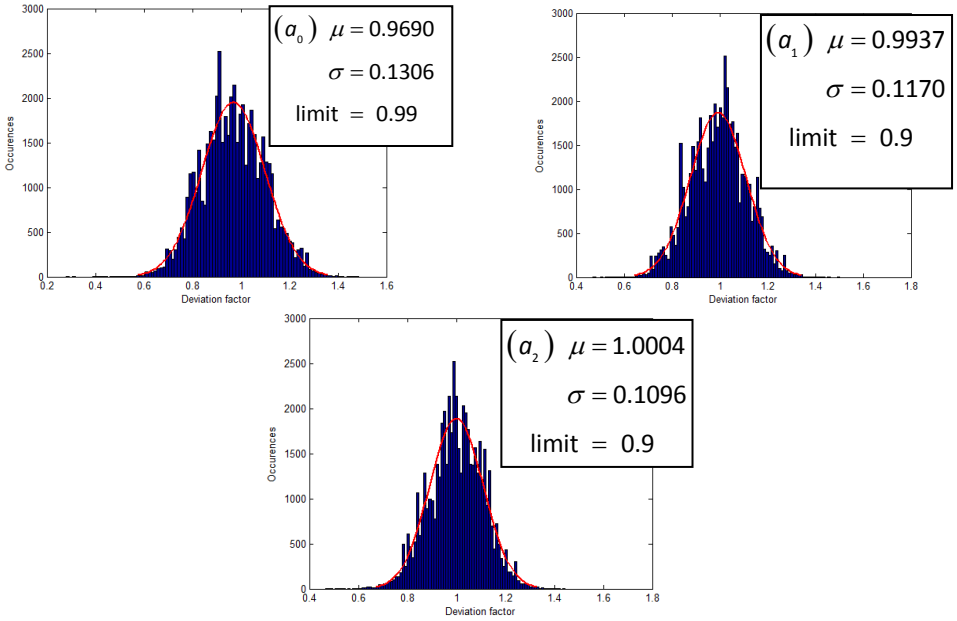

Figure 56 - Distribution produced for each material constants ("Medium 1 Variation")

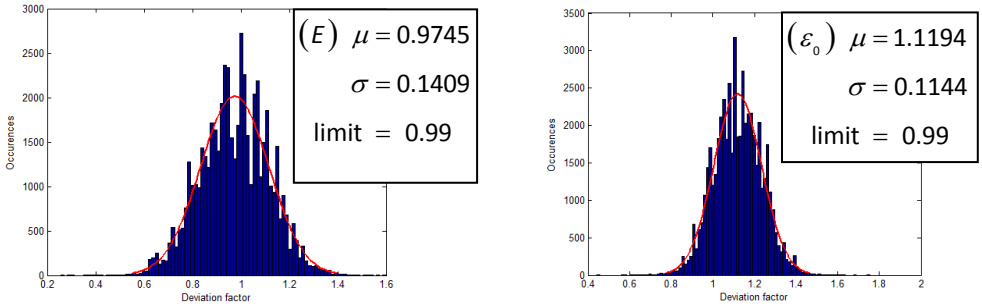

Figure 57 - Distribution produced for initial failure strain and E-modulus ("Medium 1 Variation")

The distribution produces in figure 56 and 57 above is from the "Medium 1 variation" analysis. The initial failure strain (ε_0) was given a distribution that gave an expected value of 1.1194 which is 12 percent larger than what it is supposed to be. The parametric study in chapter 10 shows that an overall increase of the initial failure strain will result in an increase in force and pressure levels. It was therefore performed 5 analyses of the same stochastic variation to check if the deviation from the perfect normal distribution could be the reason for the PPAC converges to higher level than expected. Those 5 analyses were compared, and the conclusion is that the deviation of the perfect normal distribution had neglectable effects. The hourglass energy has also increased, which is included in the LS-DYNA calculation. It can be one of the reasons to an increase in the PPAC. This hourglass energy increase was discovered relative late in this master thesis, and was therefore not further investigated.

The optimal input value for the stochastic variation of material parameters for the method developed in this master thesis is concluded to be:

Parameters	μ	σ	limit
Material constant 1 (a_0):	1	10	0.99
Material constant 2 (a_1):	1	2	0.90
Material constant 2 (a_3):	1	2	0.90
Initial failure strain (ε_0):	1	10	0.99
E-modulus (E):	1	10	0.99

Table 11 - Stochastic variation input

Table 11 is the input values that give the "Medium 1 Variation" analysis. The suggested stochastic variation of the material parameters given in table 11 is based on results obtained from performing many analyses with different stochastic variation of the material parameters. The results and knowledge obtained in the parametric study performed earlier were also used. The reason why the material constants a_1 and a_2 were given lower input values for standard deviation and limit is because they affect the same part of the model (the yielding surface). Therefore elements that are given a stochastic variation that increases the values of all 3 material constants will create elements with an unphysical high yielding surface. This can be handled by sufficiently reduce the standard deviation and limit input values of the material constants.

11.3 Discussion of the stochastic variation method

The stochastic variation of material parameters is performed element-wise, where it is no dependence or correlation between the elements. Since the iceberg model average element size is around 50x50 [mm] for the solid elements, the degree of inhomogeneity is large. The stochastic variation method suggested has no control over what the neighbor elements have as a stochastic variation. Therefore the distance between a hard element and a weak element can be as low as 50 [mm], which probably is too low. The size of hard and weak zones should be chosen and controlled, but this not easily implemented in the LS-DYNA's FORTRAN77 code, and was therefore not attempted. The suggested method in this master thesis is to incorporate a stochastic variation of the material parameters, which is the first attempt of implementing this inhomogeneous material. This suggested method should therefore be further optimized, and this discussion should bring thoughts and ideas of possible improvement to this current suggested method.

Form a relatively new experiment conducted 2012 by Kim, Daley and Ulan-Kvitberg [12], the local pressures within the contact-area were investigated. The experiment used so called "High-Precision Pressure Measurement Film" to obtain the local pressure during impact. Many contour plots were obtained, and one of the contour plots obtained from the experiment is given below:

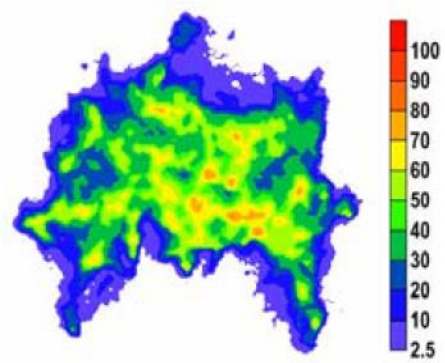

Figure 58 - Contour plot, from an earlier experiment [12]

Figure 58 shows the location and size of the high pressure zones. It also shows how the pressure is distributed over the contact-area for specific time. Comparing figure 54 and 58 clearly shows that there is some difference in the pressure distribution over the contact-area, and also the location and the size of the high pressure zones between the NLFEA and the experiment mention above. There is size difference between the experiment and the NLFEA, which makes it difficult to compare. However some clear indicative observations can be made. There is less high pressure zone located outside the center of contact-area, and the reduction rate of the pressure level from a high pressure zone seems slower. It seems that that a relative high pressure level can be observed between most of the high pressure zones. The NLFEA model gives relative faster reduction rate of the pressure levels from high pressure zones, and much less pressure is observed between the high pressure zones in the NLFEA. Due to the small ice sample size used in the experiment no concrete conclusions can be made. Nonetheless the element dependence and correlation of neighbor elements within a sub-volume of unknown but larger size than the element-size is most likely. The next step in order to improve the stochastic variation of the mechanical properties is to investigate this dependence and correlation between elements.

Another aspect of this stochastic variation that also should be further investigated is how these material parameters should be varied. The user of this method should also consider if no one or some or all of the material parameters should vary with the same stochastic variation. In this master thesis and the method above, the material parameters is assumed to be independent to each other. Therefore all the material parameters are independently varied. It is limited knowledge of the sea ice material, which makes it de difficult to produce very well-thought arguments for the decision taken for the suggested stochastic variation of the mechanical properties. It is also possible that including less material parameters might give sufficient large stochastic variation, and it would also be easier to control.

12 The “best” material model of an iceberg

The chapter 9 and 10 evaluates the iceberg material model, where a lot of analyses are performed. The main goal is to find the “best” input of the material parameters in the iceberg model. In chapter 9 one impact scenario has been analyzed 4 times, and each time with different input to the material properties. The material properties have been obtained from earlier experiments by different scientists (Derradji-Aouat, Kierkegaard, Riska and Frederking). The analyses were evaluated and compared with the “Pond Inlet 1984” experiment, which has very similar impact scenario. From the comparison between the NLFEA analyses and the experiment, one analysis gave very reasonable result. That was the analysis with input parameters obtained from Kierkegaard. The input from Kierkegaard was concluded to give the most realistic results.

In chapter 10 a parametric study was performed on the impact scenario. Kierkegaard’s obtained material parameters were set as the initial values in the parametric study. From the parametric study the sensitivity to each parameter was evaluated. Since the Kierkegaard’s material input values yielded very good result, no changes to the input parameters were performed. The material parameters could be altered in some way that would produce similar results as the Kierkegaard’s input parameters. However there is no reason to do that, since the Kierkegaard’s input parameters produce good and realistic results. Even though the parameter was not altered, the parametric study gave very good insight in the relative importance of each parameter and how important it is to give the correct input data for each parameter. It also gave interesting results, which was used to obtain a good stochastic variation of the iceberg model. Chapter 11 investigates the possibilities to implement a reasonable inhomogeneity to the material properties. A method was suggested and the results yields reasonable results. The implementation of adding an inhomogeneity to the iceberg material with a stochastic variation of the material parameters is therefore a success.

The “best” material properties for the iceberg model:

After all the analyses performed and the modification added to the iceberg model, the following input to the iceberg model is concluded to give the most reasonable results for a general iceberg impact:

	Density [kg/m^3]	E-modulus [MPa]	Poisson’s ratio [-]
	900	9500	0.3
	Bulk modulus [MPa]	Shear modulus [MPa]	E_0 [-]
	7916.6	3653.8	0.01
Cases:	Material constants		
	a_0 [MPa^2]	a_1 [MPa]	a_2 [-]
Kierkegaard (1993)	2.588	8.63	-0.163

Table 12 - The "best" input values for the material properties for the iceberg model

Parameters	μ (unchangeable)	σ	limit
Material constant 1 (a_0) :	1	10	0.99
Material constant 2 (a_1) :	1	2	0.90
Material constant 2 (a_3) :	1	2	0.90
Initial failure strain (ε_0):	1	10	0.99
E-modulus (E):	1	10	0.99

Table 13 - The “best” input values for the stochastic variation of material parameters

The input to the material constants $(a_0, a_1 \text{ and } a_2)$ and initial failure strain (ε_0) should always be set by experimental data. This means that input values for the different material parameter does not have a specific value that will give the correct iceberg material for every scenario. The icebergs material properties will vary between different arctic regions and using experiment data from iceberg that the structure is most probable going to encounter is important. Still a good general iceberg model can be developed and used for numerical design purposes that will be acceptable for many impact scenarios. It assumed that the “Pond inlet 1984” experiments were performed on very general iceberg that should represent an iceberg that can be encountered in many of the arctic regions. Table 12 and 13 shows the “best” input parameters for producing the “best” material properties that will give the most reasonable iceberg results for a general iceberg impact.

13 Iceberg impact analyses

It is unknown to what extent the variation of the mechanical properties is important with respect to assessment of damage in maritime and offshore structures during iceberg impacts. Now a “best” material model with stochastic variation of the mechanical properties of an iceberg is established. It would be interesting to see the amount of damage the iceberg model will give the colliding structure, and especially the relative strength between the iceberg and the colliding structure.

This damage assessment for the structure during iceberg impacts can be found by performed ice-structure interaction analysis for abnormal-level ice events (ALIE). ALIE impacts allow large deformation, and therefore share-energy design is used. The setup of the ALIE impact scenario is given in chapter 8.2. In this master thesis a large focus has been on the material properties, therefore limited amount of geometrical shapes has been analyzed. Figure 28 in chapter 8.2 shows the geometrical shapes that have been analyzed during this master thesis. Two similar icebergs are analyzed, where one is sharper shaped than the other. It will be interesting to compare how easily the sharper shaped iceberg is crushed relative to the blunter shaped iceberg. From the analysis the level and distribution of structural damage is shown by looking at the internal energy. The structural damage output can also be evaluated by comparing the relative displacement of the most critical node in the outer plate of the panel vs. the ice crushing distance of the iceberg in x-direction (see figure 59). How the ice crushing distance is found is also mathematically explained by equation (5.1) in chapter 5.

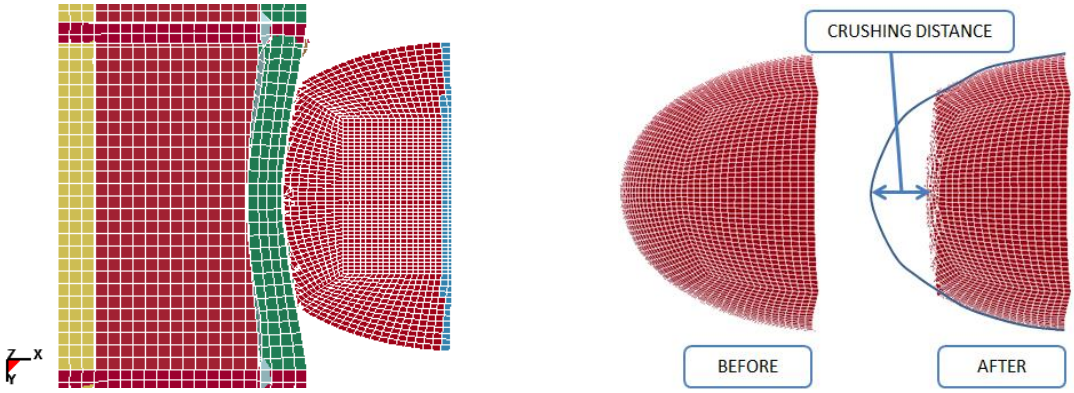

Figure 59 - Overview of the impact scenario, and definition of the crushing distance

The panels used in the share-energy design analyses are modeled by Torstein Myhre. Myhre has developed 3 panels with 3 different ice classes. The structural strength of each panel can be viewed in table 4, where the dimension of the structural components within the panel is given. The most critical position for penetration of inner and also outer hull for an iceberg collision will be between the girders and stringers (see figure 60). Therefore impact location on the panel given in figure 60 will be analyzed.

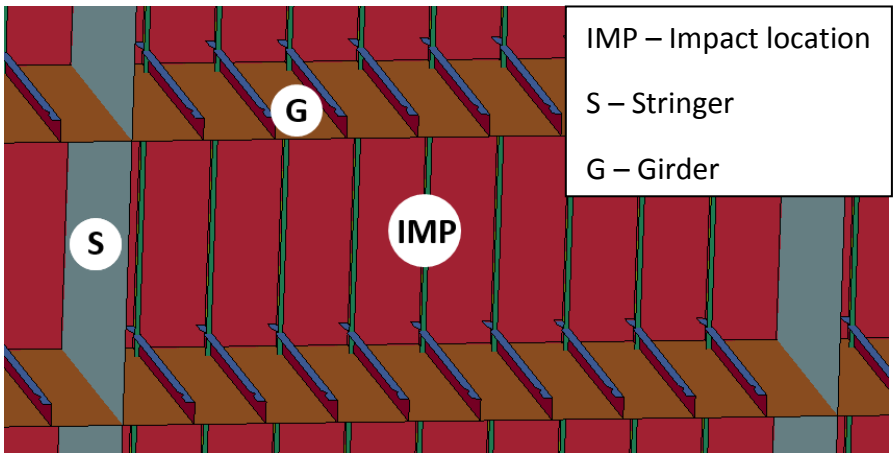

Figure 60 - Impact location analyzed

It will now be presented results of the structural damage produced between the colliding objects from 6 different analyses. The same collision scenario is analyzed 6 times, where both panels and iceberg shapes have been varied. This will show how the 3 panels perform against a blunt and sharper shaped iceberg, and how the panels perform against each other:

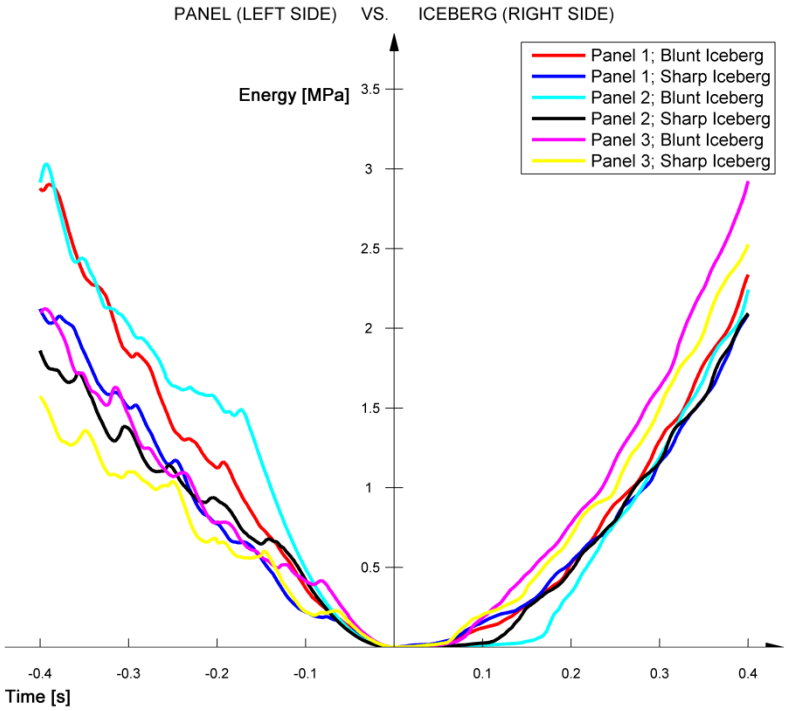

Figure 61 - Relative internal energy between panel and iceberg

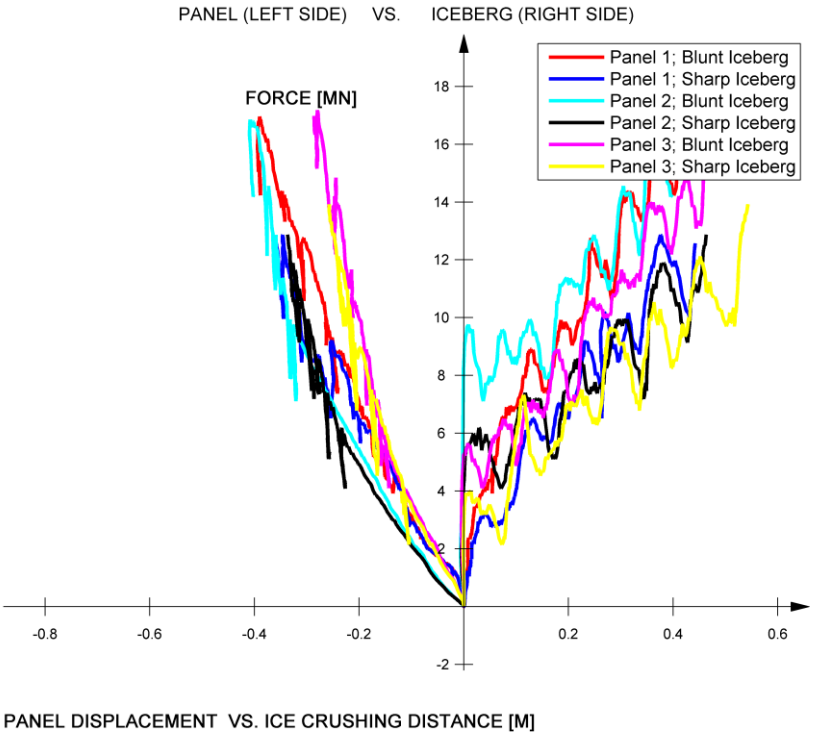

Figure 62 - Relative displacement between outer hull and ice crushing distance

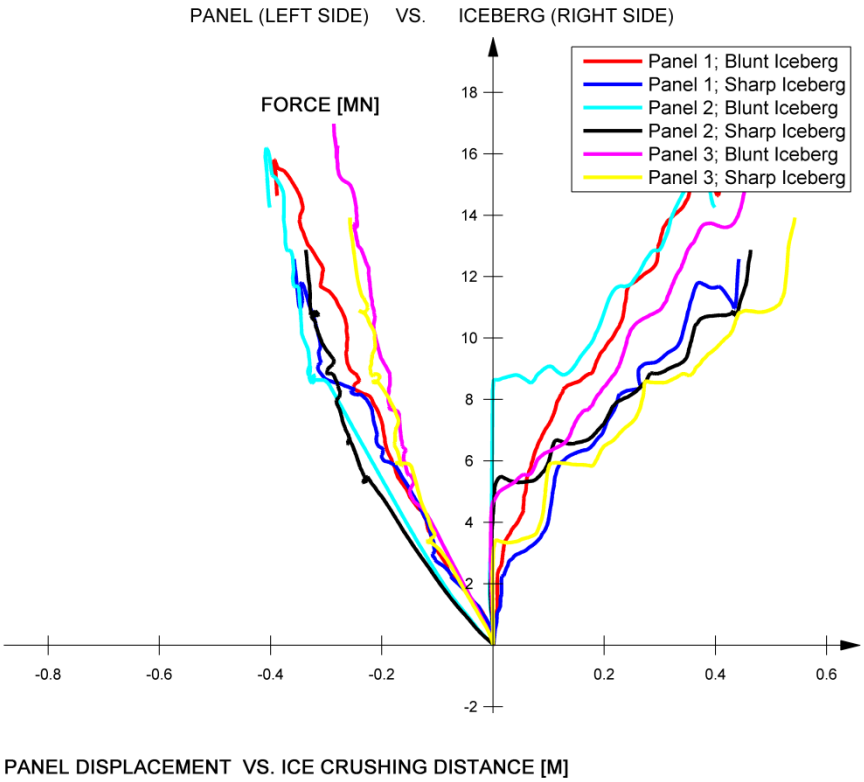

Figure 63 - Smooth curve of figure 62 (50 closest points averaged)

Figure 61 to 63 shows minor differences between the different analyses. The size of the iceberg and the duration of the impact should probably be increased. This would have given a deeper indentation length and more structural damage would occur. This would most probably give a larger deviation between the analyses in figure 61 to 63. A laptop with 2 GHz processor and 8GB RAM performed all the share-energy design analyses, which restricted the size and duration of the analyses. However figure 61 to 63 still gives interesting results.

Figure 61 shows the internal energy, which is on way to assess the structural damage output. Panel 3 has the lowest amount of internal energy between those 3 panels, and is therefore strongest one of these panels. Panel 1 and 2 seem to have similar strength, since figure 61 gives very similar internal energy curves. The shape of the iceberg changes the structural damage level in the panels, and the shape of the iceberg is therefore important. The blunter shaped iceberg gives larger amount of structural damage; due to larger amount of ice is force into the panel. Even though the sharper shaped iceberg gives less structural damage, the sharper shaped iceberg could still be more critical. The sharper shaped iceberg can still give larger displacement of the outer hull, if the sharper shaped iceberg is as strong as the blunt iceberg. Figure 62 and 63 show the total force verses displacement (x-direction) of the most critical node at the outer plate, and the total force verses the crushing distance (x-direction) of the iceberg (See figure 59). The figures 62 and 63 confirm the same as figure 61. Panel 3 is the strongest panel; it gives the lowest displacement length of the outer hull. The most interesting results in the figures 62 and 63 is that even do the sharper shaped iceberg give less structural damage, it still gives larger or the same displacement length to the outer hull. From figures 63 it seems like the sharper shaped iceberg does not easier get crushed, and therefore gives the same indentation length to the outer hull. It would be very interesting to do more analyses were longer impacts duration is analyzed, so that the effect due to the iceberg shape can be further investigated. Also even a sharper shaped iceberg than used in this master thesis would be important to investigate. For if the sharper shaped icebergs do not easier get crushed the critical shape for inner hull puncturing will easily be sharper shaped icebergs.

The effect on the structural damage due to the stochastic variation of material parameters would be interesting to investigate. Therefore it will below be presented one impact scenario, where iceberg model has been given the following stochastic variation of the material parameters:

- No variation
- Medium 1 variation (see chapter 11)
- Large variation $\begin{pmatrix} \sigma_{a_1} = 4, \text{limit}_{a_1} = 0.99 \text{ and } \sigma_{a_2} = 4, \text{limit}_{a_2} = 0.99, \\ \text{else similar to Medium 1 Variation} \end{pmatrix}$

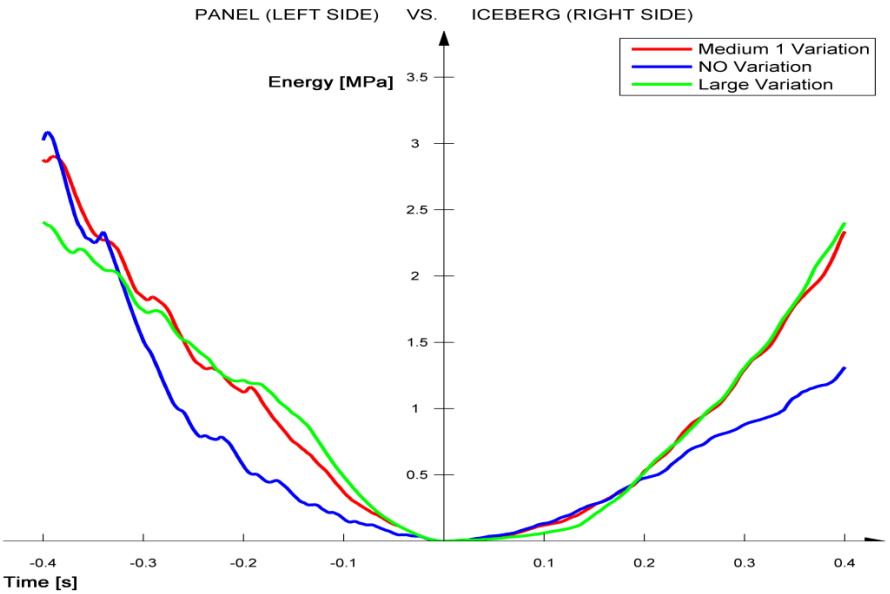

Figure 64 - Relative strength; internal energy plotted for panel and iceberg

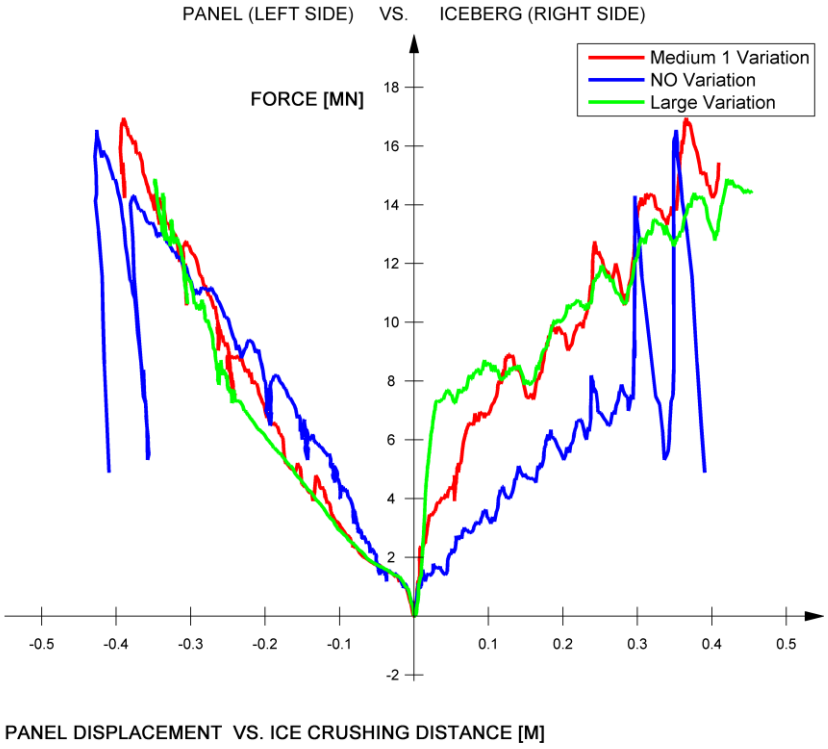

Figure 65 - Relative displacement between outer hull and Ice crushing distance

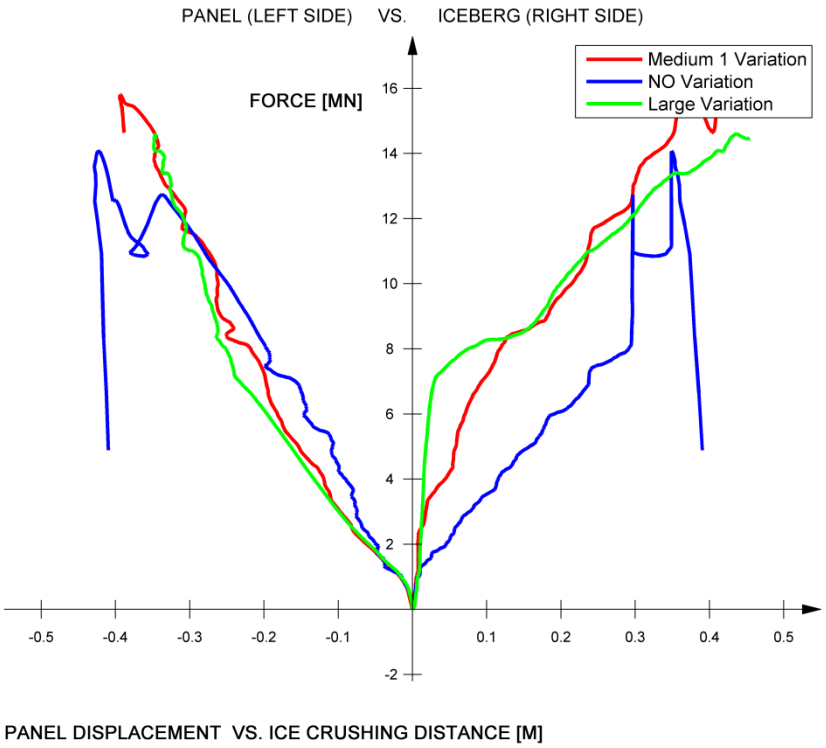

Figure 66 - Smooth curve of figure 65 (50 closest points averaged)

Figure 64 shows that the mixtures of hard and weak zones do contribute to the structural damage output. The internal energy curve is larger for the panel side when the iceberg is given stochastic variation of mechanical properties. However after 0.3 [s] does the homogenous iceberg gives equal internal energy which is very interesting. Figure 65 indicates the same as figure 64, which is that the inhomogeneous iceberg gives larger displacement to the outer plate in the beginning. It also shows that the homogeneous iceberg gives equally displacement of outer hull after 0.3 [s]. These figures indicate that in the beginning of the impact where the contact-area is fairly small, the mixture of hard and weak zones contribute to structural damage. But after a larger contact-area the mixture of hard and weak zones seems to weaken the iceberg strength, which seems a little peculiar. The effect of numerical error and the amplitude of the total force increases heavily at the end of the analysis (see figure 65), therefore it is high uncertainties around the later stages of the impact results. Therefore the later part of the impact will not be further discussed.

14 Conclusion

It has been developed both process and spatial pressure-area curves. The development of the spatial pressure-area curves gave great insight in the local pressures within the nominal contact-area. The spatial pressure-area curve confirmed also what is already well-known. That it exist high pressure zones within the contact-area, and therefore iceberg impacts has to be consider for both local as well as global design. There have been created 5 different spatial pressure-area curves, where especially 2 of them are good curves for structural design purposes. There is also one that describes physics and the pressure distributions within the nominal contact-area very well:

- Box-averaging method (good for structural design purposes)
- Iterative-search method (good for structural design purposes)
- Contour-averaging method (describes the physics and the pressure distribution)

The reanalysis of an earlier project work was performed in chapter 9 to see what input values that should be chosen in the material model of the iceberg. 4 analyses were performed, where the input values was obtained from earlier experiments executed by different scientist. Two of the analyses gave reasonable results, that were the analyses performed with Derradji-Aouat and Kierkegaard input parameters. The Kierkegaard's input parameter produces very similar results as the "Pond Inlet 1984" experiment. "Pond Inlet 1984" was a well-performed, where the impact scenario is very similar. The Kierkegaard's input material parameters are therefore concluded to be the "best" input parameters to representing a general iceberg, assuming that the iceberg used in the "Pond Inlet 1984" tests is representing a general iceberg.

The parametric study of the iceberg given in chapter 10 gave great insight in how sensitive the different material parameters were. The following material parameters were varied; material constants $(a_0, a_1 \text{ and} a_2)$, mesh-size and initial failure strain (ε_0). The parametric study gave the following findings. The yield surface is very sensitive to the material constants a_1 and a_2, and the yield surface is very important to the material model. Therefore the material model is very sensitive to the material constants a_1 and a_2, and the parametric study shows exactly that. The analysis is also very sensitive to the initial failure strain. The initial failure strain decides the amount of strain that is allowed before erosion is activated, and a higher allowed strain clearly leads to higher load and pressure levels. The mesh-size was also investigated in the parametric study, and the results converges for a mesh-size around 50[mm]. 50 [mm] mesh-size is therefore concluded to be the optimal mesh-size to use for the iceberg model. This mesh-size gives reasonable results, and still is reasonable efficient with respect to CPU-time.

The stochastic variation of the material properties to the iceberg model has been successfully implemented. The suggested stochastic variation method gives a new and better distribution of the local pressures compared to the homogenous iceberg model. The local pressures and high pressure zones have now a more irregular pattern where the locations of the high pressure zones have a more physical correct position. The overall force and pressure levels still are of similar size as the model before the stochastic variation. This is good since the model before the stochastic variation already gave decent load and pressure levels.

After the “best” iceberg model was developed, where the stochastic variation of material parameters is included. The distribution and level of structural damage output for the new iceberg model has been investigated. From the share-energy design analysis the structural damage output was obtained. The results from the analysis were that a blunter shape iceberg will cause more structural damage. This quite obvious since the iceberg is forced to a certain length into the panel, and a blunter shaped iceberg will force more ice into the panel. Still considering structural scantlings; i.e. stiffener/frame spacing, the relative strength between displacement of outer hull and ice crushing distance, the sharper shaped iceberg could be critical. Figures 62 and 63 show that the sharper shaped iceberg actually displaces the outer hull equally much if not more. Therefore possibility of puncturing inner hull and producing larger local displacement of the outer hull seems to be more critical for sharper shaped icebergs. The share-energy design analyses with sharper shaped iceberg gave similar indentation length of the outer hull of the panel, which indicated that the sharper shaped iceberg is not easier to crush than the blunter shaped iceberg.

The importance of the stochastic variation of the material parameters due to structural damage was also investigated. It seems the analysis produces results with large uncertainties, due to the large force amplitude in figure 65. Therefore only the beginning of the analyses is analyzed and compared. The stochastic variation seems to have a relative large effect on the structural damage output on the panel, due to more internal energy is produced in the panel for the inhomogeneous iceberg collision, and also larger displacement of the outer plate was produced. Therefore the inhomogeneous iceberg model seems to produce more structural damage to the panel compared to the homogenous iceberg model.

15 Recommendations for further work

There has been develop many MATLAB-scripts, and it is especially one script that is more comprehensive than the other MATLAB scripts. That is the PRO_SPA_CALC script that calculates the process pressure-area curve and spatial pressure-area curves for specific time-steps. The calculation of the spatial pressure-area curves is very extensive and there is no definite method to calculate the curves. The script has in total 5 methods to calculate the spatial pressure-area curves, some of the method area more robust than others. The Contour-averaging method and Iterative-search method are the most robust methods of those 5 methods developed. The algorithms these methods use can be further optimized and the expand-maxima method and box-averaging method should be more generalized.

There has been large focus on what forces and pressures the iceberg model produces. There are still more results that should be investigated. One of them is the strain and stress levels in the iceberg model. The amount of allowed straining before an element is eroded should be investigated. Since it lacks knowledge of how the stresses and strains are behaving in the sea ice material, due to the complexity of the ice material. There has been no experimental data to compare the stress and strain levels obtained in the iceberg model, and therefore stress and strain levels have been neglected in this master thesis.

The problem that occurred in the FORTRAN77 code was not solved. It should be investigated how the current code can be modified to obtain the same distribution as the MATLAB script. It is also unknown how inhomogeneous real icebergs are; the average size of each hard and weak zone and the intensity of the mixture of hard and weak zones are some questions that should be researched and investigated. From earlier experiments there is some indication that a larger part can be more confined than other parts. The current suggested method does not give the opportunity to decide the size or the intensity of the weak and hard zones. A method to actual control the size and intensity will probably give a more physical correct iceberg model. If such method could be implemented, investigating the effects on the distribution and level of structural damage on a colliding structure due to the change of size and intensity of hard and weak zones would be very interesting.

The lack of knowledge also gives uncertainties to what type of distribution the stochastic variation should have. The normal distribution was chose to obtain similar total load and pressure levels as it had before the stochastic variation. The process pressure-area curve gave larger values after the stochastic variation of the material parameters than before, and therefore other distribution should be investigated.

It has been a large focus on applying the correct material properties and implementing a good stochastic variation of material parameters, and therefore there has been performed limited amount of deformable analysis with various iceberg shapes and geometries. It would be valuable to see have this new modified iceberg model, with this stochastic variation of

material parameters will perform with different geometries. The share-energy design analysis should be performed with a lot of iceberg shapes where the effect of how easily the ice is crushed for a sharper shaped iceberg should be further analyzed. This master thesis did investigate the difference of sharper shaped iceberg compared to blunter shaped iceberg. The results obtained were difficult to analyze, due to the small iceberg model and the short impact duration chosen for the analysis. Both the size of the iceberg model and the impact duration was limited due lack of CPU-resources.

16 References

[1] *ICEBERG LOCATIONS* [Online]. U.S Department of Homeland Security, Navigation center. Available: http://www.navcen.uscg.gov/?pageName=IcebergLocations [Accessed 23.11 2012].

[2] *Patran, Complete FEA Modeling Solution* [Online]. MSC Software. Available: http://www.mscsoftware.com/Products/CAE-Tools/Patran.aspx [Accessed 23.11 2012].

[3] CHRIS ULAN-KVITBERG, H. K. A. C. D. 2011. Comparison of Pressure-Area Effects for Various Ice and Steel Indenters.

[4] D.M. MASTERSON, R. M. W. F., B. WRIGHT, T. KARNA AND W.P. MADDOCK 2007. A REVISED ICE PRESSURE-AREA CURVE.

[5] DALEY, C. 1994. *MSI Ice Loads Data: Compilation of Medium Scale Ice Indentation Test Results and Comparison to ASPPR*, Daley R&E.

[6] DALEY, C. 2007. Reanalysis of Ice Pressure-Area Relationships. *Marine Technology,* 44**,** 234-244.

[7] DERRADJI-AOUAT, A. 2003. Multi-surface failure criterion for saline ice in the brittle regime. *Cold Regions Science and Technology,* 36**,** 47-70.

[8] FREDERKING, R. The Local Pressure-Area Relation in Ship Impact with Ice. Proceedings 15th International Conference on Port and Ocean Engineering under Arctic Conditions, POAC'99, 1999. 687-696.

[9] GAGNON, R. E. & WANG, J. 2012. Numerical simulations of a tanker collision with a bergy bit incorporating hydrodynamics, a validated ice model and damage to the vessel. *Cold Regions Science and Technology,* 81**,** 26-35.

[10] GUDIMETLA, P. S. R., ST JOHNS, N., COLBOURNE, B., DALEY, C., BRUNEAU, S. E. & GAGNON, R. Strength and Pressure Profiles from Conical Ice Crushing Experiments.

[11] HALLQUIST, J. O. March 2006. LS-DYNA theory manual.

[12] HYUNWOOK KIM, C. D., CHRIS ULAN-KVITBERG 2012. Reappraisal of Pressure Distribution Induced by Ice-Structure Interaction Using High-Precision Pressure Measurement Film.

[13] ISO 2010. INTERNATIONAL STANDARD 19906 Petroleum and natural gas industries Arctic offshore structures.

[14] JONES, S. J. 1982. The confined compressive strength of polycrystalline ice. *Journal of Glaciology,* 28**,** 171-177.

[15] JONES, S. J. 2006. Comparison of the strength of iceberg and other freshwater ice and the effect of temperature.

[16] JORDAAN, I., LI, C., MACKEY, T., NOBAHAR, A. & BRUCE, J. 2005. Design Ice Pressure-Area Relationships: Molikpaq Data.

[17] KENNETH J. BIRD, R. R. C., DONALD L. GAUTIER (CARA PROJECT CHIEF), DAVID W. HOUSEKNECHT, TIMOTHY R. KLETT, JANET K. PITMAN, THOMAS E. MOORE, CHRISTOPHER J. SCHENK, MARILYN E. TENNYSON AND CRAIG J. WANDREY. 2008. Circum-Arctic Resource Appraisal: Estimates of Undiscovered Oil and Gas North of the Arctic Circle.

[18] LIU, Z. 2011. *Analytical and numerical analysis of iceberg collisions with ship structures,* Trondheim, Norwegian University of Science and Technology.

[19] LONG, W. F. 1992. Refraction by Spherical Surfaces.

[20] LSTC. *LS-DYNA* [Online]. Livemore Software Technology Corporation. Available: http://www.lstc.com/products/ls-dyna [Accessed 23.11 2012].
[21] LSTC 2012. LS-DYNA ® KEYWORD USER'S MANUAL VOLUME II Material Models. *Material Models.*
[22] NASA. *Arctic Sea Ice* [Online]. NASA, Earth Observatory. Available: http://earthobservatory.nasa.gov/Features/SeaIce/page3.php [Accessed 23.11 2012].
[23] NORSOK 2004. NORSOK STANDARD N-004. *Design of steel structures.*
[24] SCHULSON, E. M. & DUVAL, P. 2009. *Creep and fracture of ice,* Cambridge, Cambridge University Press.
[25] USGS. 2008. *90 Billion Barrels of Oil and 1,670 Trillion Cubic Feet of Natural Gas Assessed in the Arctic* [Online]. U.S. Geological Survey. Available: http://www.usgs.gov/newsroom/article.asp?ID=1980#.UK9aHofAcSO [Accessed 23.11 2012].
[26] WELLS, J., JORDAAN, I., DERRADJI-AOUAT, A. & TAYLOR, R. 2011. Small-scale laboratory experiments on the indentation failure of polycrystalline ice in compression: Main results and pressure distribution. *Cold Regions Science and Technology,* 65**,** 314-325.
[27] WRIGGERS, P. 2008. *Nonlinear Finite Element Methods,* Berlin, Heidelberg, Springer Berlin Heidelberg.

Appendices

Contents of the Appendices:

A. Additional files

Along with thesis a zip-file delivered with additional files, which includes the following:

- MATLAB scripts
- FORTRAN subroutine
- Poster of the master thesis
- Additional results
- A few input files (LS-DYNA)

The input files to LS-DYNA and the model files from MSC PATRAN are too large for the 60MB limit DIAM sets for the zip-file. Therefore these files have been delivered on a network drive created by Martin Storheim.

- Name of the network drive is: “isfjell”
- Folder name is: “MASTER_THESIS_ADITIONAL_FILES_SIMENBO”

B. MATLAB scripts

The MATLAB scripts are given in the following order:

```
%*************************************************************************
% FILE NAME: MAIN.m
% STRENGTH DESIGN METHOD MAIN POST-PROCESSING SCRIPT:
%*************************************************************************

clear
clc
close all

% COUNTS number of time-steps, nodes and finds the meshsize:
run('COUNT_IT')
% COUNT_IT gives/finds the needed input to the rest of the scripts!

% READS the NCFORC-FILE:
run('NCFORC_READ')

% Post-processing CALCULATION (PRESSURE-AREA CURVES)
run('PRO_SPA_CALC')

% PLOTS (PRESSURE-AREA CURVES)
run('PLOT')

% READS the MATSUM-FILE and Caclulates energy curves and plots
run('MATSUM')

%{
DEACTIVETED
%*************************************************************************
% SHARED ENERGY DESIGN METHOD MAIN POST-PROCESSING SCRIPT:
%*************************************************************************
clear
clc
close all

run('MATSUM')
run('RCFORC')
%}
```

```
%*************************************************************************
% FILENAME: COUNT_IT.m
%*************************************************************************
%   Counts different tings by use of NCFORC-file:
%       - Counts NODES
%       - Counts TIME-STEPS
%       - FINDS MESH-SIZE ON RIGID PLATE
%*************************************************************************
%-------------------------------->>        DEVELOPED BY: SIMEN BØHLERENGEN
%*************************************************************************
% COUNT NODES:
%-------------------------------------------------------------------------
fud = fopen('ncforc');
cou = 1;
for i=1:15
    tline = fgets(fud);
end

cou_node = 0;
c_node = 0;
f_cou_node = fscanf(fud,'%d',[1,1]);
while c_node == cou_node
    fgets(fud);
    fgets(fud);
    cou_node = fscanf(fud,'%d',[1,1]);

    c_node = f_cou_node + cou;
    cou = cou + 1;
end
NR_NODES = cou-1;
fclose(fud);

% COUNT TIMESTEP:
%-------------------------------------------------------------------------
fod = fopen('ncforc');

for i=1:7
    tline = fgets(fod);
end
TIME1=0;
TIME2=0.1;
cou_ts = 0;
while TIME1 < TIME2
    cou_ts = cou_ts + 1;
    tline = fgets(fod);
    tline = fgets(fod);
    tline = fgets(fod);
    TIME1 = fscanf(fod,'%*s %*c %*c %*c %f',[1,1]);

    for i=1:NR_NODES*2+3
        tline = fgets(fod);
    end

    tline = fgets(fod);
    tline = fgets(fod);
    tline = fgets(fod);
    TIME2 = fscanf(fod,'%*s %*c %*c %*c %f',[1,1]);

    for i=1:NR_NODES*2+3
```

```
        tline = fgets(fod);
    end
end
NR_TS = cou_ts*2-1;
fclose(fod);

% MESH SIZE:
%-------------------------------------------------------------------------
fud = fopen('ncforc');
cou = 1;
for i=1:15
    tline = fgets(fud);
end
fgets(fud);
coord1(1:3) = fscanf(fud,'%f %f %f',[1,3]);
fgets(fud);
fgets(fud);
coord2(1:3) = fscanf(fud,'%f %f %f',[1,3]);
Meshsize = (coord2(1)-coord1(1))+(coord2(2)-coord1(2))+...
           (coord2(3)-coord1(3));
fclose(fud);

% PRINTER UT:
%-------------------------------------------------------------------------
PRINT_TS = sprintf('ANTALL TIMESTEP:    %d',NR_TS);
PRINT_N = sprintf('ANTALL NODES:       %d',NR_NODES);
PRINT_MS =sprintf('MESHSIZE:           %f',Meshsize);
disp(PRINT_TS)
disp(PRINT_N)
disp(PRINT_MS)
```

```
%*************************************************************************
% FILE NAME: NCFORC_READ.m
%*************************************************************************
%                    Post-processing of the NCFORC-FILE
%*************************************************************************
%                          READS THE NCFORC-FILE
% PART 1: INPUT
% PART 2: READ FILE
%*************************************************************************
%------------------------------>>        DEVELOPED BY: SIMEN BØHLERENGEN
%*************************************************************************

fid = fopen('ncforc');
%*************************************************************************
%PART 1)    INPUT DATA
%*************************************************************************
% VELOCITY CHOSEN IN ANALYSIS, AND THE RADIUS OF THE ICEBERG:
v = 2;          % [m/s] velocity
r = 1.5;        % [m] radius of the Iceberg
%*************************************************************************

NR_W = sqrt(NR_NODES);
NR_H = sqrt(NR_NODES);

% Structure dimension:
%Width:
minW = -(NR_W-1)/2*Meshsize;
maxW = (NR_W-1)/2*Meshsize;
%Hight:
minH = -(NR_H-1)/2*Meshsize;
maxH = (NR_H-1)/2*Meshsize;

NR_TS = NR_TS-1;
%%
%*************************************************************************
% PART 2:    READ FILE:
%*************************************************************************
for i=1:7
tline = fgets(fid);
end
TIME = zeros(1,NR_TS);
 dyna = zeros(NR_W,NR_H,8,NR_TS);
for t=1:NR_TS
  tline1 = fgets(fid);
  tline2 = fgets(fid);
  tline3 = fgets(fid);
  % READ TIME at each time-step:
  TIME(t) = fscanf(fid,'%*s %*c %*c %*c %f',[1,1]);

for i=1:4
  tline = fgets(fid);
end

 for y = 1:NR_H
     for x = 1:NR_W
         % READ rest of the VALUES from NCFORC-file:
         % Cordinates, forces and the pressures is read
         dyna(x,y,1:8,t) = fscanf(fid,'%d %f %f %f %f %f %f %f',[1,8]);
     end
 end
```

```
end
fclose(fid);

savefile = 'VARIABLES/dyna.mat';
save(savefile, 'dyna');
```

```
%*************************************************************************
% FILE NAME: PRO_SPA_CALC.m
%*************************************************************************
%                    Post-processing of the NCFORC-FILE
%*************************************************************************
%      Process and Spatial pressure-area Curves calculation SCRIPT
% PART 1: Process pressure-area curve calculations
% PART 2: Spatial pressure-area curves calculations
%*************************************************************************
%------------------------------>>        DEVELOPED BY: SIMEN BØHLERENGEN
%*************************************************************************
% PART 1: Process presssure-area curve CALCULATION:
%*************************************************************************
indent = zeros(NR_TS,1);
force = zeros(NR_TS,1);
asum_cont_area = zeros(NR_TS,1);

for t=1:NR_TS

% FORCE OBTAINED:
%-------------------------------------------------------------------------
% Force in y-direcion (2D): (Activated)
force(t)= abs(sum(sum(dyna(:,:,2,t))));

% Resultant force: (Deactivated)
% force(t)= sqrt((sum(sum(dyna(:,:,2,t))))^2+...
%           (sum(sum(dyna(:,:,3,t))))^2+(sum(sum(dyna(:,:,4,t))))^2);


% Analytical , calculation, based on SAGITTA (geometry) relationship:
%-------------------------------------------------------------------------
% Finding the SAGITTA length (S):
if sum(sum(dyna(:,:,2,t))) == 0
ini_s = v*TIME(t);              % inital length (before impact)
start_impact = t+1;             % impact timestep
else
indent(t) = v*TIME(t);          % indentation length

% Radius of the circular contact-area (h):
seg_r = sqrt(2*(indent(t)-ini_s)*r-(indent(t)-ini_s)^2);

% Analytical contact area (based on SAGITTA relation):
asum_cont_area(t) = pi*seg_r^2;
end
end
%%
% Nonimal area vs Actual area:
%-------------------------------------------------------------------------
act_area = zeros(NR_TS,1);
area_ratio = zeros(NR_TS,1);
for i = 1:NR_TS
act_area(i) = sum(sum(dyna(:,:,2,i)~=0))*(Meshsize)^2;
area_ratio(i)  = act_area(i)/asum_cont_area(i);
end
%SAVE VARIABLES:
%-------------------------------------------------------------------------
savefile = 'VARIABLES/p_pa_c.mat';
p_pa_c = (10^(-6)*force)./asum_cont_area;
save(savefile, 'p_pa_c');
```

```
savefile = 'VARIABLES/s_pa_c.mat';
s_pa_c= (10^(-6)*force)./act_area;
save(savefile, 's_pa_c');

savefile = 'VARIABLES/time.mat';
save(savefile, 'TIME');

savefile = 'VARIABLES/indent.mat';
save(savefile, 'indent');

MN_F = force*10^-6;
savefile = 'VARIABLES/MN_F.mat';
save(savefile, 'MN_F');

savefile = 'VARIABLES/ppac.mat';
ppac = smooth(asum_cont_area,abs(p_pa_c),0.05,'loess');
save(savefile, 'ppac');

PRINT_CALC = sprintf('Forces, pressures and areas calculated');
disp(PRINT_CALC)
%%
%*************************************************************************
% PART II)   Spartial pressure-area curves CALCULATION:
%*************************************************************************
% CHOOSE TIME-STEPS:    (INPUT)
%-------------------------------------------------------------------------
% CHOSEN/SPECIFIC TIME-STEPS: (activeted)
disp('TIME-STEPS:')
locs = [11 21 41 61 81 111 141 171 200]

% TIME-STEP ON FORCEPEAKS: (deactivated)
%[pks,locs]=findpeaks(force,'minpeakdistance',30,'NPEAKS',9);

% Choose accuracy how many elements that are summed together:
% NB!! SHOULD SET TO 1, and 1 is default!
OppdTall = 1;
% Number of Maximum Analysed:
% NB, higher increase the matlab code significantly!
% 5 is default, and are know to give acceptable results.
ant_max = 5;
%Choose accuracy or number of points on x-axis for method number 3:
NR_CON = 40;
%-------------------------------------------------------------------------

STP = locs;

%Skriver ut oppdelingen:
OppdW = floor(NR_W/OppdTall);    % rectangle
OppdH = floor(NR_H/OppdTall);    % rectangle
Oppd = floor((OppdH+OppdW)/2);   % squares

elem = zeros(OppdH,OppdW,length(locs));
start_impact_area_values = zeros(OppdH,OppdW);
sy = zeros(ant_max,length(locs));
sx = zeros(ant_max,length(locs));

% SPLITT TOTAL AREA INTO SUB-AREAS:
for ste = 1:length(locs)
```

```
    n1= -OppdTall+1;
    n2= 0;
for x = 1:Oppd
    n1 = n1+OppdTall;
    n2 = n2+OppdTall;
    m1 = -OppdTall+1;
    m2 = 0;

 for c = 1:Oppd
    m1 = m1+OppdTall;
    m2 = m2+OppdTall;

elem(c,x,ste) = (sum(sum(dyna(m1:m2,n1:n2,2,STP(ste)))));
start_impact_area_values(c,x) = sum(sum(dyna(m1:m2,n1:n2,5,start_impact)));
 end
end
end

% FINDING MAXIMUM PRESSURES and OBTAIN ACTUAL AREA:
act_ar_sum = zeros(length(locs),1);
act_ar_sum_k = zeros(length(locs),1);
act_ar_sum_r = zeros(length(locs),1);

for ste = 1:length(locs)

act_ar=elem(:,:,ste);
act_ar(act_ar == 0) = NaN;
act_ar = ~isnan(act_ar);
act_ar_sum(ste,1) = sum(sum(act_ar(:,:)));
act_ar_r = sum(act_ar,2);
act_ar_r(act_ar_r == 0) = NaN;
act_ar_r = ~isnan(act_ar_r);
act_ar_k = sum(act_ar,1);
act_ar_k(act_ar_k == 0) = NaN;
act_ar_k = ~isnan(act_ar_k);
act_ar_sum_r(ste,1) = sum(act_ar_r);
act_ar_sum_k(ste,1) = sum(act_ar_k);


Arraycopy = elem(:,:,ste);
Array_dup = elem(:,:,ste);

for j = 1:ant_max
   [num, Index(j)] = min(Arraycopy(:));
   Arraycopy(Index(j)) = 0;
   maximumValues = Array_dup(Index);
   maxVal = find(Array_dup==maximumValues(j));
   [sx(j,ste) sy(j,ste)] = ind2sub(size(Array_dup),maxVal(1));
end
end
%%



%-------------------------------------------------------------------------
% CALCULATION of METHOD 1A
% Expand-Maxima Method (rectangular shape areas):
%-------------------------------------------------------------------------
PRINT_CALC = sprintf('Calculation of method 1A:');
```

```
disp(PRINT_CALC)

ar_con1a = zeros(OppdW,OppdH,ant_max,length(locs));

for ste = 1:length(locs)     % TIME-STEPS
for sa = 1:ant_max           % High presssure zones
x=sx(sa,ste);
y=sy(sa,ste);
copy_elem=elem(:,:,ste);
act_ar1a = act_ar_sum_r+act_ar_sum_k-1;

sum_area = 0;
sum_pressure = 0;
k=0;
clear rp kp rad_max rad_min kol_min kol_max
runde = 0;

while sum(sum(copy_elem(:,:))) ~= Oppd*Oppd*0
    k = 1+k;
    rp(k) = x(1);
    kp(k) = y(1);

    rad_max = max(rp(:));
    rad_min = min(rp(:));
    kol_max = max(kp(:));
    kol_min = min(kp(:));
    rad = rad_min:rad_max;
    kol = kol_min:kol_max;

% Element with zeros pressure
trek_zero = sum(sum(elem(rad_min:rad_max,kol_min:kol_max,ste)==0));
% Actual area for each TIME-STEP and for each area expansion:
sum_area = (rad_max-rad_min+1)*(kol_max-kol_min+1)*...
    (Meshsize*OppdTall)^2-(Meshsize*OppdTall)^2*trek_zero;
M1A.SA(k,ste) = sum_area;

% Pressure for each TIME-STEP and for each area expansion:
    sum_pressure = sum(sum(elem(rad_min:rad_max,kol_min:kol_max,ste)));
    M1A.spac(sa,k,ste) = sum_pressure/M1A.SA(k,ste);
    M1A.SP(k,ste) = min(M1A.spac(:,k,ste));

% Creating COLOUR LEVELS for the contour-plot in script: PLOT.m
    if k/act_ar1a <= 0.005
        ar_con1a(x,y,sa,ste) = 10;
    elseif k/act_ar1a <= 0.10
        ar_con1a(x,y,sa,ste) = 9;
    elseif k/act_ar1a <= 0.20
        ar_con1a(x,y,sa,ste) = 8;
    elseif k/act_ar1a <= 0.30
        ar_con1a(x,y,sa,ste) = 7;
    elseif k/act_ar1a <= 0.40
        ar_con1a(x,y,sa,ste) = 6;
    elseif k/act_ar1a <= 0.50
        ar_con1a(x,y,sa,ste) = 5;
    elseif k/act_ar1a <= 0.60
        ar_con1a(x,y,sa,ste) = 4;
    elseif k/act_ar1a <= 0.70
        ar_con1a(x,y,sa,ste) = 3;
    elseif k/act_ar1a <= 0.80
        ar_con1a(x,y,sa,ste) = 2;
```

```
    elseif k/act_ar1a <= 0.90
        ar_con1a(x,y,sa,ste) = 1;
    elseif k/act_ar1a <= 0.99
        ar_con1a(x,y,sa,ste) = 0;
    else
    end

    copy_elem(rad_min:rad_max,kol_min:kol_max) = 0;

    right = sum(copy_elem(rad_min:rad_max,kol_max+1)/...
        (Meshsize*(rad_max-rad_min)));
    left = sum(copy_elem(rad_min:rad_max,kol_min-1)/...
        (Meshsize*(rad_max-rad_min)));
    up = sum(copy_elem(rad_min-1,kol_min:kol_max)/...
        (Meshsize*(kol_max-kol_min)));
    down = sum(copy_elem(rad_max+1,kol_min:kol_max)/...
        (Meshsize*(kol_max-kol_min)));

    mat_check = [right,left,up,down];
    pos_check = find(mat_check==min(min(mat_check)));

    if pos_check == 1
        x = rad;
        y = kol_max + 1;
    elseif pos_check == 2
        x = rad;
        y = kol_min - 1;
    elseif pos_check == 3
        x = rad_min - 1;
        y = kol;
    elseif pos_check == 4
        x = rad_max + 1;
        y = kol;
    else

        runde = runde + 1;
        if runde == 5
            runde = 1;
        else
        end

        if runde == 1
            x = rad;
            y = kol_max + 1;
        elseif runde == 2
            x = rad;
            y = kol_min - 1;
        elseif runde == 3
            x = rad_min - 1;
            y = kol;
        elseif runde == 4
            x = rad_max + 1;
            y = kol;
        else
        end
    end
end
end
end
disp('Method 1A DONE')
```

```
%% ------------------------------------------------------------------------
% CALCULATION of METHOD 1B
% Expand-Maxima Method (rectangular shape areas):
%-------------------------------------------------------------------------
PRINT_CALC = sprintf('Calculation of method 1B:');
disp(PRINT_CALC)

ar_con1b = zeros(OppdW,OppdH,ant_max,length(locs));

for ste = 1:length(locs)
    for sa = 1:ant_max
        x=sx(sa,ste);
        y=sy(sa,ste);
        copy_elem=elem(:,:,ste);
        sum_area = 0;
        sum_pressure = 0;
        k=0;
        clear rp kp

while sum(sum(copy_elem(:,:))) ~= Oppd*Oppd*0
    k = 1+k;

% Actual area for each TIME-STEP and for each area expansion:
    sum_area = sum_area + (Meshsize*OppdTall)^2;
    M1B.SA(k,ste) = sum_area;
% Pressure for each TIME-STEP and for each area expansion:
    sum_pressure = sum_pressure + elem(x,y,ste);
    M1B.spac(sa,k,ste) = sum_pressure/M1B.SA(k,ste);
    M1B.SP(k,ste) = min(M1B.spac(:,k,ste));
    copy_elem(x,y) = 0;

% Creating COLOUR LEVELS for the contour-plot in script: PLOT.m
    if k/act_ar_sum(ste,1) <= 0.005
        ar_con1b(x,y,sa,ste) = 10;
    elseif k/act_ar_sum(ste,1) <= 0.01
        ar_con1b(x,y,sa,ste) = 9;
    elseif k/act_ar_sum(ste,1) <= 0.05
        ar_con1b(x,y,sa,ste) = 8;
    elseif k/act_ar_sum(ste,1) <= 0.10
        ar_con1b(x,y,sa,ste) = 7;
    elseif k/act_ar_sum(ste,1) <= 0.20
        ar_con1b(x,y,sa,ste) = 6;
    elseif k/act_ar_sum(ste,1) <= 0.30
        ar_con1b(x,y,sa,ste) = 5;
    elseif k/act_ar_sum(ste,1) <= 0.40
        ar_con1b(x,y,sa,ste) = 4;
    elseif k/act_ar_sum(ste,1) <= 0.50
        ar_con1b(x,y,sa,ste) = 3;
    elseif k/act_ar_sum(ste,1) <= 0.60
        ar_con1b(x,y,sa,ste) = 2;
    elseif k/act_ar_sum(ste,1) <= 0.80
        ar_con1b(x,y,sa,ste) = 1;
    elseif k/act_ar_sum(ste,1) <= 0.95
        ar_con1b(x,y,sa,ste) = 0;
    else
    end

    rp(k) = x;
```

```
    kp(k) = y;

    for i=1:k

     %CHECKS left, right, up and down elements:
     check1 = min((copy_elem(rp(i)-1,kp(i))),(copy_elem(rp(i),kp(i)-1)));
     check2 = min((copy_elem(rp(i)+1,kp(i))),(copy_elem(rp(i),kp(i)+1)));
     check11 = min(check1,check2);

%CHECKS DIAGONAL elements:
%check3 = min((copy_elem(rp(i)-1,kp(i)-1)),(copy_elem(rp(i)+1,kp(i)+1)));
%check4 = min((copy_elem(rp(i)-1,kp(i)+1)),(copy_elem(rp(i)+1,kp(i)-1)));
%check22 = min(check3,check4);

         next_HPA = min(check11);  %INCLUDE for diagonal search,(check22)
         HPA(i) = next_HPA;
    end

    HPAlist = min(HPA(:));

    if HPAlist == 0
    search = 1;
    while search<=20 && HPAlist == 0 && min(rp)-search >= 2 ...
           && min(kp)-search >= 2 ...
           && max(rp)+search <= length(elem(:,:,ste))-1 ...
           && max(kp)+search <= length(elem(:,:,ste))-1

       search = search +1;
       for i=1:k
            %CHECKS left, right, up and down elements:
            check1 = min((copy_elem(rp(i)-search,kp(i))),...
                (copy_elem(rp(i),kp(i)-search)));
            check2 = min((copy_elem(rp(i)+search,kp(i))),...
                (copy_elem(rp(i),kp(i)+search)));
            check11 = min(check1,check2);

%CHECKS DIAGONAL elements:
%check3 = min((copy_elem(rp(i)-1,kp(i)-1)),(copy_elem(rp(i)+1,kp(i)+1)));
%check4 = min((copy_elem(rp(i)-1,kp(i)+1)),(copy_elem(rp(i)+1,kp(i)-1)));
%check22 = min(check3,check4);

         next_HPA = min(check11); %INCLUDE for diagonal search,(check22)
         HPA(i) = next_HPA;
       end
    HPAlist = min(HPA(:));
    end
    else
    end
    [x y] = ind2sub(size(copy_elem),find(copy_elem==HPAlist));
    x=x(1);
    y=y(1);
end
end
end
disp('Method 1B DONE')

%% ------------------------------------------------------------------------
% EXPANDING AREA PROCESS ITERATION: NUMBER 2
% Box-Averaging Method
```

```
%-------------------------------------------------------------------------
PRINT_CALC = sprintf('Calculation of method 2:');
disp(PRINT_CALC)

ar_con2 = zeros(OppdW,OppdH,length(locs));

for ste = 1:length(locs)

% Starting/first sub-area, before expanding uniformaly to each side!
% Chosen to be at first impact position.
    max_siav = min(min(start_impact_area_values(:,:)));
    [x y] = ind2sub(size(start_impact_area_values),...
        find(start_impact_area_values==max_siav));

    m1 = x;
    n1 = y;
    m2 = x;
    n2 = y;

    sum_pressure = 0;
    sum_area = 0;
    k = 0;

    act_ar2 = min(act_ar_sum_r,act_ar_sum_k);

while length(elem(:,:,ste))> m2 && length(elem(:,:,ste))>n2...
        && 1<m1 && 1<n1

    k=k+1;
    m1 = m1-1;
    n1 = n1-1;
    m2 = m2+1;
    n2 = n2+1;

% Actual area for each TIME-STEP and for each area expansion:
    trek_zero = sum(sum(elem(m1:m2,n1:n2,ste)==0));
    M2.SA(ste,k) = ((m2-m1+1)*Meshsize*OppdTall)^2 -...
        (Meshsize*OppdTall)^2*trek_zero;
% Pressure for each TIME-STEP and for each area expansion:
    M2.SP(ste,k) = sum(sum(elem(m1:m2,n1:n2,ste)))/ M2.SA(ste,k);


% Creating COLOUR LEVELS for the contour-plot in script: PLOT.m
    if k/act_ar2(ste) <= 0.05
        ar_con2(m1:m2,n1:n2,ste) = ar_con2(m1:m2,n1:n2,ste)+ 1;
    elseif k/act_ar2(ste) <= 0.15
        ar_con2(m1:m2,n1:n2,ste) = ar_con2(m1:m2,n1:n2,ste)+ 1;
    elseif k/act_ar2(ste) <= 0.30
        ar_con2(m1:m2,n1:n2,ste) = ar_con2(m1:m2,n1:n2,ste)+ 1;
    elseif k/act_ar2(ste) <= 0.50
        ar_con2(m1:m2,n1:n2,ste) = ar_con2(m1:m2,n1:n2,ste)+ 1;
    elseif k/act_ar2(ste) <= 0.80
        ar_con2(m1:m2,n1:n2,ste) = ar_con2(m1:m2,n1:n2,ste)+ 1;
    else
    end
end
end
disp('Method 2 DONE')
```

```
%% ------------------------------------------------------------------------
% EXPANDING AREA PROCESS ITERATION: NUMBER 3
% Contour-Averaging Method
%-------------------------------------------------------------------------
PRINT_CALC = sprintf('Calculation of method 3:');
disp(PRINT_CALC)

ar_con3 = zeros(OppdW,OppdH,length(locs));

for ste = 1:length(locs)
c = 0;
list_elem = zeros(1,(length(elem(:,:,ste)))^2);

for k = 1:length(elem(:,:,ste))
    for h = 1:length(elem(:,:,ste))
        c = c+1;
        list_elem(c) = elem(k,h,ste);
    end
end

sort_list_elem = sort(list_elem);
level_down = abs(sort_list_elem(1)):-abs(sort_list_elem(1)/NR_CON):0;
level_down(1) = level_down(1)-1;

if exist('M3') == 0
M3.SP = zeros(length(locs),NR_CON+1);
M3.SA = zeros(length(locs),NR_CON+1);
else
end

for i=1:NR_CON+1
    k = 1;
    sum1 = 0;

    while abs(sort_list_elem(k)) > level_down(i)
% Actual area for each TIME-STEP and for each area expansion:
        M3.SA(ste,i) = (Meshsize*OppdTall)^2*k ;

        sum1 = sum1 + abs(sort_list_elem(k));
        M3.F(i) = sum1;

% Pressure for each TIME-STEP and for each area expansion:
        M3.SP(ste,i) = M3.F(i)/M3.SA(ste,i);

        k = k + 1;
    end
end
max_fo = min(min(elem(:,:,ste)));

for y=1:OppdH
    for x=1:OppdW

% Creating COLOUR LEVELS for the contour-plot in script: PLOT.m
    if abs(elem(x,y,ste)/max_fo) <= 0
        ar_con3(x,y,ste) = 0;
    elseif abs(elem(x,y,ste)/max_fo) <= 0.001
        ar_con3(x,y,ste) = 1;
    elseif abs(elem(x,y,ste)/max_fo) <= 0.005
        ar_con3(x,y,ste) = 2;
```

```
    elseif abs(elem(x,y,ste)/max_fo) <= 0.01
        ar_con3(x,y,ste) = 3;
    elseif abs(elem(x,y,ste)/max_fo) <= 0.10
        ar_con3(x,y,ste) = 4;
    elseif abs(elem(x,y,ste)/max_fo) <= 0.20
        ar_con3(x,y,ste) = 5;
    elseif abs(elem(x,y,ste)/max_fo) <= 0.30
        ar_con3(x,y,ste) = 6;
    elseif abs(elem(x,y,ste)/max_fo) <= 0.40
        ar_con3(x,y,ste) = 7;
    elseif abs(elem(x,y,ste)/max_fo) <= 0.50
        ar_con3(x,y,ste) = 8;
    elseif abs(elem(x,y,ste)/max_fo) <= 0.70
        ar_con3(x,y,ste) = 9;
    elseif abs(elem(x,y,ste)/max_fo) <= 0.80
        ar_con3(x,y,ste) = 10;
    else
    end

    end
end
end
disp('Method 3 DONE')

%% ------------------------------------------------------------------------
% EXPANDING AREA PROCESS ITERATION: NUMBER 4
% Iteration-Maxima Method
%-------------------------------------------------------------------------
PRINT_CALC = sprintf('Calculation of method 4:');
disp(PRINT_CALC)

Oppd_length = ceil(Oppd/3);
arsize = zeros(Oppd_length,1);
for i=1:Oppd_length
    arsize(i) = Oppd-3*i;
end
length_trek = (sum(arsize))*2;
area_length = Oppd^2-length_trek;


ar_con4_all = zeros(OppdH,OppdW,length(locs));
M5t = zeros(area_length,2,length(locs));

max_sub = zeros(area_length,1);
pressure_sub = zeros(area_length,1);
area_sub = zeros(area_length,1);
subyy = zeros(area_length,1);
subxx = zeros(area_length,1);
exrad = zeros(area_length,1);
exkol = zeros(area_length,1);
M4 = zeros(area_length,2);
M4sort = zeros(area_length,2);

for ste = 1:length(locs)

    calc_mat = zeros(OppdH,OppdW,area_length);

    ex_rad=0;
    ex_kol = 0;
```

```
    maxnu =0;
    ifcount=0;

for exd = 1:OppdH
   ex_rad = ex_rad + 1;

    while  ex_kol < Oppd && ex_kol/ex_rad < 3
        ex_kol = ex_kol + 1;
        maxnu = maxnu+1;
        rs=0;

        while rs <= (OppdH-ex_rad)
            rs = rs + 1;
            re = rs + ex_rad-1;
            ks = 0;

           while ks <= (OppdW-ex_kol)
                ks = ks + 1;
                ke = ks + ex_kol-1;

                calc_mat(rs,ks,maxnu) = sum(sum(elem(rs:re,ks:ke,ste)));
           end
        end
        max_sub(maxnu) = min(min(calc_mat(:,:,maxnu)));
        [suby subx] = ind2sub(size(calc_mat(:,:,maxnu)),...
            find(calc_mat(:,:,maxnu)==max_sub(maxnu)));

%Zero pressure elements:
trek_zero = sum(sum(elem(suby(ceil(length(suby)/2)):...
(suby(ceil(length(suby)/2))+ex_rad-1),...
subx(ceil(length(subx)/2)):(subx(ceil(length(subx)/2))+ex_kol-1),ste)==0));
% Actual area for each sub-area:
area_sub(maxnu) = ex_rad*ex_kol*(Meshsize*OppdTall)^2 -...
    (Meshsize*OppdTall)^2*trek_zero;
% Pressure for each sub-area:
pressure_sub(maxnu) = max_sub(maxnu)/area_sub(maxnu);

    subyy(maxnu) = suby(ceil(length(subx)/2));
    subxx(maxnu) = subx(ceil(length(subx)/2));
    exrad(maxnu)=ex_rad;
    exkol(maxnu)=ex_kol;
    end
            if mod(ex_rad,3) == 0 && ex_rad > 0
                ifcount = ifcount + 1;
                ex_kol = ifcount;
            else
                ex_kol = ifcount;
            end
end

    M4(:,1) = area_sub(:);
    M4(:,2) = pressure_sub(:);
    M4sort(:,:) = sortrows(M4(:,:),[1 2]);
    M5t(:,:,ste) = M4sort(:,:);

    M5maxar = zeros(area_length,2);
    M5maxar(:,:) = M5t(:,:,ste);
    M5maxar(:,2) = abs(M5maxar(:,2))*10^-6;
    [M5_pks,M5_locs]=findpeaks(M5maxar(:,2),'minpeakdistance',10);
```

```
% Creating COLOUR LEVELS for the contour-plot in script: PLOT.m
ar_con4_all(subyy(area_length):(subyy(area_length)+exrad(area_length)-1)...
  ,subxx(area_length):(subxx(area_length)+exkol(area_length)-1),ste) = 0;
ar_con4_all(subyy(ceil(M5_locs(end)*0.8)):(subyy(ceil(M5_locs(end)*0.8))...
  +exrad(ceil(M5_locs(end)*0.8))-1),subxx(ceil(M5_locs(end)*0.8)):...
  (subxx(ceil(M5_locs(end)*0.8))+exkol(ceil(M5_locs(end)*0.8))-1),ste) = 1;
ar_con4_all(subyy(ceil(M5_locs(end)*0.6)):(subyy(ceil(M5_locs(end)*0.6))...
  +exrad(ceil(M5_locs(end)*0.6))-1),subxx(ceil(M5_locs(end)*0.6)):...
  (subxx(ceil(M5_locs(end)*0.6))+exkol(ceil(M5_locs(end)*0.6))-1),ste) = 2;
ar_con4_all(subyy(ceil(M5_locs(end)*0.5)):(subyy(ceil(M5_locs(end)*0.5))...
  +exrad(ceil(M5_locs(end)*0.5))-1),subxx(ceil(M5_locs(end)*0.5)):...
  (subxx(ceil(M5_locs(end)*0.5))+exkol(ceil(M5_locs(end)*0.5))-1),ste) = 3;
ar_con4_all(subyy(ceil(M5_locs(end)*0.4)):(subyy(ceil(M5_locs(end)*0.4))...
 +exrad(ceil(M5_locs(end)*0.4))-1),subxx(ceil(M5_locs(end)*0.4)):...
 (subxx(ceil(M5_locs(end)*0.4))+exkol(ceil(M5_locs(end)*0.4))-1),ste) = 4;
ar_con4_all(subyy(ceil(M5_locs(end)*0.3)):(subyy(ceil(M5_locs(end)*0.3))...
  +exrad(ceil(M5_locs(end)*0.3))-1),subxx(ceil(M5_locs(end)*0.3)):...
  (subxx(ceil(M5_locs(end)*0.3))+exkol(ceil(M5_locs(end)*0.3))-1),ste) = 5;
ar_con4_all(subyy(ceil(M5_locs(end)*0.2)):(subyy(ceil(M5_locs(end)*0.2))...
  +exrad(ceil(M5_locs(end)*0.2))-1),subxx(ceil(M5_locs(end)*0.2)):...
  (subxx(ceil(M5_locs(end)*0.2))+exkol(ceil(M5_locs(end)*0.2))-1),ste) = 6;
ar_con4_all(subyy(ceil(M5_locs(end)*0.1)):(subyy(ceil(M5_locs(end)*0.1))...
  +exrad(ceil(M5_locs(end)*0.1))-1),subxx(ceil(M5_locs(end)*0.1)):...
  (subxx(ceil(M5_locs(end)*0.1))+exkol(ceil(M5_locs(end)*0.1))-1),ste) = 7;
ar_con4_all(subyy(ceil(M5_locs(end)*0.05)):...
    (subyy(ceil(M5_locs(end)*0.05))+exrad(ceil(M5_locs(end)*0.05))-1),...
    subxx(ceil(M5_locs(end)*0.05)):(subxx(ceil(M5_locs(end)*0.05))+...
    exkol(ceil(M5_locs(end)*0.05))-1),ste) = 8;
ar_con4_all(subyy(ceil(M5_locs(end)*0.01)):...
    (subyy(ceil(M5_locs(end)*0.01))+exrad(ceil(M5_locs(end)*0.01))-1),...
    subxx(ceil(M5_locs(end)*0.01)):(subxx(ceil(M5_locs(end)*0.01))+...
    exkol(ceil(M5_locs(end)*0.01))-1),ste) = 9;
ar_con4_all(subyy(ceil(M5_locs(end)*0.005)):...
    (subyy(ceil(M5_locs(end)*0.005))+exrad(ceil(M5_locs(end)*0.005))-1),...
    subxx(ceil(M5_locs(end)*0.005)):(subxx(ceil(M5_locs(end)*0.005))+...
    exkol(ceil(M5_locs(end)*0.005))-1),ste) = 10;

 PRINT_CALC = sprintf('Calculated SPACs for TIME-STEPS:    %d/9',ste);
 disp(PRINT_CALC)
end
disp('Method 4 DONE')
```

```
%*************************************************************************
% FILE NAME: MATSUM.m
%*************************************************************************
%                  Post-processing of the MATSUM-FILE
%*************************************************************************
% PART 1: Read MATSUM-file
% PART 2: Calculate different energies
% PART 3: ENERGY CURVES PLOTSENERGIES
%*************************************************************************
%------------------------------>>        DEVELOPED BY: SIMEN BØHLERENGEN
%*************************************************************************
% MAKE USE OF A WORD-COUNT FUNCTION:
NR_TS = wordcount2('matsum');    % counts number of the word = time
                                 % gives number of time-step
%%
close all
%*************************************************************************
% PART 1: READ IN MATSUM-FILE
%*************************************************************************
fid = fopen('matsum');
for i=1:5
    tline = fgets(fid);
end
b = fscanf(fid,'%d %*s',[1,inf]);
NR_MAT = length(b);
tline = fgets(fid);

TIME = zeros(1,NR_TS);
values = zeros(NR_MAT,11,NR_TS);
for t = 1:NR_TS
    for i = 1:3
        tline = fgets(fid);
    end
TIME(t) = fscanf(fid,'%*s %*c %f',[1,1]);
for m = 1:NR_MAT
    fscanf(fid,'%*s %s',[1,1]);
    values(m,1:11,t) = fscanf(fid,'%*s %f',[1,11]);
    tline = fgets(fid);
    tline = fgets(fid);
end
end
fclose(fid);
%*************************************************************************
% PART 2: Calculate Different ENERGIES from LS-DYNA ANALYSIS
%*************************************************************************
Etot = zeros(NR_MAT,NR_TS);
Ekin = zeros(NR_MAT,NR_TS);
Eint = zeros(NR_MAT,NR_TS);
Eero_int = zeros(NR_MAT,NR_TS);
Eero_kin = zeros(NR_MAT,NR_TS);
Ehge = zeros(NR_MAT,NR_TS);
Eint_tot = zeros(NR_MAT,NR_TS);
Ekin_tot = zeros(NR_MAT,NR_TS);
Etot_totm = zeros(1,NR_TS);
Ekin_totm = zeros(1,NR_TS);
Eint_totm = zeros(1,NR_TS);

Eship_tot = zeros(1,NR_TS);
Eship_kin = zeros(1,NR_TS);
Eship_int = zeros(1,NR_TS);
```

```
Eship_ero_int = zeros(1,NR_TS);
Eship_ero_kin = zeros(1,NR_TS);
Eship_hge = zeros(1,NR_TS);
Eship_int_tot = zeros(1,NR_TS);
Eiceberg_tot = zeros(1,NR_TS);
Eiceberg_kin = zeros(1,NR_TS);
Eiceberg_int = zeros(1,NR_TS);
Eiceberg_ero_int = zeros(1,NR_TS);
Eiceberg_ero_kin = zeros(1,NR_TS);
Eiceberg_hge = zeros(1,NR_TS);
Eiceberg_int_tot = zeros(1,NR_TS);

for t = 1:NR_TS
    for m = 1:NR_MAT
Ekin(m,t) = Ekin(m,t) + values(m,2,t);
Eint(m,t) = Eint(m,t) + values(m,1,t);
Eero_int(1,t) = Eero_int(1,t) + values(m,3,t);
Eero_kin(1,t) = Eero_kin(1,t) + values(m,4,t);
Ehge(m,t) = Ehge(m,t) + values(m,11,t);

Ekin_tot(m,t) = Ekin_tot(m,t) + values(m,2,t) + values(m,4,t);
Eint_tot(m,t) = Eint_tot(m,t) + values(m,1,t) + values(m,3,t);

Etot(m,t) = Etot(m,t) + values(m,1,t) + values(m,2,t) +...
    values(m,11,t) + values(m,3,t) + values(m,4,t);

   end
Etot_totm(1,t) = Etot_totm(1,t) + sum(Etot(:,t));
Ekin_totm(1,t) = Ekin_totm(1,t) + sum(Ekin(:,t));
Eint_totm(1,t) = Eint_totm(1,t) + sum(Eint(:,t));

% NB! ICEBERG MODEL NEED TO BE MATERIAL 1 AND 2!

%SHIP ENERGIES:
Eship_tot(t) = sum(Etot(3:end,t));          % TOTAL ENERGY
Eship_int(t) = sum(Eint(3:end,t));          % INTERNAL
Eship_ero_int(t) = sum(Eero_int(3:end,t));  % ERODED INTERNAL
Eship_int_tot(t) = sum(Eint_tot(3:end,t));  % TOTAL INTERNAL
Eship_kin(t) = sum(Ekin(3:end,t));          % KINETIC
Eship_ero_kin(t) = sum(Eero_kin(3:end,t));  % ERODED KINETIC
Eship_hge(t) = sum(Ehge(3:end,t));          % HOURGLASS
%ICEBERG ENERGIES:
Eiceberg_tot(t) = sum(Eint(1:2,t));         % TOTAL ENERGY
Eiceberg_int(t) = sum(Eint(1:2,t));          % INTERNAL
Eiceberg_ero_int(t) = sum(Eero_int(1:2,t));  % ERODED INTERNAL
Eiceberg_int_tot(t) = sum(Eint_tot(1:2,t));  % TOTAL INTERNAL
Eiceberg_kin(t) = sum(Ekin(1:2,t));          % KINETIC
Eiceberg_ero_kin(t) = sum(Eero_kin(1:2,t));  % ERODED KINETIC
Eiceberg_hge(t) = sum(Ehge(1:2,t));          % HOURGLASS
end

%TRANSFORM UNIT FROM PA -> MPa:
Ekin = Ekin*10^-6;
Eint =Eint*10^-6;
Eero_int = Eero_int*10^-6;
Eero_kin  = Eero_kin*10^-6;
Ehge = Ehge*10^-6;
Ekin_tot = Ekin_tot*10^-6;
Eint_tot = Eint_tot*10^-6;
Etot_totm =Etot_totm*10^-6;
```

```
Ekin_totm = Ekin_totm*10^-6;
Eint_totm = Eint_totm*10^-6;

%SHIP:
Eship_tot = Eship_tot*10^-6;
Eship_int = Eship_int*10^-6;
Eship_ero_int =Eship_ero_int*10^-6;
Eship_int_tot = Eship_int_tot*10^-6;
Eship_kin = Eship_kin*10^-6;
Eship_ero_kin = Eship_ero_kin*10^-6;
Eship_hge = Eship_hge*10^-6;
%ICEBERG:
Eiceberg_tot = Eiceberg_tot*10^-6;
Eiceberg_int = Eiceberg_int*10^-6;
Eiceberg_ero_int = Eiceberg_ero_int*10^-6;
Eiceberg_int_tot = Eiceberg_int_tot*10^-6;
Eiceberg_kin = Eiceberg_kin*10^-6;
Eiceberg_ero_kin = Eiceberg_ero_kin*10^-6;
Eiceberg_hge = Eiceberg_hge*10^-6;

% PRODUCING X-axis for the ship graphs:
NEG_TIME = -TIME;

%%
%%************************************************************************
% PART 3: ENERGY CURVES PLOTSENERGIES
%%************************************************************************
% RELATIVE STRENGTH BETWEEN STRUCTURE AND ICEBERG PLOT:
%-------------------------------------------------------------------------
figure(100)
centeraxes(gca,0);
set(gcf,'color','w');
plot(NEG_TIME,Eship_int_tot,'r-',TIME,Eiceberg_int_tot,'b-', 'LineWidth',1)
title('SHIP (RIGHT SIDE)     VS      ICEBERG (LEFT SIDE)')
xlabel('Time [s]')
ylabel('Energy [MPa]')
opt.fontname = 'helvetica';
opt.fontsize = 8;
centeraxes(gca,opt);
box on
hold off

%%
print -dpng FIGURES\MATSUM_F01_RELATIVE_STRENGTH.png -r600
%%
% INTERNAL ENERGY PLOTS:
%-------------------------------------------------------------------------
figure(2)
plot(TIME,Eint_tot(1,:),'r-',TIME,Eint(1,:),'b-', TIME,Eero_int(1,:),...
    'm-','LineWidth',1)
title('Total internal energy vs Internal energy vs Eroded internal energy')
set(gcf,'color','w');
legend('Total internal energy','Internal energy','Eroded internal energy')
xlabel('Time [s]')
ylabel('Energy [MPa]')
box on
hold off
%%
print -dpng FIGURES\MATSUM_F01_INT_EN_and_HG_EN.png -r600
%%
```

```
figure(3)
plot(TIME,Ehge(1,:),'r-', TIME, Eint(1,:),'b-','LineWidth',1)
title('Hourglass energy VS Internal total')
legend('Hourglass energy','Internal energy')
xlabel('Time [s]')
ylabel('Energy [MPa]')
set(gcf,'color','w');
box on
hold off
%%
print -dpng FIGURES\MATSUM_F02_INT_EN_NotEROD_and_HG_EN.png.png -r600
%%
figure(4)
plot(TIME,Ehge(1,:),'r-', TIME, Eint_tot(1,:),'b-','LineWidth',1)
title('Hourglass energy VS total Internal energy')
set(gcf,'color','w');
xlabel('Time [s]')
ylabel('Energy [MPa]')
legend('Hourglass energy','Total internal energy')
box on
hold off
%%
print -dpng FIGURES\MATSUM_F03_Eint_tot_VS_Ehge.png -r600
%%
% HOURGLASS ENERGY PLOT:
%%-------------------------------------------------------------------------
figure(5)
plot(TIME,Ehge(1,:),'b-','LineWidth',1)
title('Hourglass energy')
xlabel('Time [s]')
ylabel('Energy [MPa]')
set(gcf,'color','w');
box on
hold off
%%
% TOTAL ENERGY ALL Materials PLOTS:
%%-------------------------------------------------------------------------
figure(7)
plot(TIME,Etot_totm,'b-',TIME,Ehge(1,:),'r-','LineWidth',1)
title('Total energy for all materials VS Hourglass energy')
legend('Total energy for all materials','Hourglass energy')
xlabel('Time [s]')
ylabel('Energy [MPa]')
set(gcf,'color','w');
box on
hold off
%%
print -dpng FIGURES\MATSUM_F04_TOT_EN_VS_HGEN.png -r600
%%
%*************************************************************************
% SAVING WORKPLACE!!!!
savefile =  'VARIABLES/MATSUM_WS.mat';
save(savefile)
```

```
%*************************************************************************
% FILE NAME: RCFORC.m
%*************************************************************************
%                  Post-processing of the RCFORC-FILE
%*************************************************************************
% - Read RCFORC-file
% - Calculates reaction forces (total force)
% - Calculates displacments
% - PLOTS RELATIVE STRENGTH BETWEEN COLLIDING OBJECTS
%   by plotting total force versus relative dispacements.
%*************************************************************************
%------------------------------>>        DEVELOPED BY: SIMEN BØHLERENGEN
%*************************************************************************
% MAKE USE OF A WORD-COUNT FUNCTION:
NR_TS = wordcount2('rcforc');    % counts number of the word = time
NR_TS = NR_TS/4;                 % gives number of time-step;


close all
%*************************************************************************
% PART 1: READ IN RCFORC-FILE
%*************************************************************************
fid = fopen('rcforc');
for i=1:5
    tline = fgets(fid);
end

b = fscanf(fid,'%d %*s',[1,inf]);
NR_MAT = length(b);
tline = fgets(fid);


SV = zeros(8,NR_TS,2);
MV = zeros(8,NR_TS,2);
for t = 1:NR_TS
    for w = 1:5
    tline0 = fgets(fid);
    end
    for q = 1:2
    fscanf(fid,'%*s %d',[1,1]);
    SV(1:8,t,q) = fscanf(fid,'%*s %f',[1,8]);
    fscanf(fid,'%*s %d',[1,1]);
    MV(1:8,t,q) = fscanf(fid,'%*s %f',[1,8]);
    end
end
fclose(fid);

%*************************************************************************
%%
TIME = SV(1,:);
NEG_TIME = -TIME;
RCFORC_MX_P = MV(2,:,1)*10-6;
RCFORC_MX_R = MV(2,:,2)*10-6;

RCFORC_SX_P = SV(2,:,1)*10-6;
RCFORC_SX_R = SV(2,:,2)*10-6;

RCFORC_MX_S = zeros(1,NR_TS);
RCFORC_SX_S = zeros(1,NR_TS);
```

```
for t=1:NR_TS
RCFORC_MX_S(1,t) = (sum(MV(2,t,1)+MV(2,t,2)))*10-6;
RCFORC_SX_S(1,t) = (sum(SV(2,t,1)+SV(2,t,2)))*10-6;
end
RCFORC_MALL = zeros(1,NR_TS);
RCFORC_SALL = zeros(1,NR_TS);

RCFORC_MALL_S = zeros(1,NR_TS);
RCFORC_SALL_S = zeros(1,NR_TS);

for t=1:NR_TS
RCFORC_MALL(t)= (sqrt((MV(2,t,1))^2+(MV(3,t,1))^2+(MV(4,t,1))^2))*10-6;
RCFORC_SALL(t)= (sqrt((SV(2,t,1))^2+(SV(3,t,1))^2+(SV(4,t,1))^2))*10-6;

RCFORC_MALL_S(t)= (sqrt((sum(MV(2,t,:)))^2+(sum(MV(3,t,1)))^2+...
    (sum(MV(4,t,1)))^2))*10-6;
RCFORC_SALL_S(t)= (sqrt((sum(SV(2,t,1)))^2+(sum(SV(3,t,1)))^2+...
    (sum(SV(4,t,1)))^2))*10-6;
end


Dpush = zeros(1,NR_TS);
ini_s = 0;
v = 2;

for t=1:NR_TS
if RCFORC_MALL(t) == 0
ini_s = v*TIME(t);              % inital length (before impact)
else
Dpush(t) = v*TIME(t)-ini_s;     % indentation length
end
end

%%
NR_POINTS = wordcount3('P1BRR');
NR_POINTS = NR_POINTS/2;
%%
fud = fopen('P1BRR');

for i=1:5
    tline = fgets(fid);
end

Dp = zeros(2,NR_TS,NR_POINTS);

for i = 1:NR_POINTS
    tline = fgets(fid);
    tline = fgets(fid);
    tline = fgets(fid);
    tline = fgets(fid);
    for t = 1:NR_TS
        Dp(1:2,t,i) =  fscanf(fid,'%f %f',[1,2]);
    end
    tline = fgets(fid);
    tline = fgets(fid);

end
fclose(fud);
```

```
MAX = zeros(1,NR_TS);
for t=1:401
    for i=1:NR_POINTS-1
        if i == 1;
        MAX(t) = min(Dp(2,t,i),Dp(2,t,i+1));
        else
        MAX(t) = min(MAX(t),Dp(2,t,i+1));
        end
    end
end
Dplate = -abs(MAX);

Dice = Dpush + Dplate;

%%

figure(100)
centeraxes(gca,0);
set(gcf,'color','w');
plot(Dplate,RCFORC_MALL_S,'r-',Dice,RCFORC_MALL_S,'b-', 'LineWidth',1)
title('SHIP (RIGHT SIDE)     VS      ICEBERG (LEFT SIDE)')
xlabel('Time [s]')
ylabel('Energy [MPa]')
opt.fontname = 'helvetica';
opt.fontsize = 8;
centeraxes(gca,opt);
box on
hold off

%************************************************************************
% SAVING WORKPLACE!!!!
savefile =  'VARIABLES/RCFORC_WS.mat';
save(savefile)
```

```
%*************************************************************************
% FILE NAME: PLOT.m
%*************************************************************************
%                    Post-processing of the NCFORC-FILE
%*************************************************************************
%                     RESULTS AND PLOTS of NCFORC-file
% PART 1: Actual vs Nominal area
% PART 2: Force vs indentation and time
% PART 3: Process pressure-area curve
% PART 4: Spatial pressure-area curves
% PART 5: Compare Process pressure-area curves
%*************************************************************************
%-------------------------------->>        DEVELOPED BY: SIMEN BØHLERENGEN
%*************************************************************************

% X-axis; for ISO curve:
x_axis = 0:10/(NR_TS-1):10;

z_axis = minH:Meshsize:maxH;
y_axis = minW:Meshsize:maxW;

% ISO Curve:
ISO = 7.40*x_axis.^(-0.70);

%%
%-------------------------------------------------------------------------
% PART 1: Actual area vs Nominal area
%-------------------------------------------------------------------------
nom_area = asum_cont_area;

figure(1)
plot(nom_area, area_ratio,'b-')
title('Actual area vs Nominal area')
xlabel('Area [m^2]')
ylabel({'Area-ratio';'Actual/Nominal';'[MPa]'})
set(gcf,'color','w');
box on
hold off

print -dpng FIGURES\NCFORC_F01_ACTUAL_VS_NOMINAL_AREA.png -r600

%% -----------------------------------------------------------------------
%       Force vs indentation and Time
%-------------------------------------------------------------------------

figure(2)
if exist('ax')==1
    cla 'reset'
else
end

set(gcf,'color','w');
box on
x1 = TIME;
y1 = abs(MN_F);
y2 = abs(MN_F);
x2 = indent;
hl1=line(x1,y1,'Color','r');
ylim([0 max(abs(MN_F))]);
```

```
ax(1)=gca;
set(ax(1),'Position',[0.12 0.12 0.75 0.70])
set(ax(1),'XColor','k','YColor','k');
xlabel('Time[s]')

ax(2)=axes('Position',get(ax(1),'Position'),...
   'XAxisLocation','top',...
   'YAxisLocation','left',...
   'Color','none',...
   'XColor','k','YColor','k');

hl2=line(x2,y2,'Color','r','Parent',ax(2));
ylim([0 max(abs(MN_F))]);
title({'Force vs Time and Indentation'})
box on

xlabel('Indentation [m]')
ylabel({'Force';'[MN]'})
hold off

print -dpng FIGURES\NCFORC_F02_FORCE_VS_TIME_AND_INDENTATION.png

%% ------------------------------------------------------------------------
% PART 2: Process pressure-area curve
%-------------------------------------------------------------------------

figure(3);

if exist('ax')==1
    cla 'reset'
else
end

set(gcf,'color','w');
box on
x1 = TIME;
y1 = abs(p_pa_c);
x2 = indent;
y2 = abs(p_pa_c);
hl1=line(x1,y1,'Color','k');
ylim([0 max(abs(p_pa_c))]);
ax(1)=gca;
set(ax(1),'Position',[0.12 0.12 0.75 0.70])
set(ax(1),'XColor','k','YColor','k');
xlabel('Time[s]')

ax(2)=axes('Position',get(ax(1),'Position'),...
   'XAxisLocation','top',...
   'YAxisLocation','left',...
   'Color','none',...
   'XColor','k','YColor','k');

hl2=line(x2,y2,'Color','r','Parent',ax(2));
ylim([0 max(abs(p_pa_c))]);
title({'Process prssure-area curve VS time and indentation'})
box on

xlabel('Indentation [m]')
ylabel({'Pressure';'[MPa]'})
```

```
hold off

print('-dpng', 'FIGURES\NCFORC_F03_PPAC_VS_TIME_AND_INDENTATION.png',...
    '-r600')

%% ------------------------------------------------------------------------
% PART 3: Spatial PRESSURE-AREA CURVES
%-------------------------------------------------------------------------
% Method 1A,SPAC compared with PPAC and ISO Curve (ACTUAL AREA)
%-------------------------------------------------------------------------

figure(20)
set(gcf,'color','w');
box on
clear legendInfo
clear pl
cd('FUNCTIONS')
colorM = distinguishable_colors(length(locs));
cd('../')

for i = 1:length(locs)
    m1aa(:,i) = M1A.SA(:,i);
    m1aa(m1aa == 0) = NaN;

    p1 = colorM(i,1);
    p2 = colorM(i,2);
    p3 = colorM(i,3);

        m1asp(:,i) = abs(M1A.SP(:,i))*10^-6;
        m1asp(m1asp == 0) = NaN;

    pl(i) = plot(m1aa(:,i),m1asp(:,i),'Color', [p1 p2 p3],...
        'LineStyle', '-', 'LineWidth',2);
    hold on
    legendInfo{i} = ['TS = ' num2str(locs(i))];

end

    pl(i+1) = plot(act_area,abs(s_pa_c),'b.','markersize', 14);

    for i = 1:length(locs)
    plot(act_area(locs(i)), abs(s_pa_c(locs(i))),'gp','markersize', 10);
    hold on
    plot(act_area(locs(i)), abs(s_pa_c(locs(i))),'bo','markersize', 10);
    hold on
    plot(act_area(locs(i)), abs(s_pa_c(locs(i))),'r.','markersize', 20);
    hold on
    end

    pl(i+2) = plot(x_axis,ISO,'--r', 'MarkerSize',3, 'LineWidth',2);

title('Method 1A, SPACs compared with PPAC and ISO curve (ACTUAL AREA)')
axis([ 0 max(max(m1aa)) 0 max(max(max(m1asp)))])
    xlabel('Area [m^2]')
    ylabel('Pressure [MPa]')
    legendInfo{length(locs)+1} = 'PPA values';
    legendInfo{length(locs)+2} = 'ISO Curve';
    legend(pl,legendInfo)
    hold off
```

```
print -dpng FIGURES\NCFORC_F20_M1A_SPACs_CW_PPAC_AND_ISO_ACTUAL_AREA.png...
    -r600
%%
choose_line = zeros(ant_max,length(locs));
sxs = zeros(length(locs),1);
sys = zeros(length(locs),1);

for i=1:length(locs)
for s=1:ant_max

choose_line(s,i) = sum(M1A.spac(s,:,i));
end
line_val = min(choose_line(:,i));
[sxs(i) sys(i)] = ind2sub(size(choose_line),find(choose_line==line_val));
end

figure(21)
cd('FUNCTIONS')
for i = 1:length(locs)
subplot_tight(ceil(sqrt((length(locs)/2))),...
    ceil(sqrt((length(locs)/2))),i, .025)
set(figure(21),'Units','Normalized','OuterPosition',[0 0 1 1])
pos=get(gca,'pos');
set(gca,'pos',[pos(1) pos(2) pos(3) pos(4)*0.95]);
pos=get(gca,'pos');
contourf(y_axis,z_axis,ar_con1a(:,:,sxs(i),i))
colorbar;
legend(num2str(locs(i)))
hc=colorbar('location','eastoutside','position',...
    [pos(1) pos(2)+pos(4) pos(3), 0.01]);
set(hc,'xaxisloc','top');
axis off
set(gca, 'color', [1 1 1])
set(gcf, 'color', [1 1 1])
end
hold off
cd('../')

print -dpng FIGURES\NCFORC_F21_M1A_CONTROL_AREA.png -r600

%% ------------------------------------------------------------------------
% Method 1B,SPAC compared with PPAC and ISO Curve (ACTUAL AREA)
%------------------------------------------------------------------------
figure(22)
set(gcf,'color','w');
box on
clear legendInfo
clear pl
cd('FUNCTIONS')
colorM = distinguishable_colors(length(locs));
cd('../')

for i = 1:length(locs)
    m1ba(:,i) = M1B.SA(:,i);
    m1ba(m1ba == 0) = NaN;

    p1 = colorM(i,1);
    p2 = colorM(i,2);
    p3 = colorM(i,3);
```

```
        m1bsp(:,i) = abs(M1B.SP(:,i))*10^-6;
        m1bsp(m1bsp == 0) = NaN;

    pl(i) = plot(m1ba(:,i),m1bsp(:,i),'Color',...
        [p1 p2 p3], 'LineStyle', '-', 'LineWidth',2);
    hold on
    legendInfo{i} = ['TS = ' num2str(locs(i))];

end

    pl(i+1) = plot(act_area,abs(s_pa_c),'b.','markersize', 14);

    for i = 1:length(locs)
    plot(act_area(locs(i)), abs(s_pa_c(locs(i))),'gp','markersize', 10);
    hold on
    plot(act_area(locs(i)), abs(s_pa_c(locs(i))),'bo','markersize', 10);
    hold on
    plot(act_area(locs(i)), abs(s_pa_c(locs(i))),'r.','markersize', 20);
    hold on
    end

    pl(i+2) = plot(x_axis,ISO,'--r', 'MarkerSize',3, 'LineWidth',2);

title('Method 1B, SPACs compared with PPAC and ISO curve (ACTUAL AREA)')
axis([ 0 max(max(m1ba)) 0 max(max(max(m1bsp)))])
    xlabel('Area [m^2]')
    ylabel('Pressure [MPa]')
    legendInfo{length(locs)+1} = 'PPA values';
    legendInfo{length(locs)+2} = 'ISO Curve';
    legend(pl,legendInfo)
    hold off

print -dpng FIGURES\NCFORC_F22_M1B_SPACs_CW_PPAC_AND_ISO_ACTUAL_AREA.png...
    -r600
%%
choose_line = zeros(ant_max,length(locs));
sxs = zeros(length(locs),1);
sys = zeros(length(locs),1);

for i=1:length(locs)
for s=1:ant_max

choose_line(s,i) = sum(M1B.spac(s,:,i));
end
line_val = min(choose_line(:,i));
[sxs(i) sys(i)] = ind2sub(size(choose_line),find(choose_line==line_val));
end

figure(23)
cd('FUNCTIONS')
for i = 1:length(locs)
subplot_tight(ceil(sqrt((length(locs)/2))),...
    ceil(sqrt((length(locs)/2))),i, .025)
set(figure(23),'Units','Normalized','OuterPosition',[0 0 1 1])
pos=get(gca,'pos');
set(gca,'pos',[pos(1) pos(2) pos(3) pos(4)*0.95]);
pos=get(gca,'pos');
contourf(y_axis,z_axis,ar_con1b(:,:,sxs(i),i))
```

```
colorbar;
legend(num2str(locs(i)))
hc=colorbar('location','eastoutside','position',...
    [pos(1) pos(2)+pos(4) pos(3), 0.01]);
set(hc,'xaxisloc','top');
axis off
set(gca, 'color', [1 1 1])
set(gcf, 'color', [1 1 1])
end
hold off
cd('../')


print -dpng FIGURES\NCFORC_F23_M1B_CONTROL_AREA.png -r600

%% ------------------------------------------------------------------------
% Method 2,SPAC compared with PPAC and ISO Curve (ACTUAL AREA)
%-------------------------------------------------------------------------
figure(24)
set(gcf,'color','w');
box on
clear legendInfo
clear pl
cd('FUNCTIONS')
colorM = distinguishable_colors(length(locs));
cd('../')

for i = 1:length(locs)

    m2a(i,:) = M2.SA(i,:);
    m2a(m2a == 0) = NaN;
    hold on

    p1 = colorM(i,1);
    p2 = colorM(i,2);
    p3 = colorM(i,3);

    m2sp(i,:) = abs(M2.SP(i,:))*10^-6;
    m2sp(m2sp == 0) = NaN;

    pl(i) = plot(m2a(i,:),m2sp(i,:),'Color', [p1 p2 p3],...
        'LineStyle', '-', 'LineWidth',2);
    legendInfo{i} = ['TS = ' num2str(locs(i))];

end
    s_act_area = (act_area);
    pl(i+1) = plot(s_act_area,abs(s_pa_c),'b.', 'LineWidth',2,...
    'markersize', 14);

    for i = 1:length(locs)
    plot(act_area(locs(i)), abs(s_pa_c(locs(i))),'gp','markersize', 10);
    hold on
    plot(act_area(locs(i)), abs(s_pa_c(locs(i))),'bo','markersize', 10);
    hold on
    plot(act_area(locs(i)), abs(s_pa_c(locs(i))),'r.','markersize', 20);
    hold on
    end

     pl(i+2) = plot(x_axis,ISO,'--r', 'MarkerSize',3, 'LineWidth',2);
```

```
    title('Method 2, SPACs compared with PPAC and ISO curve (ACTUAL AREA)')
    axis([ 0 max(max(m2a)) 0 max(max(m2sp))])
    xlabel('Area [m^2]')
    ylabel('Pressure [MPa]')
    legendInfo{length(locs)+1} = 'PPA values';
    legendInfo{length(locs)+2} = 'ISO Curve';
    legend(pl,legendInfo)
    hold off

print -dpng FIGURES\NCFORC_F24_M2_SPACs_CW_PPAC_AND_ISO_ACTUAL_AREA.png...
    -r600
%%

figure(25)
cd('FUNCTIONS')
for i = 1:length(locs)
subplot_tight(ceil(sqrt((length(locs)/2))),...
    ceil(sqrt((length(locs)/2))),i, .025)
set(figure(25),'Units','Normalized','OuterPosition',[0 0 1 1])
pos=get(gca,'pos');
set(gca,'pos',[pos(1) pos(2) pos(3) pos(4)*0.95]);
pos=get(gca,'pos');
contourf(y_axis,z_axis,ar_con2(:,:,i))
colorbar;
legend(num2str(locs(i)))
hc=colorbar('location','eastoutside','position',...
    [pos(1) pos(2)+pos(4) pos(3), 0.01]);
set(hc,'xaxisloc','top');
axis off
set(gca, 'color', [1 1 1])
set(gcf, 'color', [1 1 1])
end
hold off
cd('../')


print -dpng FIGURES\NCFORC_F25_M2_CONTROL_AREA.png -r600

%% ------------------------------------------------------------------------
% Method 3,SPAC compared with PPAC and ISO Curve (ACTUAL AREA)
%-------------------------------------------------------------------------
figure(26)
set(gcf,'color','w');
box on
clear legendInfo
clear pl
cd('FUNCTIONS')
colorM = distinguishable_colors(length(locs));
cd('../')

for i = 1:length(locs)

    m3a(i,:) = M3.SA(i,:);
    m3a(m3a == 0) = NaN;
    hold on

    p1 = colorM(i,1);
    p2 = colorM(i,2);
```

```
    p3 = colorM(i,3);

    m3sp(i,:) = abs(M3.SP(i,:))*10^-6;
    m3sp(m3sp == 0) = NaN;

    pl(i) = plot(m3a(i,:),m3sp(i,:),'Color',...
        [p1 p2 p3], 'LineStyle', '-', 'LineWidth',2);
    legendInfo{i} = ['TS = ' num2str(locs(i))];

end
    s_act_area = (act_area);
    pl(i+1) = plot(s_act_area,abs(s_pa_c),'b.', 'LineWidth',2,...
    'markersize', 14);

    for i = 1:length(locs)
    plot(act_area(locs(i)), abs(s_pa_c(locs(i))),'gp','markersize', 10);
    hold on
    plot(act_area(locs(i)), abs(s_pa_c(locs(i))),'bo','markersize', 10);
    hold on
    plot(act_area(locs(i)), abs(s_pa_c(locs(i))),'r.','markersize', 20);
    hold on
    end

     pl(i+2) = plot(x_axis,ISO,'--r', 'MarkerSize',3, 'LineWidth',2);

title('Method 3, SPACs compared with PPAC and ISO curve (ACTUAL AREA)')
axis([ 0 max(max(m3a)) 0 max(max(m3sp))])
    xlabel('Area [m^2]')
    ylabel('Pressure [MPa]')
    legendInfo{length(locs)+1} = 'PPA values';
    legendInfo{length(locs)+2} = 'ISO Curve';
    legend(pl,legendInfo)
    hold off

print -dpng FIGURES\NCFORC_F26_M3_SPACs_CW_PPAC_AND_ISO_ACTUAL_AREA.png...
    -r600
%%

figure(27)
cd('FUNCTIONS')
for i = 1:length(locs)
subplot_tight(ceil(sqrt((length(locs)/2))),...
    ceil(sqrt((length(locs)/2))),i, .025)
set(figure(27),'Units','Normalized','OuterPosition',[0 0 1 1])
pos=get(gca,'pos');
set(gca,'pos',[pos(1) pos(2) pos(3) pos(4)*0.95]);
pos=get(gca,'pos');
contourf(y_axis,z_axis,ar_con3(:,:,i))
colorbar;
legend(num2str(locs(i)))
hc=colorbar('location','eastoutside','position',...
    [pos(1) pos(2)+pos(4) pos(3), 0.01]);
set(hc,'xaxisloc','top');
axis off
set(gca, 'color', [1 1 1])
set(gcf, 'color', [1 1 1])
end
hold off
cd('../')
print -dpng FIGURES\NCFORC_F27_M3_CONTROL_AREA.png -r600
```

```
%% ------------------------------------------------------------------------
% Method 4,SPAC compared with PPAC and ISO Curve (ACTUAL AREA)
%-------------------------------------------------------------------------

M5t(:,2,:) = abs(M5t(:,2,:)).*10^-6;

figure(28)
set(gcf,'color','w');
box on
clear legendInfo
clear pl
cd('FUNCTIONS')
colorM = distinguishable_colors(length(locs));
cd('../')

for i = 1:length(locs)
    clear M5t_pks M5t_locs M5_pks M5_locs M5tpks M5tlocs

    M5t_pks(:,1) = M5t(:,2,i);
    M5t_locs(:,1) = M5t(:,1,i);

    [M5_pks,M5_locs]=findpeaks(M5t(:,2,i),'minpeakdistance',10);


    M5t_pks(M5_locs(1):M5_locs(end)) = 0;
    M5t_pks(M5t_pks == 0) = NaN;

    M5plot(:,1) = M5t_locs;
    M5plot(:,2) = M5t_pks;

    for j = 1:length(M5_pks)
        M5plot(M5_locs(j),2) = M5_pks(j);
    end

    M5p = M5plot(0== sum(isnan(M5plot), 2), :);

    p1 = colorM(i,1);
    p2 = colorM(i,2);
    p3 = colorM(i,3);

    pl(i) = plot(M5p(:,1),M5p(:,2),'Color', [p1 p2 p3],...
        'LineStyle', '-', 'LineWidth',2);
    legendInfo{i} = ['TS = ' num2str(locs(i))];
    hold on
end

    s_act_area = (act_area);
    pl(i+1) = plot(s_act_area,abs(s_pa_c),'b.', 'LineWidth',2,...
    'markersize', 14);

    for i = 1:length(locs)
    plot(act_area(locs(i)), abs(s_pa_c(locs(i))),'gp','markersize', 10);
    hold on
    plot(act_area(locs(i)), abs(s_pa_c(locs(i))),'bo','markersize', 10);
    hold on
    plot(act_area(locs(i)), abs(s_pa_c(locs(i))),'r.','markersize', 20);
    hold on
    end
```

```
     pl(i+2) = plot(x_axis,ISO,'--r', 'MarkerSize',3, 'LineWidth',2);

    title('Method 3, SPACs compared with PPAC and ISO curve (ACTUAL AREA)')
    axis([ 0 max(max(M5p(:,1))) 0 max(max(M5p(:,2)))])
    xlabel('Area [m^2]')
    ylabel('Pressure [MPa]')
    legendInfo{length(locs)+1} = 'PPA values';
    legendInfo{length(locs)+2} = 'ISO Curve';
    legend(pl,legendInfo)
    hold off

print -dpng FIGURES\NCFORC_F28_M4_SPACs_CW_PPAC_AND_ISO_ACTUAL_AREA.png...
    -r600
%%

figure(29)
cd('FUNCTIONS')
for i = 1:length(locs)
subplot_tight(ceil(sqrt((length(locs)/2))),...
    ceil(sqrt((length(locs)/2))),i, .025)
set(figure(29),'Units','Normalized','OuterPosition',[0 0 1 1])
pos=get(gca,'pos');
set(gca,'pos',[pos(1) pos(2) pos(3) pos(4)*0.95]);
pos=get(gca,'pos');
contourf(y_axis,z_axis,ar_con4_all(:,:,i))
colorbar;
legend(num2str(locs(i)))
hc=colorbar('location','eastoutside','position',...
    [pos(1) pos(2)+pos(4) pos(3), 0.01]);
set(hc,'xaxisloc','top');
axis off
set(gca, 'color', [1 1 1])
set(gcf, 'color', [1 1 1])
end
hold off
cd('../')


print -dpng FIGURES\NCFORC_F29_M4_SPACs_CONTROL_AREA.png -r600

%% ------------------------------------------------------------------------
% PART 4: CONTOUR PLOTS
%-------------------------------------------------------------------------

figure(10)
cd('FUNCTIONS')
for i = 1:length(locs)
PTS(:,:,i) = dyna(:,:,5,locs(i))*10^-6;
subplot_tight(ceil(sqrt((length(locs)/2))),...
    ceil(sqrt((length(locs)/2))),i, .025)
set(figure(10),'Units','Normalized','OuterPosition',[0 0 1 1])
pos=get(gca,'pos');
set(gca,'pos',[pos(1) pos(2) pos(3) pos(4)*0.95]);
pos=get(gca,'pos');
contourf(y_axis,z_axis,PTS(:,:,i))
colorbar;
legend(num2str(locs(i)))
hc=colorbar('location','eastoutside','position',...
    [pos(1) pos(2)+pos(4) pos(3), 0.01]);
```

```
set(hc,'xaxisloc','top');
axis off
set(gca, 'color', [1 1 1])
set(gcf, 'color', [1 1 1])
end
hold off
cd('../')


print('-dpng','FIGURES\NCFORC_F10_CONTOUR_PLOT_MANY_FORCE_PEAKS.png'...
    ,'-r1200')

%%
%CONTOUR PLOT startpoint:
%--------------------------------------------------------------------------
figure(11)
contourf(y_axis,z_axis,PTS(:,:,1))
colorbar;
title({'TIMESTEP NUMBER', num2str(locs(1))})
legend('MPA')
xlabel('[m]')
ylabel('[m]')
set(gca, 'color', [1 1 1])
set(gcf, 'color', [1 1 1])
hold off
%%
print -dpng FIGURES\NCFORC_F11_CONTOUR_PLOT_FIRST_PEAK.png -r600
%%
%CONTOUR PLOT MedianPlot:
%--------------------------------------------------------------------------
figure(12)
contourf(y_axis,z_axis,PTS(:,:,ceil(length(locs)/2)))
colorbar;
title({'TIMESTEP NUMBER', num2str(locs(ceil(length(locs)/2)))})
legend('MPA')
xlabel('[m]')
ylabel('[m]')
set(gca, 'color', [1 1 1])
set(gcf, 'color', [1 1 1])
hold off

print -dpng FIGURES\NCFORC_F12_CONTOUR_PLOT_MEDIAN_PEAK.png -r600
%%
%CONTOUR PLOT LastPlot:
%--------------------------------------------------------------------------
figure(13)
contourf(y_axis,z_axis,PTS(:,:,length(locs)))
colorbar;
title({'TIMESTEP NUMBER', num2str(locs(length(locs)))})
legend('MPA')
xlabel('[m]')
ylabel('[m]')
set(gca, 'color', [1 1 1])
set(gcf, 'color', [1 1 1])
hold off
%%
print -dpng FIGURES\NCFORC_F13_CONTOUR_PLOT_LAST_PEAK.png -r600
```

```
%% ------------------------------------------------------------------------
%   PROCESS PRESSURE-AREA CURVES
%   Compared with ISO curve and 3[m^2] Pond Inlet
%-------------------------------------------------------------------------

Kierk = load('IMPORTS/K_implot.mat','pacall');

cd('FUNCTIONS')
plotsam
cd('../')

figure(30)
title('Process prssure-area curve compared with Pond Inlet and ISO')
plot(asum_cont_area, abs(p_pa_c),'red',...
    asum_cont_area,abs(Kierk.pacall(1:200)),'b-',...
    x_axis,ISO,'m',...
    cur1(:,1), cur1(:,2),'g-',cur2(:,1),cur2(:,2),'g-',...
    cur3(:,1),cur3(:,2),'g-',cur4(:,1),cur4(:,2),'g-')
axis([ 0 6 0 40])
set(gcf,'color','w');
legend('Process pressure area curve','Kierkgaard','ISO','Pond Inlet')
hold off

print -dpng FIGURES\NCFORC_F30_CW_PONDINLET_ISO.png -r600
%%
% SAVING WORKPLACE!!!!
 savefile =  'VARIABLES/WP_NCFORC.mat';
 save(savefile)
```

```
%% ************************************************************************
% CHECKS THE DISTRIBUTION OF THE STOCHASTIC VARIATION
% OF MATERIAL PARAMETERS:
%*************************************************************************
%-------------------------------------------------------------------------
% MATERIAL CONSTANT 1: (a0)
%-------------------------------------------------------------------------
nbins = 100;
xcenters = -4:4;

fid = fopen('STO21');
for i=1:8
tline = fgets(fid);
end
filant = 53042-8;
ant = filant;
NOM = zeros(ant,1);
for i = 1:ant
NOM(i) = fscanf(fid,'%*d %f',[1,1]);
end
fclose(fid);
NM1 = [mean(NOM) std(NOM)  min(NOM)  max(NOM)]

figure(100)
set(gcf,'color','w');
histfit(NOM,nbins,'normal')
ylabel('Occurences')
xlabel('Deviation factor')


%-------------------------------------------------------------------------
% MATERIAL CONSTANT 1: (a1)
%-------------------------------------------------------------------------
nbins = 100;
xcenters = -4:4;

fid = fopen('STO22');
for i=1:8
tline = fgets(fid);
end
filant = 53042-8;
ant = filant;
NOM = zeros(ant,1);
for i = 1:ant
NOM(i) = fscanf(fid,'%*d %f',[1,1]);
end
fclose(fid);
NM2 = [mean(NOM) std(NOM)  min(NOM)  max(NOM)]

figure(101)
set(gcf,'color','w');
histfit(NOM,nbins,'normal')
ylabel('Occurences')
xlabel('Deviation factor')
```

```
%-------------------------------------------------------------------------
% MATERIAL CONSTANT 1: (a2)
%-------------------------------------------------------------------------
nbins = 100;
xcenters = -4:4;

fid = fopen('STO23');
for i=1:8
tline = fgets(fid);
end
filant = 53042-8;
ant = filant;
NOM = zeros(ant,1);
for i = 1:ant
NOM(i) = fscanf(fid,'%*d %f',[1,1]);
end
fclose(fid);
NM3 = [mean(NOM) std(NOM)  min(NOM)  max(NOM)]

figure(102)
set(gcf,'color','w');
histfit(NOM,nbins,'normal')
ylabel('Occurences')
xlabel('Deviation factor')
%-------------------------------------------------------------------------
% E-modulus: (E)
%-------------------------------------------------------------------------

nbins = 100;
xcenters = -4:4;

fid = fopen('STO24');
for i=1:8
tline = fgets(fid);
end
filant = 53042-8;
ant = filant;
NOM = zeros(ant,1);
for i = 1:ant
NOM(i) = fscanf(fid,'%*d %f',[1,1]);
end
fclose(fid);
NM4 = [mean(NOM) std(NOM)  min(NOM)  max(NOM)]

figure(103)
set(gcf,'color','w');
histfit(NOM,nbins,'normal')
ylabel('Occurences')
xlabel('Deviation factor')
%-------------------------------------------------------------------------
% Inital strain energy: (e0)
%-------------------------------------------------------------------------
nbins = 100;
xcenters = -4:4;

fid = fopen('STO25');
for i=1:8
tline = fgets(fid);
end
filant = 53042-8;
```

```
ant = filant;
NOM = zeros(ant,1);
for i = 1:ant
NOM(i) = fscanf(fid,'%*d %f',[1,1]);
end
fclose(fid);
NM5 = [mean(NOM) std(NOM)  min(NOM)  max(NOM)]

figure(104)
set(gcf,'color','w');
histfit(NOM,nbins,'normal')
ylabel('Occurences')
xlabel('Deviation factor')
```

```
%% ************************************************************************
% Equivalent MATLAB SCRIPT:
%*************************************************************************
clear RN

nbins = 100;
xcenters = -4:4;
ant = 53043-8;
my = 1;
sigma = 10;
myf = 0.5;
sigmaf = 0.1;
limit = 0.99;
RNN = zeros(ant,1);

nloop = 1;
for i = 1:ant
while nloop == 1
        RN = (normrnd(myf,sigmaf,1,1)-0.5)*sigma+my;
    if RN < (my - limit)
        nloop = 1;
    elseif RN > (my + limit)
        nloop = 1;
    else
        nloop = 0;
    end
end
nloop = 1;

RNN(i) = RN;
end
NOMchech = [mean(RNN) max(RNN) min(RNN)]
figure(6)
set(gcf,'color','w');
histfit(RNN,nbins,'normal')

%% ************************************************************************
```

C. FORTAN77 Subroutine

```
c      -----------------------------------------------------------
c      FORTRAN77 CODE
c      PART OF SUBROUTINE IMPLIMENTED IN THE LS-DYNA CODE
c      -----------------------------------------------------------
c      ---------------->      DEVELOPED BY:  SIMEN BØHLERENGEN
c      -----------------------------------------------------------
c      This code is implementation into the LS-DYNA code
c      which then will create a stochastic variation
c      of the material properties in each element
c      before the simulation starts.
c      -----------------------------------------------------------
c      Generate random numbers to scale parameters, Simenbo, 20130510
c      STOCHASTIC VARIATION
       nrandall = RAND(1)
       hsv(29)=nrandall
c      a0
              nsigma=cm(11)
              nlimit=cm(12)
              nmy=1
              nloop=1
              DO WHILE (nloop .EQ. 1)
                IF (cm(22) .LT. 0.5) THEN
                nx1= (RAN(ISEED)-.5)*nsigma +nmy
               ELSEIF ((cm(22) .GT. 0.5) .AND. (cm(22) .LT. 1.5)) THEN
                nx1= (RAND(0)-.5)*nsigma +nmy
               ELSEIF ((cm(22) .GT. 1.5) .AND. (cm(22) .LT. 2.5)) THEN
                nx1= (RAND(1)-.5)*nsigma +nmy
               ENDIF
                IF (nx1 .GT. nlimit+nmy) THEN
                 nloop=1
                ELSEIF (nx1 .LT. nmy-nlimit) THEN
                 nloop=1
                ELSE
                 nloop=0
                ENDIF
              ENDDO
              hsv(21) = nx1
c      a1
              nloop=1
              DO WHILE (nloop .EQ. 1)
              nsigma=cm(13)
              nlimit=cm(14)
              nmy=1
                IF (cm(22) .LT. 0.5) THEN
                nx1= (RAN(ISEED)-.5)*nsigma +nmy
               ELSEIF ((cm(22) .GT. 0.5) .AND. (cm(22) .LT. 1.5)) THEN
                nx1= (RAND(0)-.5)*nsigma +nmy
               ELSEIF ((cm(22) .GT. 1.5) .AND. (cm(22) .LT. 2.5)) THEN
                nx1= (RAND(1)-.5)*nsigma +nmy
               ENDIF
                IF (nx1 .GT. nlimit+nmy) THEN
                 nloop=1
                ELSEIF (nx1 .LT. nmy-nlimit) THEN
                 nloop=1
                ELSE
```

```
                nloop=0
              ENDIF
            ENDDO
            hsv(22) = nx1
c       a2
            nsigma=cm(15)
            nlimit=cm(16)
            nmy=1
            nloop=1
            DO WHILE (nloop .EQ. 1)
              IF (cm(22) .LT. 0.5) THEN
              nx1= (RAN(ISEED)-.5)*nsigma +nmy
             ELSEIF ((cm(22) .GT. 0.5) .AND. (cm(22) .LT. 1.5)) THEN
              nx1= (RAND(0)-.5)*nsigma +nmy
             ELSEIF ((cm(22) .GT. 1.5) .AND. (cm(22) .LT. 2.5)) THEN
              nx1= (RAND(1)-.5)*nsigma +nmy
             ENDIF
              IF (nx1 .GT. nlimit+nmy) THEN
               nloop=1
              ELSEIF (nx1 .LT. nmy-nlimit) THEN
               nloop=1
              ELSE
               nloop=0
              ENDIF
            ENDDO
            hsv(23) = nx1
c       E
            nsigma=cm(17)
            nlimit=cm(18)
            nmy=1
            nloop=1
            DO WHILE (nloop .EQ. 1)
              IF (cm(22) .LT. 0.5) THEN
              nx1= (RAN(ISEED)-.5)*nsigma +nmy
             ELSEIF ((cm(22) .GT. 0.5) .AND. (cm(22) .LT. 1.5)) THEN
              nx1= (RAND(0)-.5)*nsigma +nmy
             ELSEIF ((cm(22) .GT. 1.5) .AND. (cm(22) .LT. 2.5)) THEN
              nx1= (RAND(1)-.5)*nsigma +nmy
             ENDIF
              IF (nx1 .GT. nlimit+nmy) THEN
               nloop=1
              ELSEIF (nx1 .LT. nmy-nlimit) THEN
               nloop=1
              ELSE
               nloop=0
              ENDIF
            ENDDO
            hsv(24) = nx1
c       e0
            nsigma=cm(19)
            nlimit=cm(20)
            nmy=1
            nloop=1
            DO WHILE (nloop .EQ. 1)
              IF (cm(22) .LT. 0.5) THEN
              nx1= (RAN(ISEED)-.5)*nsigma +nmy
             ELSEIF ((cm(22) .GT. 0.5) .AND. (cm(22) .LT. 1.5)) THEN
              nx1= (RAND(0)-.5)*nsigma +nmy
             ELSEIF ((cm(22) .GT. 1.5) .AND. (cm(22) .LT. 2.5)) THEN
              nx1= (RAND(1)-.5)*nsigma +nmy
             ENDIF
```

```
                IF (nx1 .GT. nlimit+nmy) THEN
                 nloop=1
                ELSEIF (nx1 .LT. nmy-nlimit) THEN
                 nloop=1
                ELSE
                 nloop=0
                ENDIF
              ENDDO
              hsv(25) = nx1
      ENDIF
c     compute shear modulus, g
      g2 =cm(1)/(1.+cm(2))
      g  =.5*g2
      IF ((cm(21) . gt. 0.5) .AND. (cm(21) .LT. 1.5)) THEN
       a0=cm(5)*hsv(21)
       a1=cm(6)*hsv(22)
       a2=cm(7)/hsv(23)
       bulk=cm(3)*hsv(24)
       shear=cm(4)*hsv(24)
       fcnst=cm(10)*hsv(25)
      ELSEIF (cm(21) .gt.  1.5) THEN
       a0=cm(5)*hsv(21)
       a1=cm(6)*hsv(21)
       a2=cm(7)/hsv(21)
       bulk=cm(3)*hsv(21)
       shear=cm(4)*hsv(21)
       fcnst=cm(10)*hsv(21)
      ELSE
       a0=cm(5)
       a1=cm(6)
       a2=cm(7)
       bulk=cm(3)
       shear=cm(4)
       fcnst=cm(10)
      ENDIF
```

D. Various results from integrated analysis

Comparison of all the spatial pressure-area curve types:

(Results obtained from Medium 1 Variation analysis)

Box-averaging method

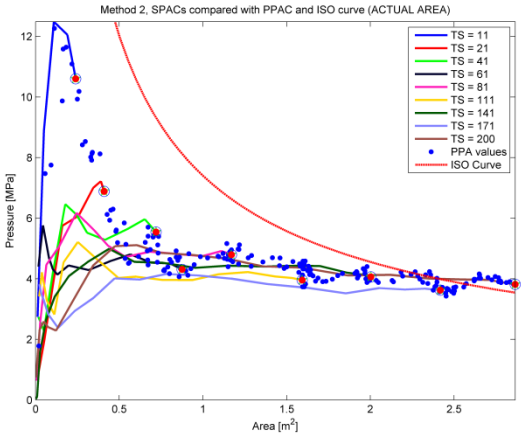

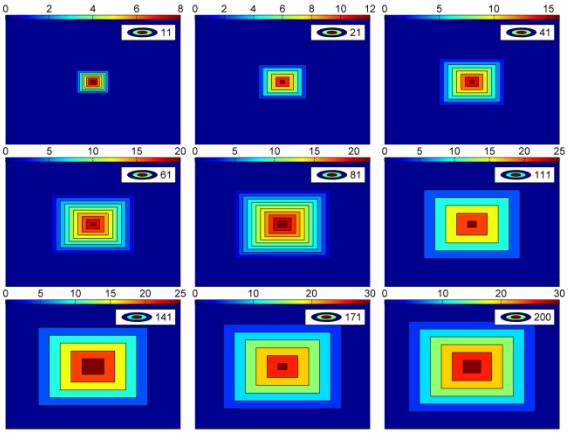

Contour-averaging method

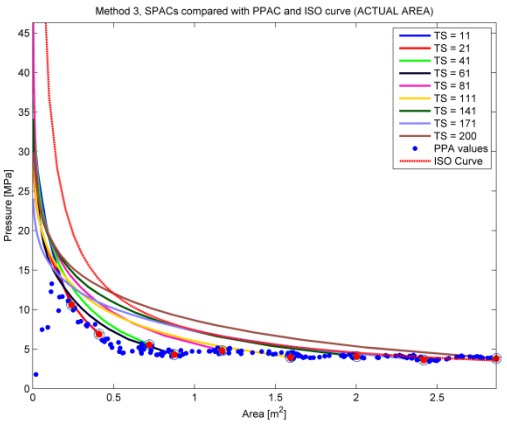

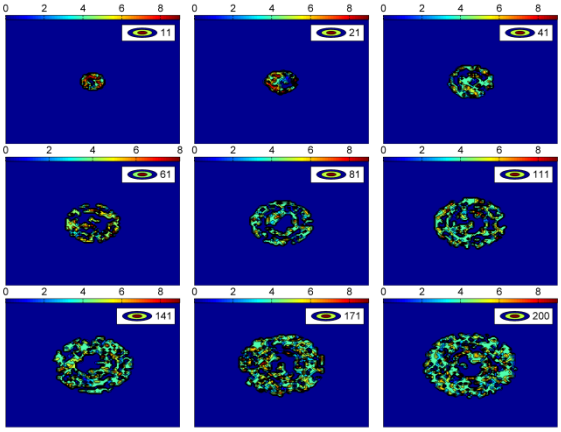

Iterative-search method

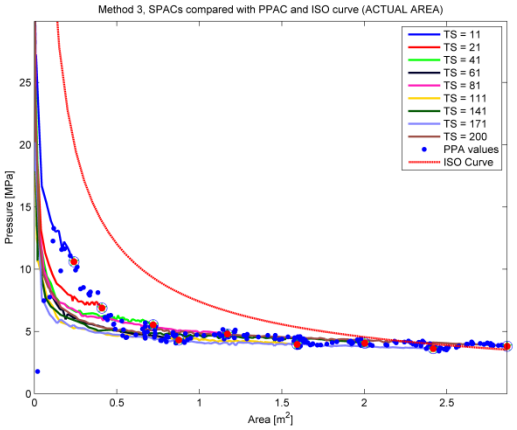

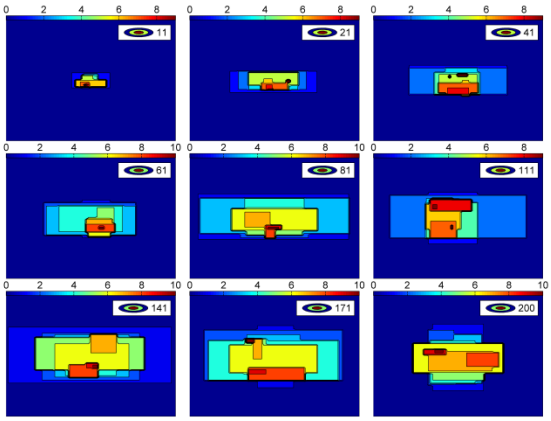

Expand-maxima Method (square areas)

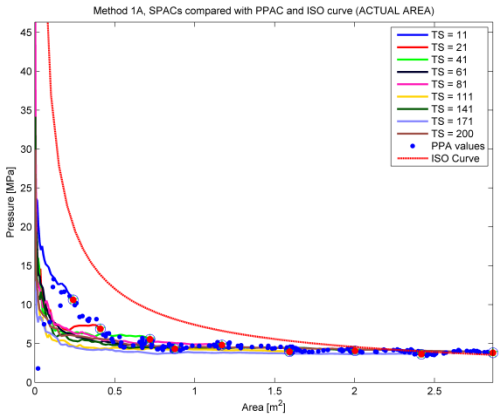

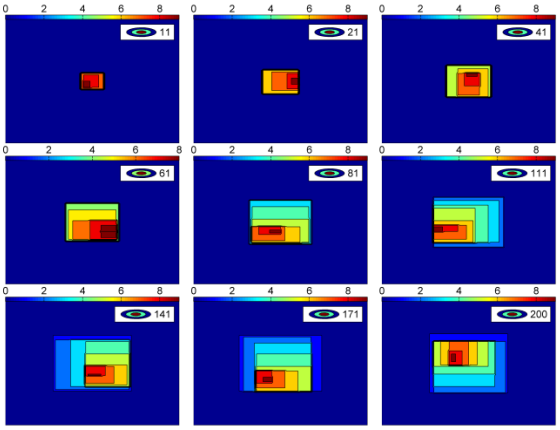

Expand-maxima Method (irregular areas)

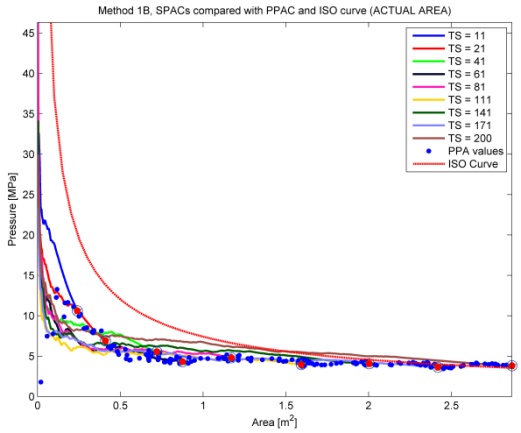

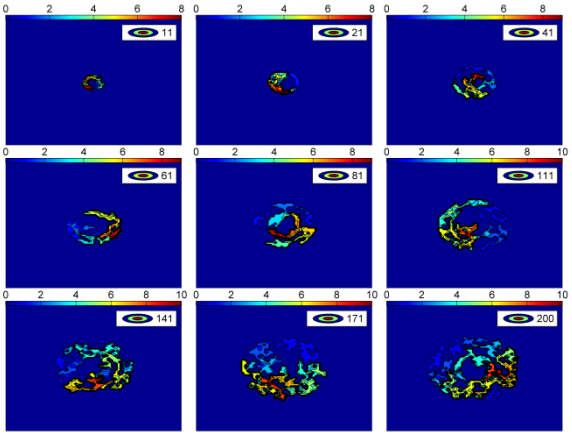

Energy curves for Medium 1 Variation:

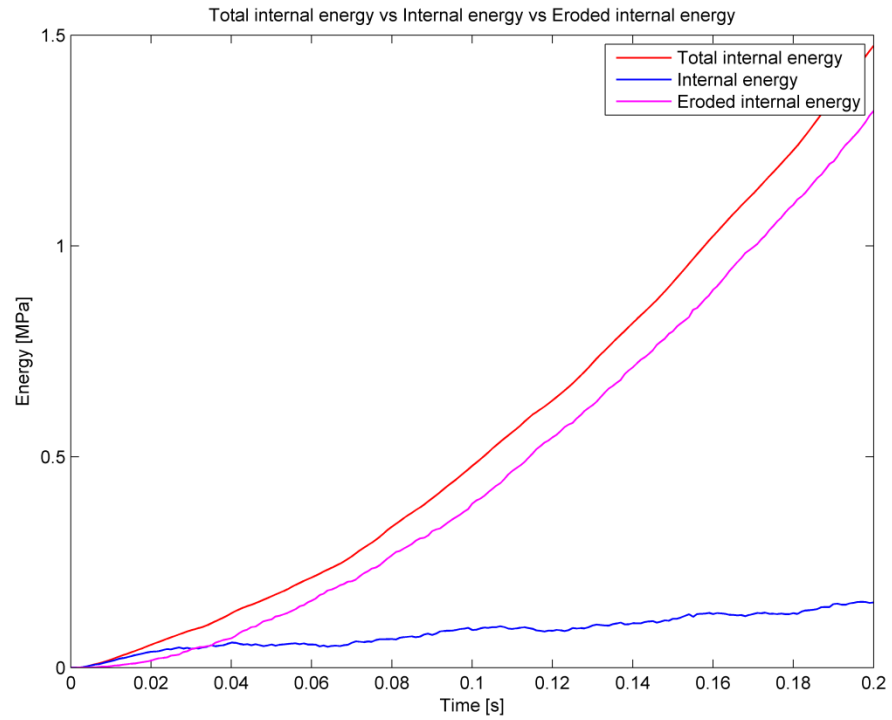

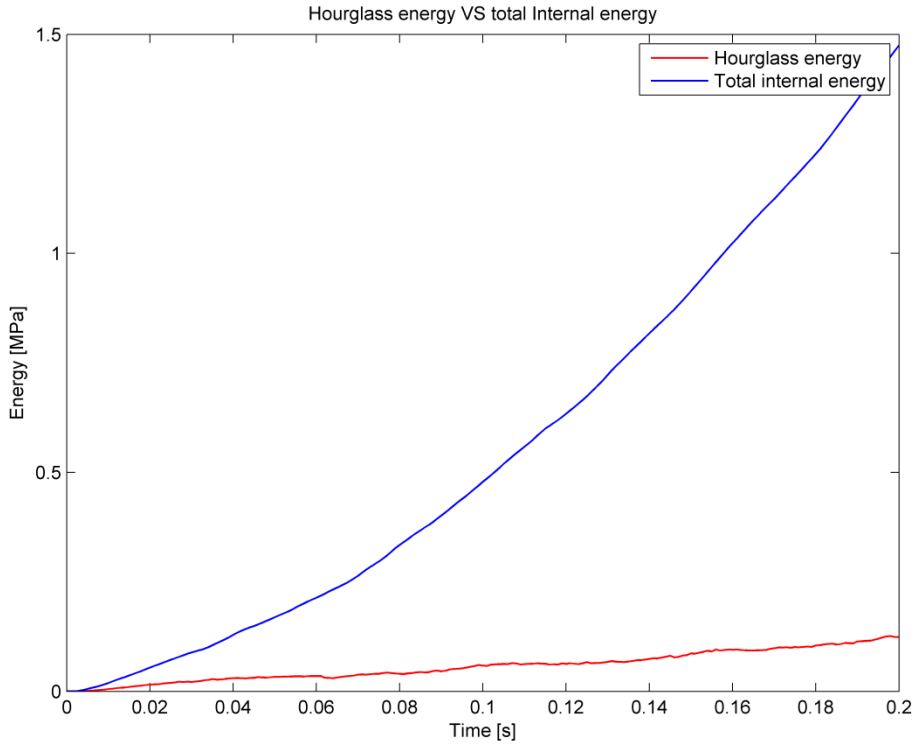

E. Nonlinear finite element method

Analyses where the nonlinear partial differential equation is involved can be comprehensive. In these types of analyses the change of state and deformation process to the solid in time has to be accounted for. These problems can be called initial boundary value problems. LS-DYNA uses of course the nonlinear finite element method to solve the analysis, which is the software used in this project work. A short introduction of the method will therefore be given below. The difference between FEM (finite element method) and NLFEM (nonlinear finite element method) is that the NLFEM accounts for all the nonlinearities. There are 3 types of nonlinearities in FLFEM:

4 Geometric nonlinearity
5 Material nonlinearity
6 Boundary condition nonlinearity

Geometric nonlinearity takes the change of geometry into account due to large deformations. Material nonlinearity accounts for nonlinear material behavior, which occurs for nonlinear materials or linear materials that is loaded over the yielding stress. Material nonlinearities are associated with the stress-stain relationship, where it now has to account for possible changes in the stress-strain curve. This will change the E-modulus and the strength of the material. Boundary condition nonlinearity accounts for boundary conditions which may not be linear, and all the contact area that is happening during an analysis.

Nonlinear finite element method programs have been developed, such as LS-DYNA, ABAQUS, etc. The different programs use different methods to solve the nonlinear finite element problem. LS-DYNA uses the explicit central difference scheme, which is optimal for impact scenarios. Impacts are very nonlinear and the importance of account for nonlinearities is therefore essential. There are many different approaches in nonlinear finite element method, and the choice of method should be chosen carefully.

Explicit versus implicit

The different method can be divided up in two different main groups, explicit and implicit methods. Which one that is most preferable will depend mostly on the duration of the analysis. In this project work explicit method has been used, since it is an impact scenario with low duration. For impacts small time increment is essential, which makes explicit method most favorable.

Explicit and implicit solver for nonlinear finite elements method is full explain in the book “Nonlinear Finite Element Methods” of Peter Wriggers, [27]. A light introduction is given below.

Explicit

Explicit methods are relatively easy to implement, since the solution t_{n+1} depends only on the quantities at time t_n. There exist different explicit methods to solve the equation of motion in solid mechanics. One of the most popular one is the central difference scheme, which also is used in LS-DYNA, the applied software. Since this method is used in LS-DYNA a short theoretical introduction will be given below. The central difference scheme approximate the velocities and accelerations at time t_n by, [27]:

$$v_n = \frac{u_{n+1} - u_{n-1}}{2\Delta t} \tag{16.1}$$

$$a_n = \frac{u_{n+1} - 2u_n + u_{n-1}}{\left(\Delta t\right)^2} \tag{16.2}$$

By implementing these approximations into the momentum balance:

$$M\ddot{u} + C\dot{u} + R\left(u\right) = P \tag{16.3}$$

The result will be an equation system where there is possible to compute the unknown displacement u_{n+1} at the time t_{n+1}:

$$M\left(u_{n+1} - 2u_n + u_{n-1}\right) + \frac{\Delta t}{2} C\left(u_{n+1} - u_{n-1}\right) + \left(\Delta t\right)^2 R\left(u_n\right) = \left(\Delta t\right)^2 P_n \tag{16.4}$$

When this equation system is established, the initial boundary conditions have to be chosen or calculated. Usually the prescribed displacement, velocity and acceleration are known. For the u_{-1} term, Taylor series expansion for the displacements at time t_{-1} can be used, and then all needed initial values are known and the integration process can start without any problems.

For calculation of acceleration and velocity there exist different approximations, which can be used:

$$u_{n+1} = u_n + \Delta t v_n + \frac{\left(\Delta t\right)^2}{2} a_n \tag{16.5}$$

$$v_{n+1} = v_n + \frac{1}{2}\Delta t\left(a_n + a_{n+1}\right) \tag{16.6}$$

Implement these approximations in the equation of motion for the $\left(\ \right)_{n+1}$ term gives:

$$Ma_{n+1} + Cv_{n+1} + R\left(u_{n+1}\right) = P_{n+1} \tag{16.7}$$

$$\left(M+\frac{\Delta t}{2}C\right)a_{n+1}=P_{n+1}-R\left(u_n+\Delta t v_n+\frac{(\Delta t)^2}{2}a_n\right)-\frac{\Delta t}{2}Ca_n \tag{16.8}$$

Equation (16.8) gives the acceleration for a_{n+1}, then displacement, velocity and acceleration can be determined, and the equation of motion can be simulated.

Since explicit method is an approximate method, there is a stability problem, where we do not have balance in the equation of motion. This makes the method unconditionally stable, which introduce an important criterion for the length of the time step. The critical time step for solid elements is generally defined as:

$$\Delta t_e=\frac{L_e}{\left\{\left[Q+\left(Q^2+c^2\right)^{\frac{1}{2}}\right]\right\}} \tag{16.9}$$

where Q is a function of the bulk viscosity coefficients C_0 and C_1 :

$$Q=\begin{cases}C_1 c+C_0 L_e\left|\dot{\varepsilon}\right| & for\ \dot{\varepsilon}_{kk}<0\\ 0 & for\ \dot{\varepsilon}_{kk}\geq 0\end{cases} \tag{16.10}$$

where L_e is the characteristic length, which for the 8 node solid element is:

$$L_e=\frac{\upsilon_e}{A_{e_{\max}}} \tag{16.11}$$

Where υ_e is the element volume, and $A_{e_{\max}}$ is the area of the largest side, and c is the adiabatic sound speed:

$$c=\left[\frac{4G}{e\rho_0}+\frac{\partial p}{\partial \rho}\right)_s\Bigg]^{\frac{1}{2}} \tag{16.12}$$

The sound speed equation (16.12) can be simplified for elastic materials with constant bulk modulus:

$$c=\sqrt{\frac{E(1-\upsilon)}{(1+\upsilon)(1-2\upsilon)\rho}} \tag{16.13}$$

For shell element the critical time step is defined as:

$$\Delta t_e = \frac{L_s}{c} \tag{16.14}$$

Where L_s is the characteristic length and c is the sound speed:

$$c = \sqrt{\frac{E}{\rho\left(1-\nu^2\right)}} \tag{16.15}$$

Implicit

Implicit integration schemes replace the time derivatives with quantities which depend upon both the last time step and the unknown quantities at $time_{n+\alpha}$. This will require that that the nonlinear equation system is solve for each time step. The nonlinear equation system can be solved by special method such as Newton-Raphson Method, [27]. This method gives some advantages and also some disadvantages. The advantage is that the equation system is allowed to be unconditional stable, and the restrictions on the time step size are only due to the requirement of accuracy. Therefore implicit method is preferable if large time step is needed.

This project work considers impacts with short duration and small time increment is therefore needed. Due to the physical case at hand, the explicit method is far more efficient. Therefore detailed explanation of for implicit method is left out, for further information about implicit method look up general nonlinear finite elements books, or [27].